AD NUMBER
AD817471
LIMITATION CHANGES

TO:

Approved for public release; distribution is unlimited.

FROM:

Distribution: Further dissemination only as directed by Space and Missile Systems Organization, AF Unit Post Office, Los Angeles, CA 90045, 28 MAR 1967, or higher DoD authority.

AUTHORITY
SAMSO/USAF ltr dtd 29 Feb 1972

AD81842 7

VARIABLE POINT GUIDANCE
AND TARGETING
FINAL REPORT

VOLUME I PART 1
BASIC PRINCIPLES AND RESULTS

Prepared by: E.B. Capen, RCA, J.J. Camiel, RCA, R.J. Mc Naughton, RCA, "et al"

DECEMBER 1966

~~This transmittal of this~~ ~~Headquarters, Sp~~ ce Systems Division (AFSC), AF Unit Post Office, ~~L~~

STATEMENT #5 UNCLASSIFIED

SPACE SYSTEMS DIVISION
AIR FORCE SYSTEMS COMMAND
LOS ANGELES, CALIFORNIA

D D C
RECEIVED
JUL 2 6 1967
C

DISCLAIMER NOTICE
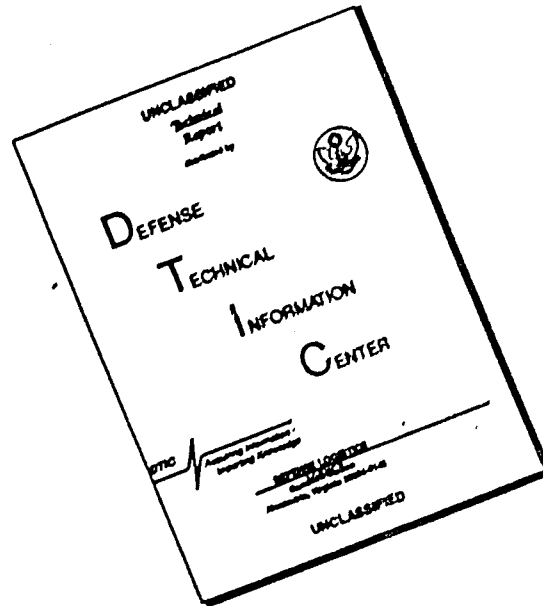
THIS DOCUMENT IS BEST QUALITY AVAILABLE. THE COPY FURNISHED TO DTIC CONTAINED A SIGNIFICANT NUMBER OF PAGES WHICH DO NOT REPRODUCE LEGIBLY.

All distribution of this report is controlled.   Qualified Defense Documentation
Center users will request through:

VARIABLE POINT GUIDANCE
AND TARGETING
FINAL REPORT

VOLUME I PART 1
BASIC PRINCIPLES AND RESULTS

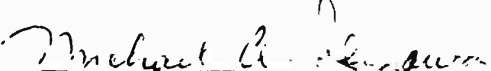Prepared by: E. B. Capen, RCA, J. J. Camiel, RCA, R. J. Mc Naughton, RCA, "et al"

FOREWORD

This document is submitted by the Aerospace Systems Division of the Radio Corporation of America to the Space Systems Divison of the U.S. Air Force Systems Command in conformance with Contract AF04(695)946.

This is part of a two-volume set of documents required by the contract. The first volume contains the theory, logic and derivation of equations as well as a complete Programmers Manual for a guided vehicle simulation program using Variable Point Guidance and Targeting. The second volume contains a coding specification and report on estimates of size and timing of the Variable Point Guidance and Targeting Method for a Univac 1824C Computer based upon actual programming.

The following personnel of the Aerospace Systems Divison, RCA, Burlington, Mass. were contributors to this report: V. K. Brenton, E. E. Hammond, J. W. Stosick, T. G. O'Brien, E. P. Wallner, E. W. Devecka, Dr. A. Baker, H. Brodie, S. Stojanov and Dr. A. M. Schneider of the University of California, La Jolla, California.

ABSTRACT

The primary objective of the development of the Variable Point Guidance and Targeting Technique is to devise a quick reaction guidance and targeting system for space vehicles which does not limit the intrinsic propulsion capability of the booster and upper stages in applications involving arbitrary rendezvous missions. Logic and equations for such a system which operate in real time and which fit a modern aerospace computer have been developed and simulated. The system is provided with the ability of accepting a revised target ephemeris or the ephemeris of a completely new target after lift-off, giving the operational flexibility which permits in-flight changing of mission objectives at any time. The purpose of the present work has been (1) to improve the efficiency and effectiveness of the techniques, (2) to verify the modifications by a detailed simulation containing a representation of a typical booster and upper-stage configuration, (3) document the complete program and (4) to code an aerospace computer to the extent that an accurate sizing and timing estimate can be made. The program was exercised by complete simulation of twelve rendezvous missions against four widely different target situations. An evaluation of the results of the rendezvous simulation studies indicates that the efficiency, effectiveness and general applicability of the computer program was improved and extended so that any satellite rendezvous mission that is within the potential capability of the booster and its associated hardware can successfully be initiated and completed by the insertion of the target ephemeris.

TABLE OF CONTENTS

TABLE OF CONTENTS (Continued)

LIST OF ILLUSTRATIONS

LIST OF ILLUSTRATIONS (Continued)

LIST OF TABLES

LIST OF ABBREVIATIONS AND SYMBOLS

(See Appendix II)

SECTION I

INTRODUCTION AND SUMMARY

1. <u>Introduction.</u> Today's capability for operating in space requires consideration of more ambitious rendezvous missions than those carried out in the Gemini program. The need to be able to rescue astronauts stranded in space requires the use of a self-contained rendezvous guidance technique which can instantaneously plan and execute rendezvous with an arbitrary target. Launching interceptor vehicles from aircraft, space stations or other mobile sites, and allowing astronauts, in orbit, to change the missile to encompass previously unplanned objectives, also call for more flexibility in flight planning and guidance.

The desirable characteristics of a guidance scheme to handle these and other generalizations of the space rendezvous mission are that it be self-targeting, have fast reaction time, be free from dependence on "nominal" trajectories, depend on a minimum number of vehicle characteristics, operate in real time, accept target ephemeris changes after launch, and be efficient, flexible, self-contained and compact.

Self-targeting means having the capability of solving the targeting problem within the on-board guidance computer, without aid from a ground-based computer. The targeting problem involves determining when to launch, where to rendezvous, and when and where to perform every intermediate maneuver. Fast reaction refers to the capability for being able to solve the targeting problem rapidly, say in one second or less, so as not to delay the launch.

The guidance should be free from dependence on nominal trajectories so that it can handle any target whose orbit is within the propulsion capability of the booster. It would depend on the minimum number of vehicle characteristics so that the payload weight or other vehicle parameters may be changed right up to the time of launch without requiring recomputation of guidance parameters. It should operate in real time to guide the vehicle in a stable manner through all phases of flight, correcting for perturbations that were not predicted when the flight plan was developed and modifying the flight plan if necessary. In a fast reaction situation, the target data may be as good before launch as after, due to the acquisition of more measurements on the target by the tracking network. Therefore, it is desirable that the system can accept an updated target ephemeris after launch and compute an effective and efficient course of action that will reliably compute the mission. The program, to be useful, must be compact enough to fit the available memory and speed capabilities of existing aerospace computers.

These capabilities are provided to a high degree by the Variable Point Guidance and Targeting Program. The approach has been to integrate the functions of targeting, flight planning and guidance. The function of targeting is to predict the target state vector at any desired time and also find an accepted flight plan for possible use. The function of flight planning is to determine the best or most efficient plan for accomplishing rendezvous.

1

The flight plans that are used, take into account the interceptor characteristics combined with the principal results of optimization theory (such as Hohmann transfers) rather than mechanizing the theory itself. Heuristic reasoning is used to make a reasonable tradeoff between time of flight and amount of propellant consumed over a wide class of targets.

The function of guidance is to generate the necessary command and control signals so that the prescribed flight plan is followed. The function of guidance in the Variable Point Guidance and Targeting Program is not only to generate the guidance commands based upon an efficient flight plan, but also to alter the flight plan itself when it is necessary or more efficient to do so. This is accomplished by the fact that the targeting routine, flight plan generator and guidance equations are integrated into a relatively simple routine which operates in real time.

As new theoretical results from astrodynamics become available and as computer capability increases, evolutionary improvements can be made to the flight plan logic and the guidance equations to approach closer and closer to optimal performance in a still wider class of cases.

2. Summary. Previous work on Variable Point Guidance and Targeting, contract AF04(695)-273 and AF04(695)-633 were involved with the development of guidance techniques applicable to the general rendezvous mission. The first contract AF04(695)-273 was a follow on to SAINT Program 706. Variable Point Guidance and Targeting, a form of Explicit Point Guidance, was developed out of the recognized need for more flexibility and faster reaction time. It was observed early in Program 706 in working with Explicit Point and other Guidance methods that launch windows were limited not only by vehicle propulsion capability but also by the limitations inherent in the targeting, flight planning and guidance method. This led to combining the targeting, flight planning and guidance into a single program as shown in Figure 1. In order to maintain efficiency and flexibility, the aim points and rendezvous point for a particular lift-off time were planned to be variable. The phasing was initially accomplished by making use of parking orbits and bi-elliptic transfers. The angle out of plane was removed at the first crossing of the line of nodes. Relatively good results were obtained from this simple system especially for missions involving near circular orbits.

In contract AF04(695)-633 means were studied for improving the performance efficiency and overall effectiveness for the general rendezvous mission. The plane change was optimally partitioned among the nodal burns, the ability to change targets at any time or update the initial ephemeris was included, the orbit transfer and phasing policies were modified to improve operation against highly elliptical target orbits and the number of burn points was decreased, therefore increasing reliability.

Alternate methods of rendezvous guidance were studied and successfully simulated using the Titan IIIC as a booster. A report on these studies (SSD-100) dated 15 July 1965, Reference (1), gives the analysis of the various methods and the simulation results for several test cases. The purpose of the present contract AF04(695)-946 is to refine and document the Variable Point Guidance and Targeting equations and logic as well as the simulation program of the guided Titan IIIC multistage booster and its environment. In addition, the simulation program is to be implemented with an SC4020 automatic plotting system and the efficiency and effectiveness of the program are to be demonstrated by a series of twelve runs against four specific targets. The equations and logic are also to be programmed for sizing in a modern aerospace computer. The work is broken into the following four tasks:

a. Task 1 - Program Improvement and Documentation. Three items were identified in past work which were considered to be of primary importance for improving the efficiency in the general rendezvous mission. The tangent transfer and full orbit phasing policy
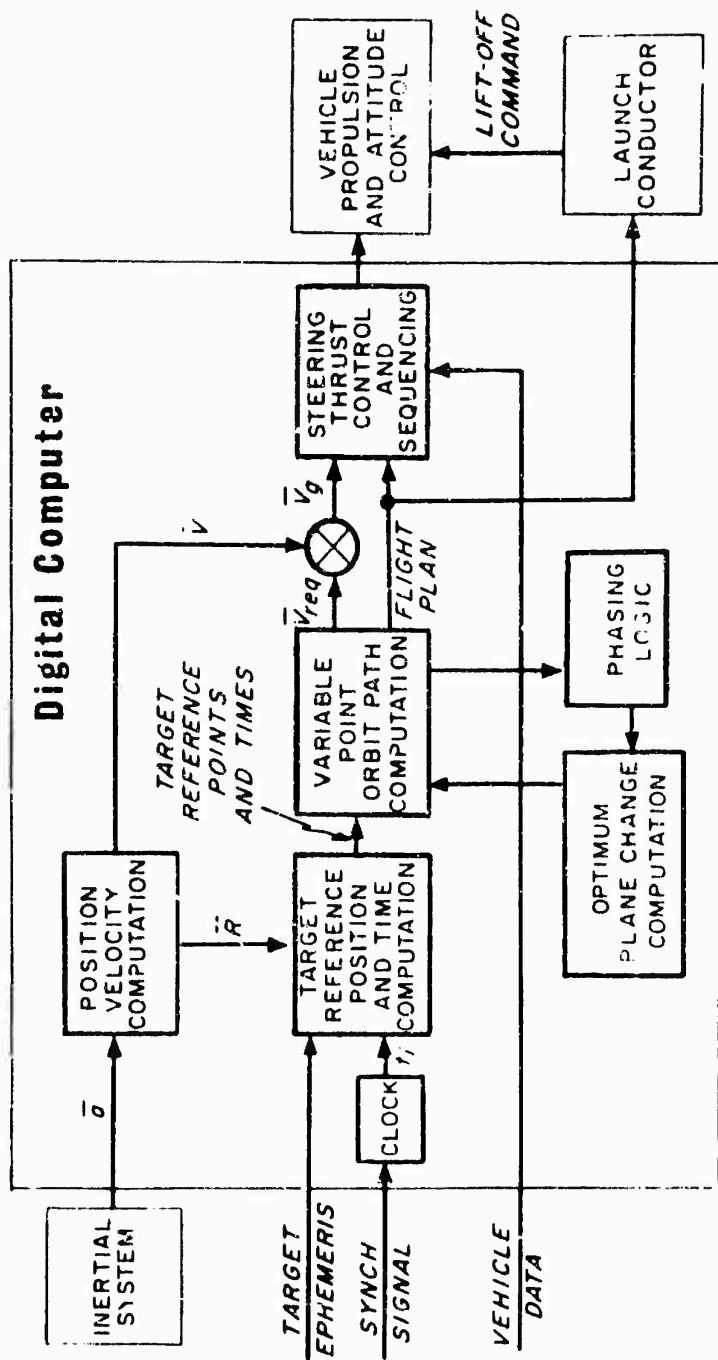
Figure 1. Variable Point Computation Guidance and Targeting

was studied in the previous contract and found to be markedly more effective in missions involving highly elliptical target orbits. The subprogram was developed and required integration into the system.

The second item for improvement involves the reference vector for orientation during coast periods in preparation for the next on-orbit burn. The method previously used did not always produce a stable reference or a correct time to start the burn. The method for correcting this defect was to use the reference vector associated with the burn point derived in the flight plan.

The third item concerned the effects of earth oblateness upon the targeting and guidance equations. The computation for predicting the future interceptor and target vehicle position and velocity should account for oblateness effects. This was done in the navigation equations and in the target prediction equations, however the correction was not made in the missile flight plan and guidance equations. The resulting trajectory therefore would cause the missile to miss the rendezvous point. The simplest solution to this problem requires only that a consistent prediction method be used for each future trajectory segment. The program was modified to include Kepler arcs in forward computation for both vehicles and correct navigation and targeting for past computations. The relative trajectory errors consequently tend to cancel out as the two vehicles approach rendezvous.

Task 1 also includes the documentation of the Variable Point Guidance and Targeting Method and a programming manual of the simulation program. The task 1 documentation is divided into two parts. Part 1 includes background theory, equations and logic, derivation of equations and simulation results. Part 2, the programmers manual, contains flow charts, the Fortran listing of guidance and targeting, the vehicle and its environment and the implementation of the SC4020 plotting routine. Task 1 also includes the demonstration and delivery of the functioning simulation program suitable for use in the system evaluation group computer facility at Wright-Patterson Air Force Base.

     b.   Task 2 - Implementation of the SC4020 Plotting Routine. This task includes the implementation of the SC4020 plotting routine with the complete guided vehicle simulation program. In addition, the complete program and instructions for automatically generating SC4020 plots of any of 68 variables are included. The plot routine has also been implemented with the flight plan generator as an added feature for examination of the launch trade off data.

     c.   Task 3 - Generation of Program Specification for Spaceborne Computer Coding. The subtasks here include actual coding of Variable Point Guidance and Targeting routines for the Univac 1824C aerospace computer. The coding of the routines in the computer is then used to obtain a basis for estimating the cycle time and storage requirement of the program. The work was divided into the following subtasks:

          1.) Generate the navigation guidance and targeting equations for coding in an aerospace computer

          2.) Code specified Variable Point Guidance and Targeting equations in 1824C assembly language

          3.) Estimate the cycle time and storage requirement of the Variable Point Guidance and Targeting Program.

          4.) Generate a document, Volume II which gives the results of the study.

Using the results of the coding, and making necessary comparisons between the simulation program, a sizing and timing study was also completed. The purpose was to verify that the Variable Point Guidance and Targeting storage requirements would fit the available space of an airborne computer. A timing study to determine if all the calculations could be done fast enough to satisfy the guidance and targeting requirements was also completed.

A summary of the Univac 1824 characteristics, program requirements and estimated size and time for the program are given in Tables I, II and III.

It is concluded from the results of this study that the Variable Point Guidance and Targeting system is self contained, it does in fact fit the available space in the 1824C computer and the program is fast enough to satisfy the guidance and targeting requirements of a general rendezvous mission. The 1824G is an 18000 word version of the 1824C. It is the same size but four pounds heavier with 6000 additional memory locations.

     d. <u>Task 4 - Terminal Guidance, Initial Conditions Study</u>. This task concerns the simulation of the Variable Point Guidance and Targeting system in specific rendezvous missions. There are twelve runs against the following four targets:

          1.) A satellite in a circular orbit at an altitude of 150 nautical miles inclined at an angle of 35 degrees

          2.) A satellite in a circular orbit at an altitude of 1000 nautical miles inclined at 49 degrees

          3.) A synchronous satellite in an elliptical orbit whose perigee is at 500 nautical miles altitude at an inclination angle of 65 degrees

          4.) A satellite in an elliptical orbit with altitude of perigee of 200 nautical miles and altitude of apogee of 300 nautical miles inclined at an angle of 90 degrees.

Three selected test cases for each of the above targets were run using three different times of lift-off. The variation in lift-off time gives a variation in the trajectories and hence a different relative velocity at the beginning of the terminal phase (when the terminal sensors would become effective). For this task the beginning of the terminal phase was defined as the time that the relative range is 100 nautical miles. SC4020 plots were made of various parameters of the boost phase of one of the runs, and plots were also made of the relative range, relative velocity, line of sight rate, body rate commands, specific force, radius vector and velocity vectors for the last 100 nautical miles of the mission.

Most simulation runs were well behaved and terminated within a reasonable rendezvous criteria. The results and detailed discussion of the simulation runs are given in Section IV, Volume I, Part 1 of this report. The results showed that modifications in the terminal guidance (the present closure mode) should be made which would lower the sensitivity and provide alternate means for carrying out the flight plan to assure that a reliable and effective reference backup is always available on the contingency that the method being used either fails to develop an acceptable terminal plan or indicates that excessive velocity changes over those derived in the original plan are required to complete the mission.

Table I. Univac Computer Characteristics

Characteristics	1824C	1824G
Size - In Cubic Inches	1300	1300
Weight In Pounds	45	49
Data Word Length In Bits	24	24
Instruction Length In Bits	16	16

Memory:

NDRO 096 (16 Bit) Instructions	12,096	18,000
DRO (24 Bit) Data Words	512	512
Storage Cycle Time in microseconds	4	4
Add Time in Microseconds	8	8
Multiply Time Averages in Microseconds	64	64

Table II. Storage Requirements

VPG Program	
(5226 Instr +300 Constants)	5676
Other (From Flight Plan VII Titan IIIC)	7858
	————
Total:	13,534
Remaining 1824G:	4466

Table III. Timing

Execution Time (Seconds) for a Typical Burn Cycle	0.09
Cycle Time Requirement to be Less Than	2.0
Execution Time (seconds) for a Typical Coast Cycle	0.177
Cycle Time Requirement to be Less Than	10.0

6

3. <u>Conclusion</u> . A computer program for the general solution of the problem of guidance of spacecraft on orbital rendezvous missions, Variable Point Guidance and Targeting, has been developed, documented, programmed for sizing on an aerospace computer, and demonstrated by simulation. In this contract, further improvements were made in the program which increased the efficiency and flexibility and extended the capability of the technique to a wider class of missions. The accuracy of the system has been improved by a better means to account for earth oblateness effects. The more efficient full orbit phasing method was integrated and a better means for controlling the vehicle in relation to coast and burn phases of orbit burns have been included. To be ready for any early specific application further modification and improvements should be made.

SECTION II

THEORETICAL BACKGROUND

1. <u>Introduction</u>. In order to specify the optimum trajectory to perform a given space mission, the entire thrust history (including both propulsive and aerodynamic forces) must be determined. This includes the specification of the number of thrusts, their location in space and time, and the thrust vector orientation at each instant during the maneuver. This task may be called flight plan selection, or targeting, since it gives an overall description of the trajectory arcs which comprise the mission. The velocity changes needed to perform the mission are those required to transfer between the successive arcs in an optimal manner. In general, the velocity requirement is much more sensitive to proper selection of the flight plan, than to the method of guidance and control during the maneuvers. In fact the fixed axis steering method used in the Variable Point Guidance mode has been shown to give results differing relatively little from the optimum. The central problem of Variable Point Guidance and Targeting is therefore the rapid and automatic generation of a near-optimum flight plan. The integration of efficient methods of propulsive and aerodynamic maneuvers into the overall plan constitutes the guidance part of the problem.

We shall here refer to targeting as the means for providing the flight plan to satisfy mission objectives and to guidance as that phase of the mission which begins after the flight plan has been chosen, and the launch process has begun. During the guidance phase the flight plan is being revised as necessary, to take account of deviations from the original plan.

The basic problem to which Variable Point Guidance and Targeting has been addressed may be formally stated as follows: "We which to direct a space vehicle from some initial trajectory in spacetime to a prescribed final trajectory, and to accomplish this transfer with minimum ΔV, minimum time, or some suitable combination of the two, subject to prescribed constraints." In this context "launch" may represent an actual launch from a ground site, or the start of a burn from orbit. Similarly "rendezvous" may represent an actual rendezvous with a target in orbit, or achievement of the desired terminal conditions. Since ΔV and flight time in general represent conflicting requirements, it cannot be established a priori just what represents the most suitable combination of the two. In fact, there are situations or missions in which one may be prepared to sacrifice ΔV to gain time, (ΔV may be budgeted and time is to be minimized).

Since it is required that our system be flexible, it must anticipate such situations. Thus the mathematics should be formulated in such a way that it will result in a family of "ideal" solutions; i.e., those for which rendezvous at various times is effected with the least ΔV. These solutions are then presented to either the computer or a human operator, who proceeds, on the basis of previously defined logical criteria, to make the tradeoff between time and ΔV which is appropriate to that particular mission. Furthermore, this process should be performed continually, in order to provide a guidance capability and to adapt to situations which may be changing in real time.

It is convenient initially to define a propulsion program in terms of "n" discrete impulse burns. There are then (4n - 6) degrees of freedom. This may be seen by noting that there are three resultant velocity components and one time associated with each impulse. (The position of the impulse is a known function of time, as defined by the previous trajectory.) This would give 4n variables. However, six of these are constrained when we prescribe the space-time target trajectory, three for target position at rendezvous time and three for velocity; hence (4n - 6) free state variables.

There are of course additional non-holonomic constraints, such as the requirement that we not pass into the earth, range safety restrictions, etc. However, total ΔV may be expressed as a function of (4n - 6) variables.

$$\Delta V \, (t_L, \, t_R, \, P_1, \, P_2 \ldots, \, P_i, \, \ldots P_{4n - 8}) \qquad \qquad (\text{II-1})$$

where the P_i's are independent variables, and launch time t_L and rendezvous time t_R have been singled out for special treatment.

The functional character of ΔV is determined by the gravitational field, and by aero-dynamic lift and drag when the vehicle is within the atmosphere. To be perfectly general, we may include continuous thrust as a limiting condition obtained by allowing n to approach infinity.

The complete set of ΔV's corresponding to all possible values of the independent state variables comprises a (4n - 6)-fold infinity of solutions. But for the various missions we are in general interested only in those satisfying the (4n - 8) equations,

$$\left(\frac{\partial \, (\Delta V)}{\partial \, P_i}\right)_{\text{const. } t_L, \, t_R} = 0 \qquad \qquad (\text{II-2})$$

i.e., only those solutions for which ΔV has been minimized with respect to all the state variables except t_L and t_R. These last two require preferential treatment; in fact, one is rarely willing to allow them to become arbitrarily large in the process of minimizing ΔV.

2.   The Exact Solution. The exact solution of the (4n - 8) equations (II-2), plus the aero-dynamic and Keplerian equations of motion and constraints, is an extremely difficult mathematical task even with unlimited computational facility, much less for a self-contained system. It has been carried out only for very special and restricted cases. However, before introducing any compromises or approximations, it would be well to carry the logical process somewhat further, in an effort to predict what the solutions may actually look like, and what one would do with them if they were available. This not only provides some insight into the design of an operational system, but it may also suggest what the nature of the approximations should be.

In order to provide a graphic model, we will consider the case of launch from earth to an arbitrary orbital rendezvous, although the principles deduced may be generalized

further. The solution of equations (II-2) comprises a two-fold infinity of solutions, corresponding to all possible values of t_L and t_R. Each of these solutions and its corresponding ΔV may be represented as a point in the (t_L, t_R) plane. Points of equal ΔV may be joined, forming uniform ΔV contours. The resulting contour map could look like that of Figure 2. All points in this plane represent minimum ΔV with respect to the state variables P_i; but t_L and t_R are retained as independent variables. Presumably there would be at least one "pit" in the contour relief map, corresponding to that combination of t_L and t_R for which ΔV approaches a total minimum. The sense of the "fall line" in this figure indicates decreasing ΔV.

The $(4n - 6)$-fold infinity of solutions has been reduced to a two-fold infinity. However, still further reduction is possible. Except for certain considerations which will be discussed subsequently. Launch time need not in general be preserved as a free parameter. What the operations officer is really concerned about in terms of most favored solutions is time of rendezvous and ΔV required. In principle he does not care when he has to launch, as long as it is not in the past. Thus the following additional minimization conditions may be imposed.

$$\left[\frac{\partial (\Delta V)}{\partial t_L}\right]_{\text{const. } t_R} = 0 \tag{II-3}$$

The set of solutions satisfying this condition is represented by the curve AB in Figure 3. It is obtained by drawing horizontal lines through all possible values of t_R, and selecting points of tangency with the smallest ΔV contour. As one moves backward in time, the curve is interrupted by the vertical line BC corresponding to launch in the present. Thus the complete set of solutions available in trading rendezvous time for ΔV is the curve ABC. (There is no merit in continuing this same curve beyond A, since this would entail increasing both ΔV and t_R, which is a bad bargain. After "the present" reaches point A, the desired solutions fall on the vertical "present" line.)

If the mission prescribes a fuel budget, the intersection of the curve ABC with the appropriate ΔV contour is the required solution. If one is prepared to sacrifice fuel to accomplish earlier rendezvous, the trade-off is effected by moving down the curve as far as fuel considerations permit. The only trajectories which are to be considered fall in this singly infinite set, and no other points in the (t_L, t_R) plane need be computed.

It should be noted that the curve AB may be obtained alternately by the following condition:

$$\left[\frac{\partial t_R}{\partial t_L}\right]_{\text{const. } \Delta V} = 0 \tag{II-4}$$

This demonstrates that, in spite of the fact that the solutions were obtained by minimizing ΔV we have simultaneously solved the minimum rendezvous time problem. Thus ΔV and t_R do not prescribe two entirely different mathematical approaches, corresponding to different mission requirements. If the equations have been properly formulated, one

11
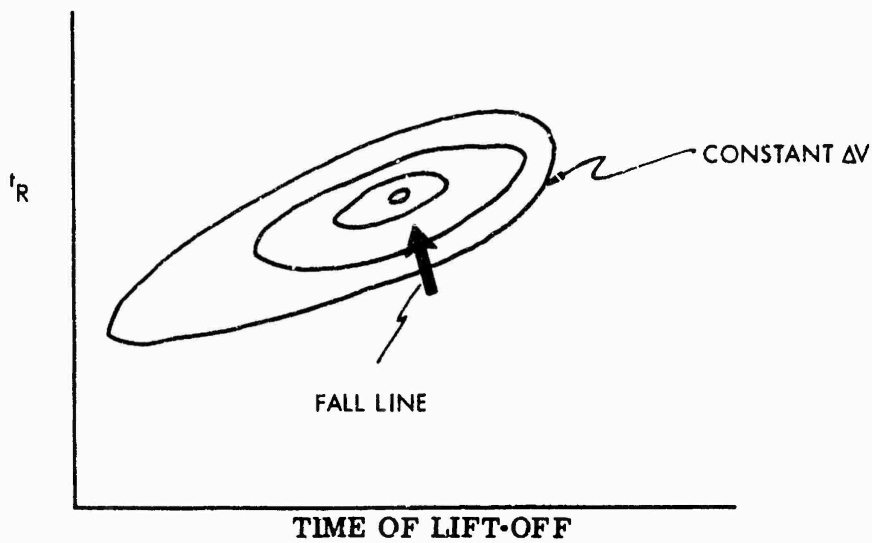
Figure 2. Delta V Contours in the Rendezvous Time,
Liftoff Time Plane
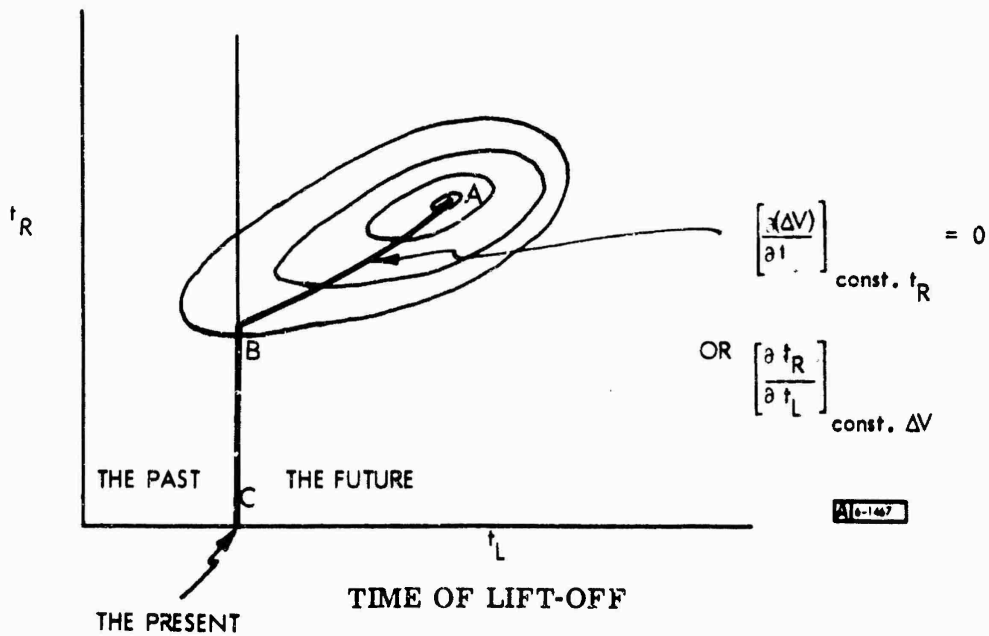
Figure 3. Rendezvous Time - Trade-off Curve

12

common computational procedure may be used for many different applications. Only in the final stage of making a logical decision is it necessary to introduce the criteria appropriate to the particular mission.

The contours of Figure 3 are conceptual. No attempt has been made above to predict their complete representation. It would therefore be useful at this point to become somewhat more specific.

The first observation that can be made is that half the (t_L, t_R) plane is a forbidden region. There is a 45 degree barrier through the origin, corresponding to the fact that rendezvous can never precede launch. In fact, as we approach this barrier the ΔV contour lines become bunched together; a relief model in which the height of the surface represents ΔV would approach infinite steepness along this 45 degree wall, corresponding to infinite ΔV for rendezvous in zero time.

Another observation to be made is the periodic character of the minimum ΔV regions, corresponding to favorable launch and rendezvous orientations which tend approximately to repeat themselves in time. There will be two such periodicities in the problem, one corresponding to the motion of the launch site, and the other that of the rendezvous target.

The fact that there is a daily launch time which is favorable with respect to ΔV is fairly obvious, since this is the time of closest approach (or crossover) between the target orbital plane and the launch site. It is somewhat less obvious that there is likewise a favorable rendezvous time. However, it can be shown analytically, and has been demonstrated by simulation studies (see Reference 9), that the most favorable (i.e., minimum ΔV) point of entry into the target orbit tends to be near the line of nodes, which is the intersection of the parking and target orbital planes. Since the target crosses this line twice per period, it introduced ΔV periodicity with respect to t_R.

In the case of launch into low earth orbit, the launch site position will have a daily period corresponding to earth's rotation, while the target trajectory will have a much shorter orbital period. The effect on ΔV is depicted in Figure 4. The contour "pit" is now seen to recur periodically with respect to t_R as the target site rotates every couple of hours. The daily earth's rotation, on the other hand, manifests itself as a slow periodicity with respect to t_L, introducing long horizontal valleys in the contour map. These tend to repeat themselves every day, but Figure 4 follows this for only about half of a daily period in t_L.

As the ΔV valleys encroach upon the 45 degree causality barrier they become foreshortened, terminating in steep cliffs. Thus the daily periodicity is interrupted by this barrier. If the diagram of Figure 4 were extended up into higher values of t_R, the diurnal periodicity with respect to t_L would manifest itself before being terminated by the barrier.

Even though we have not here solved the exact problem, or derive precisely the shapes of the contours for the multiburn problem, it is thus possible to anticipate certain symmetries, periodicities, and limits in the actual solution. The trade-off curves, designated as AB in the previous figure, and containing the family of most favorable solutions, is now repeated for each valley. If we can compute solutions along the repeated solid line segments AB, we have enough information for making the correct decision, as well as the appropriate flight plan.

13
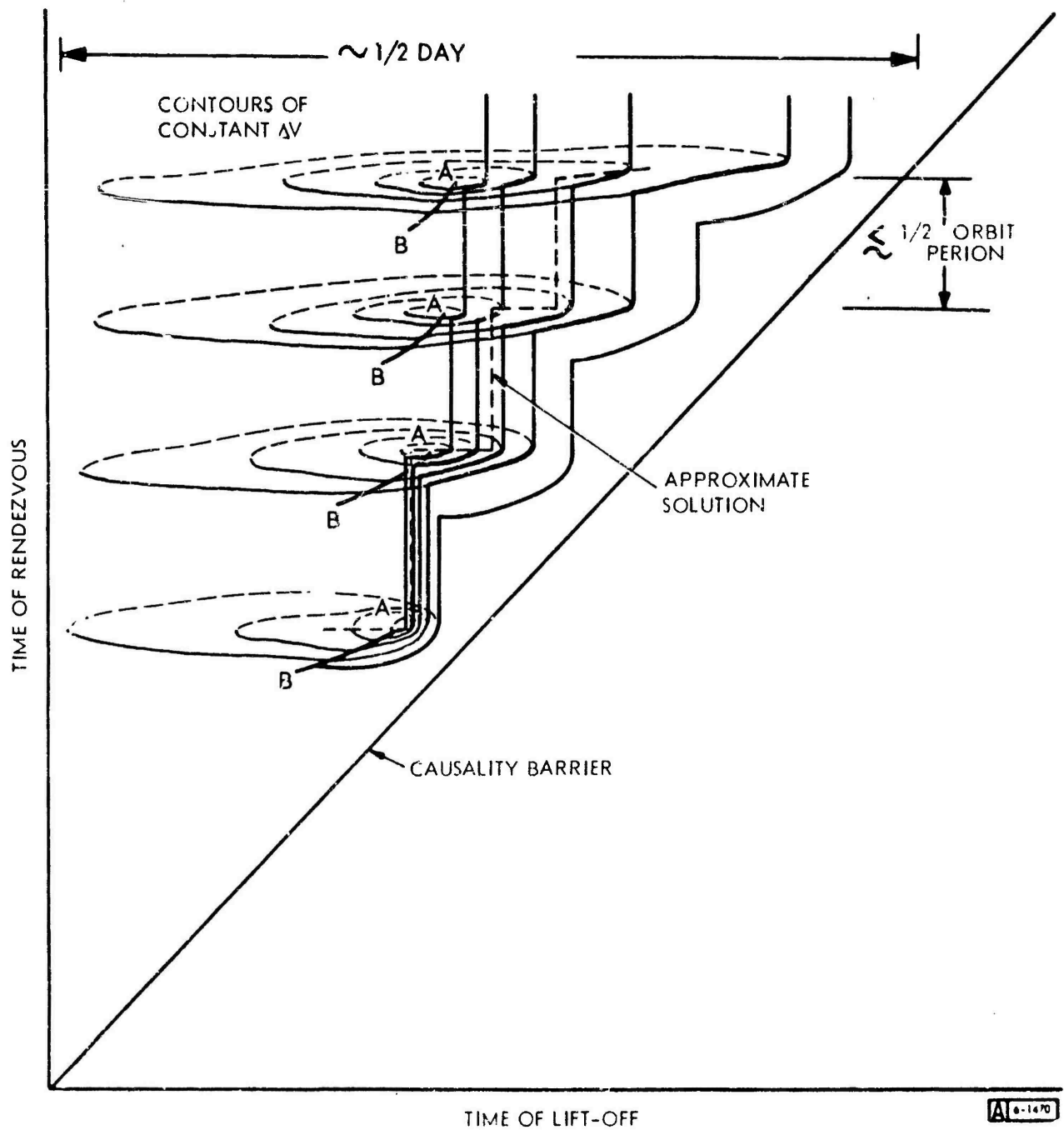
Figure 4. Contours and the Approximate Solution for a
Typical Rendezvous Problem

14

Thus we have demonstrated that a common mathematical formulation may in principle be employed for different problems, missions, and objectives; in generating a single family of solutions from the multi-dimensional hyperspace of all possible trajectories, we have reduced the requirement of mission flexibility to that of making logical decisions. The mathematics of the problem calls for the minimization of ΔV, and the favorable curves AB may be generated by considering various values of t_R, and minimizing ΔV with respect to all other variables.

3.   The Approximate Solution.   There remains of course the matter of obtaining a useful and reliable solution to this mathematical problem.   To do this within the confines of a self-contained system and reasonably finite time, it is clearly necessary at the present time to introduce approximations.   However, since we have some idea of the form of the solution, it is possible to make approximations and simplifications judiciously.

First we note that for the low earth orbits represented in Figure 4, savings in T_R obtained along one of the AB segments are at most only of the order of one half orbit.   Although it is conceivable that certain situations may eventually be encountered in which one is willing to expend extra fuel in order to gain only a few minutes of rendezvous time, it is more likely that the useful trade-off will involve hours or days, rather than minutes.   In other words, if there is to be any significant time - ΔV trade-off, it will be not so much where along a particular AB curve to find the desired solution as which of the AB curves to select.

Furthermore, restriction to flight plans falling precisely on the AB segments results in being constrained to narrow launch windows, since there are large gaps in usable t_L, corresponding to regions of excessive ΔV.   Hold problems in an actual launch process, as well as various possible military requirements, tend to make wide launch windows an important consideration.   An example of this is the failure of the Gemini 9 mission of June 1, 1966, which missed its six-minute launch window because of a hold at T minus three minutes resulting in a two-day delay.

These factors lead us rather to look for solutions following along the ΔV valleys, shown as a series of dotted steps in Figure 4.   This series of solutions is obtained by considering various values of t_L, and minimizing ΔV with respect to t_R, i.e.,

$$\left[\frac{\partial (\Delta V)}{\partial t_R} \right]_{\text{const. } t_L} = 0 \tag{II-5}$$

The jump to the subsequent step or "valley" is obtained as t_L increases whenever a ΔV is reached which exceeds the fuel budget for a particular booster-vehicle combination.   This series of steps now represents our trade-off between rendezvous time and ΔV.

It is these ΔV valleys and associated wide launch windows which are the computational objectives of the Variable Point Guidance and Targeting Program (described briefly in Paragraph 5 of this section). The targeting (or flight plan generating) portion of the program varies t_L and implicitly seeks to minimize ΔV with respect to the other state variables.

It should be noted that while the preceding discussion has suggested that the problem is being solved from earth launch, actually t_L may be regarded as starting from any initial

15

trajectory. In fact, the computation is constantly being repeated (two seconds was used as the cycle time in simulation) so that the process represents not merely a targeting program, but a guidance scheme as well. In other words, the fact that at any instant of computation the vehicle may be halfway to its target merely requires the inhibition of certain logical steps, such as those involving the actual launch process, range safety constraints, etc.; the basic mathematics remains essentially unchanged.

The exact solution of the basic mathematics would require solving simultaneously not only ballistic and aerodynamic equations, but also all the minimization and constraint requirements as well. The most obvious simplification is to break this complex problem into several lesser ones, and find solutions for each of the subsidiary problems. Clearly the resulting pieced-together solutions will not be identical to the overall optimum, but if the subdivision is accomplished properly, there should be enough uncoupling to make the results a good approximation.

The first step is to uncouple the pitch and yaw guidance through the atmosphere as a separate entity, with the exception of the determination of launch azimuth. In other words, a programmed vertical rise, roll to proper azimuth and pitch maneuver to the end of sensible atmosphere is employed. Insertion into a low parking orbit is accomplished by the generated guidance commands. The azimuthal direction of the parking orbital plane is so chosen as to minimize its dihedral angle with the target orbital plan (subject, of course, to range safety constraints, etc.). This is the extent to which the launch process is coupled to the overall requirements.

4. Guidance

a. Atmospheric Exit -- Open Loop Guidance. During the initial portions of the launch trajectory the constraints imposed by aerodynamic forces are so severe as to outweigh consideration of optimizing propellant utilization. While the launch vehicle is in the lower portion of the atmosphere, therefore, the actual trajectory cannot depart greatly from a gravity turn without exceeding the structural limits of current booster configurations. Since the bending moment on the vehicle stack is essentially proportional to the product of angle of attack and dynamic pressure, the angle of attack must be kept small, particularly over the duration of maximum dynamic pressure. The dynamics of stage separation also require a small angle of attack if appreciable dynamic pressure remains at this time. These effects are further exaggerated if the final-stage vehicle is itself a lifting body. Thus, guidance during this phase is generally considered to be best handled by a program which will achieve trajectories close to gravity turns. There are two parameters which can be varied (within the limits imposed by range safety to optimize the trajectory during the atmospheric phase. They are launch azimuth and pitch-over gain (or other equivalent gravity turn parameter). Once the overall flight planning routine has selected these parameters properly, and included an optimum trajectory beyond the atmosphere, further optimization of the trajectory within the severe angle of attack limitations will yield little improvement in overall efficiency.

The attitude control during this phase must operate to satisfy the angle of attack limits in spite of gust loads and wind shear effects. This will usually eliminate the possibility of flying the nominal trajectory with tight loop attitude control and requires aerodynamic stability augmentation. The nature of the control loop depends directly on the vehicle characteristics, including aerodynamic parameters, structural and heating limits, bending mode shapes, sensor locations and center of gravity motion during burning (including the effects of propellant slosh in liquid propellant stages).

16

b. Closed-Loop Guidance. From the point of view of overall guidance the resultant effect of atmospheric disturbances and off nominal vehicle performance will be a deviation of the vehicle stage from the nominal upon exit from the effective atmosphere. During the subsequent portion of the launch phase the desired cutoff conditions must be achieved in a near optimum manner. This is the function of the closed-loop guidance used throughout a burn phase. The ascent phase guidance is greatly simplified if all missions use a low altitude circular orbit, either as the primary orbit for the mission, or as a parking orbit. In this case, a restricted range of standard ascents is derived for all missions with a given booster, the relatively small variations with launch azimuth, payload weight and orbit altitude being dealt with in the latter portion of the ascent phase.

The simplest method of guidance for this phase which is not restricted to a limited range of orbits specifies the velocity vector as a function of position at cutoff. This method is used for two-burn entry into orbit, in the current Variable Point Guidance and Targeting Program.

In this case, a "velocity required" is defined at each instant of flight and the vehicle thrust vector oriented to reduce the velocity-to-be-gained. Pitch and yaw steering is used to maintain the velocity to be gained vector non-rotating in inertial space. Cut-off occurs when velocity-to-be-gained becomes a null value. Experience has shown that his is an efficient, though not strictly optimal method of guidance.

5. Orbital Transfer and Rendezvous. The problem of orbit transfer and rendezvous is to make a minimum ΔV transfer from an initial orbit (usually a low parking orbit, not necessarily circular) to a specified target orbit, and to rendezvous in phase.

The parking orbit, from which this phase of the problem begins, has already been optimized with respect to azimuthal direction, to the extent that the plane of this orbit makes a minimal dihedral angle with the target orbital plane; this reduces the amount of plane change. Strictly speaking, this is only approximately a valid criterion for minimizing ΔV. However, simulation studies show it to be an excellent approximation, and it accomplishes the avowed purpose of uncoupling the launch process from the rest of the problem.

The first approximation to make in solving the problem of orbital transfer and rendezvous from a parking orbit is to restrict the number of impulse burns. (The impulse is of course itself an approximation which may be shown to be very good for all burns except launch.) Here we set n = 3. However, the computer solves this 3-burn problem by looking for the minimum ΔV 2-burn solution necessary to make an orbital transfer without rendezvous. This same ΔV is then imposed on a 3-burn solution which actually effects rendezvous.

The minimum ΔV 2-burn trajectory to effect rendezvous would involve 4n - 6 = 2 free variables. However, since here we are solving the problem as though it were orbital transfer without rendezvous, the target phase is likewise left free, so that altogether there are three free variables. The desired ΔV min solution with respect to these 3 variables causes the vehicle to arrive at the target orbit with a velocity $\vec{V}_{enter}$, out of phase with the target. Instead of giving the vehicle the velocity the target has at this point, we insert with a velocity $\vec{V}_{phase}$ which causes the vehicle to overtake the target after one or more orbital periods and arrive back at this point precisely in phase, whereupon the third and last burn gives it the target velocity $\vec{V}_{target}$.

Since:

$$\vec{V}_{min} = \vec{V}_{target} - \vec{V}_{enter} = (\vec{V}_{phase} - \vec{V}_{enter}) + (\vec{V}_{target} - \vec{V}_{phase})$$

17

We can decompose the second burn of the minimum ΔV solution for 2-burn orbital transfer into two ΔV impulses, the first of which accomplishes phasing and the second rendezvous, but with the same total ΔV_{min}. Thus, orbital transfer is effectively accomplished with minimum 2-burn ΔV, and phasing into rendezvous with zero ΔV. This procedure makes the fine phasing adjustments. Larger corrections are accomplished more rapidly while in low parking orbit.

The program for solving the minimum ΔV 2-burn transfer problem by searching over three state variables has been programmed and tested on various target orbits. However, it has been observed that the optimum point for transferring to target orbit always falls very close to the line of nodes, which is the intersection of the parking and target orbital planes. If we introduce this as an arbitrary constraint, and add further the requirement that transfers from parking orbit to transfer orbit, and transfer orbit to target orbit, are always to be tangent transfers, then we have eliminated all three free variables. Previous studies have shown the results of this simplifying approximation to be very close to those of the exact minimization process; hence, the simplified version has been incorporated into the Variable Point Guidance and Targeting Program.

The solution of the rendezvous problem described here has involved approximation by subdivision into phases; namely, launch, orbital transfer, and rendezvous. Now one unifying final step is introduced; the plane changes are redistributed over the nodal burns in an optimal manner. The computation minimizes ΔV with respect to each of the plane changes, subject to the constraint that the total plane change is conserved. This adjustment makes the last correction in the approximate solution of the minimum ΔV problem.

After lift-off, when the engines are on, the guidance commands are derived from the flight plan requirements. After each burn phase and as the mission progresses the consideration of various computational alternatives is suppressed, in accordance with the fact that the existing state of the system is the result of previous logical commitments. Terminal guidance or the closure mode introduces no changes in the guidance equations themselves, except for the time or distance between burns and a coordinate transformation which converts on-board sensor data from relative coordinates to inertial coordinates. Mid-course and terminal maneuvers are thus reduced to a special case of orbital transfer and rendezvous.

SECTION III

EQUATIONS AND LOGIC

1. Introduction. The purpose of this section is to describe how the Variable Point Guidance and Targeting technique works. The basic equations and logic as well as the required inputs and outputs of the system are given and discussed. The derivation of the equations are given in Appendix I. The guidance and targeting requirements for the various phases of the rendezvous mission from before launch to the beginning of the station keeping phase are considered.

The phases of the mission are given in Table IV. A summary of the computational operations performed during the various phases of a typical rendezvous mission are also included.

The flight plans used by Variable Point Guidance and Targeting are selected from among several possible plans, involving the use of an ascent burn, plus any or all of the following: parking orbits, transfer orbits, plane change maneuvers, small corrections maneuvers, and an adaptation maneuver into the target orbit. Although the number of burns used is discrete ($n \geq 2$), the flight plans span a continuum in the sense that they tend to vary continuously with time. The type of flight plan to be used in a given situation is selected in the Variable Point Guidance and Targeting computation, based on the instantaneous geometry of target and vehicle. The vehicle can be guided to any target whose orbit is within the physical capability of the vehicle's propulsion. Last-minute changes in vehicle configuration (payload weight, propellant load, etc.) can be accepted with a minimum amount of reprogramming and corrections for weight and thrust deviations, winds, variation in lift-off time, steering lags, etc., can be made in flight.

The scheme requires a knowledge of the vehicle's position and velocity, which can be obtained from data supplied by any form of inertial measurement unit IMU, inertial platforms, strapped down inertial, stellar-monitored inertial, etc., are all compatible with Variable Point Guidance and Targeting. A navigation error analysis, which necessarily must be performed for any hardware configuration, depends primarily on the inertial and computing devices, and not on Variable Point Guidance, whose mathematical errors are small by comparison. The Variable Point Guidance equations can be solved in the ground based computer of a radio-command system, provided the measurement of vehicle position and velocity, and the communication link to the vehicle can be maintained.

Table IV. Phases of Rendezvous Mission

1. Prelaunch	Targeting and Flight Planning
2. Lift-off Through Boost to First Cut-off	Boost Guidance Steering, Staging, Navigation, Cut-off Computation
3. Coast and Parking Orbit	Orientation Control, Flight Plan Updating, Time to Start Next Burn, Navigation
4. Transfer Burn	Guidance Steering, Staging, Navigation, Cut-off, Computation
5. Coast	See (3)
6. Phasing Control Burn	See (4)
7. Phasing Orbit	Continue (3) until Closure Mode (Terminal Phase*)
Closure Mode (Terminal)	Series of Burn-Coast Phases to Rendezvous Point
Burn	Navigation and Guidance Steering and Cut-off
Coast	Navigation and Orientation Control with Start Burn Computation for Shorter Segments

*Terminal guidance usually refers to the phase of a mission in which onboard sensors (such as radar) are used to acquire a target and furnish information which can be processed and used to provide guidance signals for further corrective action.

The prime functions of the Variable Point Guidance and Targeting computation in the pre-launch phase are navigation (position and velocity), targeting and flight planning and providing information to the launch conductor. The targeting function is performed by generating the flight plan from which data can be fed to a display for the launch conductor. In the present Variable Point Guidance and Targeting formulation, the launch conductor commands liftoff.

After liftoff, the prime functions are navigation, targeting, guidance, steering, and issuance of discretes. The navigation and targeting functions are performed continuously. Guidance determines the present action needed to implement the flight plan and translates this into vehicle commands. The scheme is based on a restart capability in stages beyond those that are burned to depletion in the first burn. This is essential to gain the fullest and most efficient use of the propulsion capability of the vehicle to rendezvous with targets in the widest variety of orbits. It is primarily a mission requirement and not a guidance limitation.

The inputs to Variable Point Guidance and Targeting are shown in Figure 5. The target ephemeris is the only target data which need be furnished to the computer prior to the terminal phase. Typical IMU inputs are increments of velocity and gimbal angle. A "Go-inertial" signal, signifying that the IMU has entered its operating mode, causes the normal navigation computation to begin. The time synchronization signal references the computer clock to Greenwich mean time. The lift-off signal instructs the computer to take over active control of the vehicle. The vehicle's ΔV budget is supplied for the purpose of determining launch windows. An instant of time is within a launch window if the ΔV required for rendez-vous (launching at that instant) is less than the ΔV budget. A pitch program and multiplier suitably defined for the particular vehicle configuration are furnished to assure compliance with the heating and structural constraints in the atmospheric exit phase.

The outputs furnished to the launch conductor during the prelaunch phase are indicated in Figure 5. The outputs after lift-off include steering commands during both thrust and coast periods; engine ignition and cutoff; and sequencing discretes for staging, search, etc. The steering commands are typically angular rate commands about each of the three body axes. Precision engine cut-off commands are issued at the end of each burn. Ignition commands are given to initiate burns or to complete burns as required following the jettisoning of a depleted stage. Staging commands are issued when the propellant of a given stage is depleted. Search is initiated when the predicted relative range to the target is within the terminal sensor capability. Flight plans are generated, each cycle before lift off and revised periodically during coast periods.

Guidance commands are generated each cycle during a burn phase based upon a generally fixed flight plan. Major changes in the target orbit or changes in the mission can be in-serted any time, however, in the present program the modified flight plan for a major change is initiated only during a coast period. Minor changes such as ephemeris updating can be accommodated at any time. In the terminal phase where radar data would be used to refine the target ephemeris, the flight plan is modified between each burn.

2. Targeting and Flight Planning. The types of flight plans established by the present Variable Point Guidance and Targeting logic handle the complete three-dimensional rendez-vous problem, in which:

        1.) The launch site generally lies outside the target orbit plane

        2.) The target is in any arbitrary elliptical earth-orbit with any phase in its orbit.

        3.) Launch can occur at any time.

Flight plans are built up from segments involving ascent into a low-altitude parking orbit, transfer orbit, phasing orbit, plane change maneuver, and entry into the target orbit with corresponding equivalent position and velocity.

The use of two burn direct ascent, in which the time constraint is satisfied by trajectory phasing is not at present included since the launch window for this method is relatively narrow. The direct intercept case falls out as a singular point in the present program. If time of lift-off is controlled closely enough a direct ascent solution will result. In the present program pulsing orbits and full orbit phasing are used as the primary flight plan; bielliptic flight plans are used only in the closure mode, that is only during the last 360 degree of flight before the planned rendezvous point.
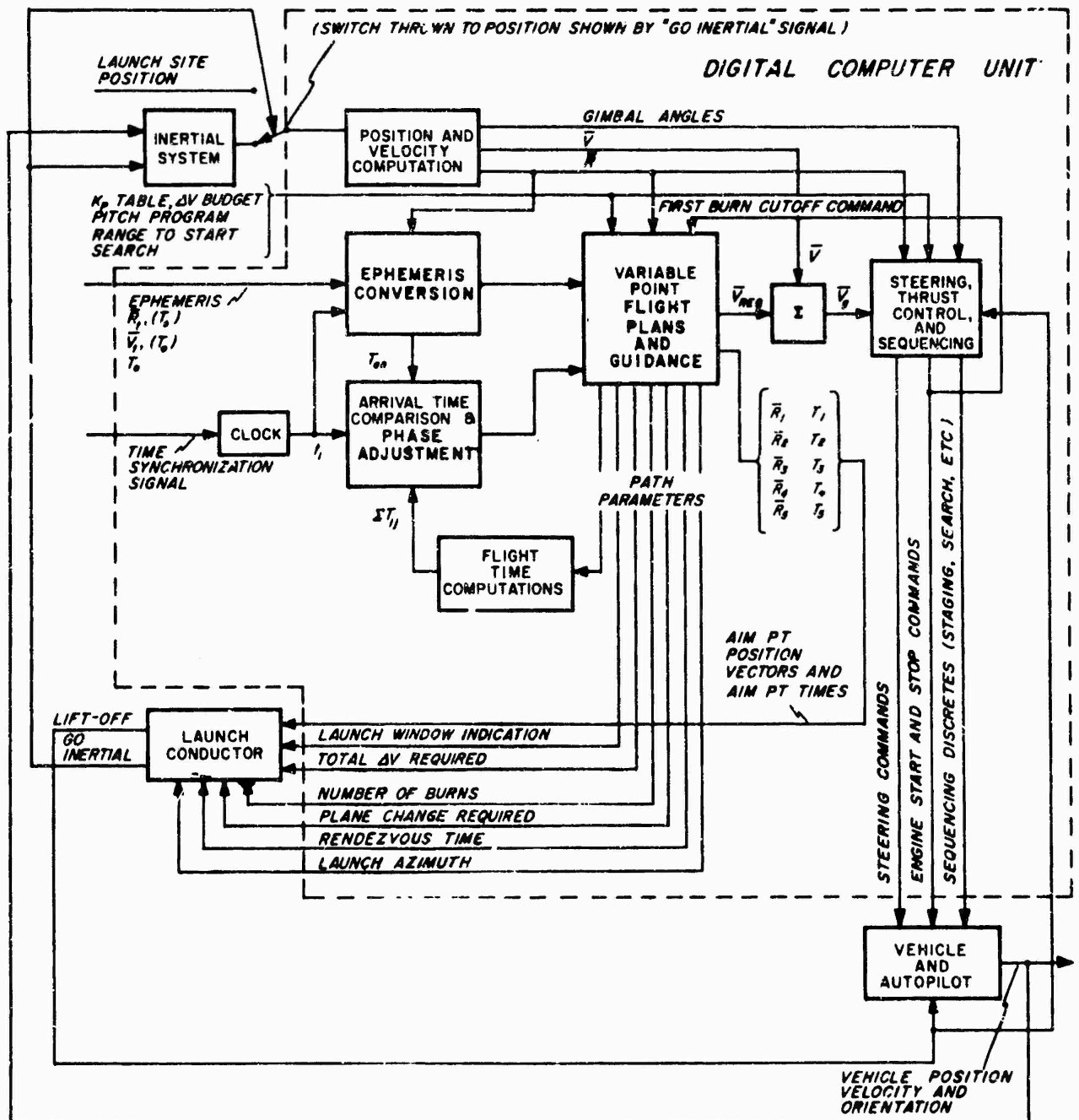
21

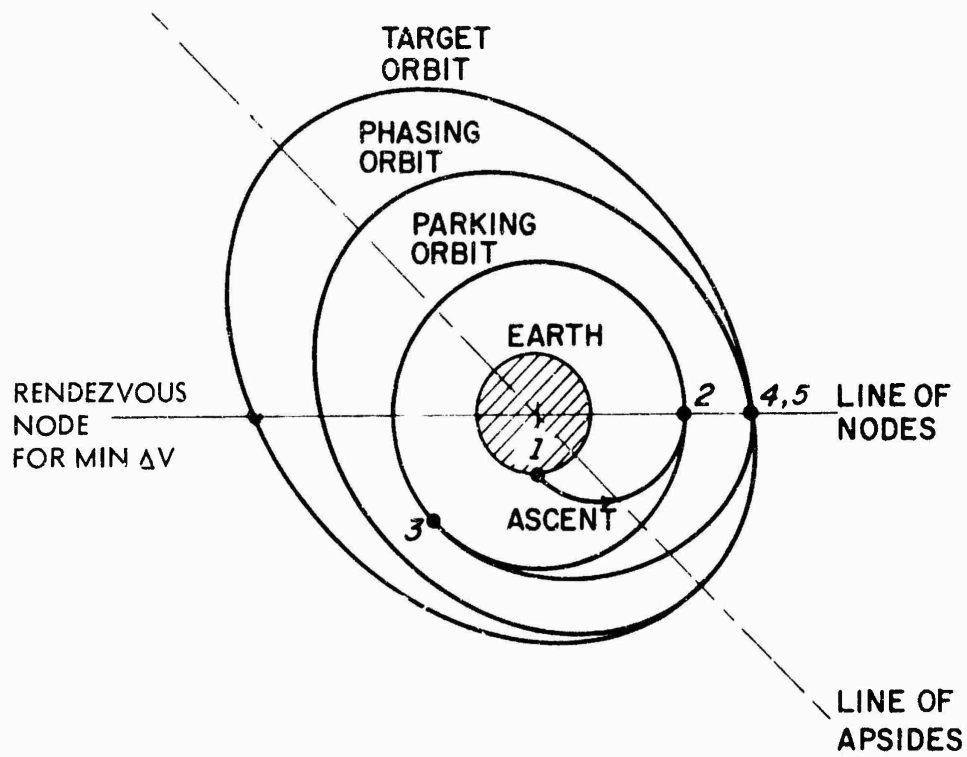Figure 5. Variable Point Guidance and Targeting Block Diagram

22

The mission starts with ascent into a nominally circular low-altitude parking orbit, the second burn being 90 degree downrange from the launch site. The vehicle spends 0, 1/2, 1, 1 1/2 ... periods in the parking orbit until the desired relative phase between target and vehicle is grossly established. Then a third burn, initiates a transfer to the target orbit altitude, reaching the target orbit at the line of nodes, as shown in Figure 6. The shape of the transfer orbit is chosen so that, if the plane of the parking orbit were rotated about the line of nodes into the plane of the target orbit, the transfer would be tangent at the initial and final points. Since both nodes are considered as potential rendezvous point this policy gives close to the optimum transfer for one of the nodes even for final orbits of relatively high eccentricity and plane change. The policy generates an essentially optimal transfer when the final orbit line of apsides is coincident with the line of nodes. A fourth burn at the target altitude initiates a full phasing orbit whose major axis is adjusted to give precise control over time of return to the point of initiation. A fifth burn completes the rendezvous.

Both chase and lob solutions are used in this type of flight plan. In chase, the phasing orbit is below the target orbit, and in lob, it is above. The lob type flight plan has been found to be useful in maintaining wide launch windows for low altitude target orbit situations. Low altitude orbits are considered to be those below about 1000 nautical miles. For target above 1000 nautical miles phasing can be effectively accomplished for any time of lift-off below the target orbit. For targets at very high altitudes (such as synchronous) several alternative phasing solutions may exist in which the phasing can be accomplished below the target orbit and the alternatives increase with increasing altitude. It has been observed that the best solution for all cases is to maintain phasing as near to the target orbit as possible without sacrificing flight time. This is accomplished by proper selection of the number of parking orbits. If the target is high enough, the phasing orbit can be made equal, within a small time increment of the target orbit and the phasing orbit become unnecessary. These are regions about the singular points. The synchronous satellite orbit allows fifteen singular solutions. The lunar orbit allows about 268 singular solutions. The distinction between high and low orbits is made in the program by testing the difference between the target orbit period and the sum of the transfer orbit period and the parking orbit period.

The distinction is necessary because not all phasing orbits can be used due to the finite size of earth. The minimum perigee for a phasing orbit must be greater than or equal to the radius of the earth plus atmosphere. Since tangent transfers are used from a low altitude parking orbit the minimum size of the phasing orbit must be about equal to the transfer orbit.

For the higher targets orbit the period of the phasing orbit does not need to approach the minimum and when the difference is large enough (between parking orbit and target orbit) the minimum period is arbitrarily set at one parking orbit period smaller than the target orbit period. When the sum of the transfer orbit period and the parking orbit period is greater than the target orbit period, the phasing orbit must be between the transfer orbit and the target. If the target orbit is exceptionally low several phasing orbits may be required to remain beneath the target orbit. For these cases it is preferable for most of the launch windows to allow the phasing orbit to lob or pass outside the target orbit.

In either case the number of parking orbits are first computed based upon the use of one minimum phasing orbit for each node. The number is obtained by truncating to full

23

TARGET ORBIT

PHASING ORBIT

PARKING ORBIT

EARTH

RENDEZVOUS NODE FOR MIN ΔV

2

4,5 LINE OF NODES

3

ASCENT

LINE OF APSIDES

NOTE: NUMBERS REPRESENT MAJOR BURNS

Figure 6. Full Orbit Phasing

24

increment the minimum solution. The phasing orbit is then trimmed upward for a usable solution. The solution to be used after lift-off is chosen from the two possibilities (one at each node).

The Greenwich time of rendezvous T_R can be expressed in terms of target motion from an initial reference time and a target flight time:

$$T_R = T_t + n_t \tau_t \tag{III-1}$$

where T_t is the Greenwich time of the next arrival of the target at a prescribed rendezvous point, τ_t is the period of the target orbit and n_t is the number of full target orbits before rendezvous. The equation (III-1) accounts for the fact that several full orbits after first time of arrival of the target at the selected rendezvous point may be required to allow the satellite interceptor to arrive at the same time. The time of rendezvous may similarly be expressed in terms of the interceptor flight plan as follows:

$$T_R = T_i + n_i \tau_i + n_\phi \tau_\phi \tag{III-2}$$

where T_i is the Greenwich time of next arrival of the interceptor at a prescribed point, (the point of the entry into the parking orbit, for example) n_i is the number of parking orbits, τ_i is the period of the parking orbit.

The rendezvous time is found by solving these equations simultaneously in an iterative procedure. In this process, T_t and τ_t are found from the target ephemeris. τ_i is fixed by the altitude of the parking orbit, T_i is known from the characteristic flight time of the payload booster configuration to reach and enter the parking orbit. The unknowns are the number of interceptor parking orbits, the size and number of phasing orbits, and the number of target orbits. The method for solving the equation is as follows:

First solve for the above equation with $n_t = n_i = 0$

Assume first that one phasing orbit is used and set its period at its limiting value, then, solve for the only remaining unknown:

$$n_i = \frac{T_t - T_i + n_t \tau_t - n_\phi \tau}{T_i} \tag{III-3}$$

$(n_\phi = 1$ on first trial).

The limiting value τ_L is equal to τ_X the transfer orbit period for low altitude target orbits or it is equal to $\tau_t - \tau_i$ for high orbits. A test is made on $(\tau_t - \tau_i - \tau_X)$ to determine which limit to use. If the quantity is greater than zero the high limit is used, if the quantity is negative the low limit τ_X is used. If n_i is negative n_t must be increased. When n_i is positive, it is then truncated and the period τ_ϕ is computed.

25

$$T_\phi = \frac{T_t - T_i + n_t \tau_t - n_i \tau_i}{n_\phi} \qquad \text{(III-4)}$$

If τ_ϕ is greater than τ_i then n_ϕ is increased by one unit.

Similar solutions are made for both of the intersections of the line of nodes of the target. The solutions are compared and one is chosen for the flight plan for that particular case. For lifting off from a ground station account is taken of the placement of the line of nodes by azimuth control and the off-flight to the node from lift-off is accounted for in the total time of arrival at the rendezvous point. A flow chart of this process is shown in Figure 7. The maximum number of target orbits before rendezvous is limited by an input setting, $n_{T max}$. The launch director can vary this setting depending on his willingness to trade fuel for time. If he wishes to obtain the greatest fuel efficiency he must set in a large enough number to assure that only chase solutions will be obtained. ($n_{max} = 3$ was large enough for a 1000 mile altitude, circular orbit case). Setting in a smaller number will result in generating lob solutions when they are required.

With the complete planar trajectory laid out, the velocity and flight path angle entering and leaving every burn is known. This data is the input to the plane change split routine, whose output then completes the solution. The problem is solved twice, once for a trail rendezvous point at each end of LN, providing two options with different rendezvous times and/or ΔV requirements.

The total required plane change is removed at burns 2, 4 and 5. A pure plane change maneuver is made at point "b" or "c" if its inclusion decreases the total mission ΔV. The amount of plane changes removed at each of these burns is determined by optimally splitting the total.

If one wanted to rendezvous by the most fuel-efficient means on every flight, one would restrict the flight plan to launch when the launch site lies in the target orbit plane, since ΔV requirements are minimum when the required plane change is zero. The vehicle should then be launched into circular parking orbit at the lowest altitude commensurate with atmospheric heating and drag constraints. It should remain in that orbit until the phase is grossly correct, then enter a Hohmann transfer to the apogee of the target orbit, and complete fine control over phasing with a full orbit tangent at the target orbit apogee. The program produces this flight plan for in plane launch since for this special case the line of nodes is arbitrarily set along the major axis of the target orbit.

The efficiency of the full-orbit tangent-tangent method compared to an optimum non-rendezvous trajectory into the same final orbit from the same launch site location ranges from good to excellent, depending on the orbit eccentricity, the angle between the line of nodes and the line of apsides and the angles between the planes. As the angle between LA and LN decreases from 90 degree to 0 degree, and/or as the eccentricity of the target orbit varies from unity to zero, the tangent transfer becomes essentially optimal over a wide range of out-of-plane angles.

The full-orbit method of phasing has the desirable characteristic that, for a given inertial location of the launch site, and a given final target orbit to be attained, the final time of rendezvous has no effect on ΔV. That is, for mission situations in which only the phase of target is varied, the resulting trajectories all use the same ΔV, but rendezvous occurs

26
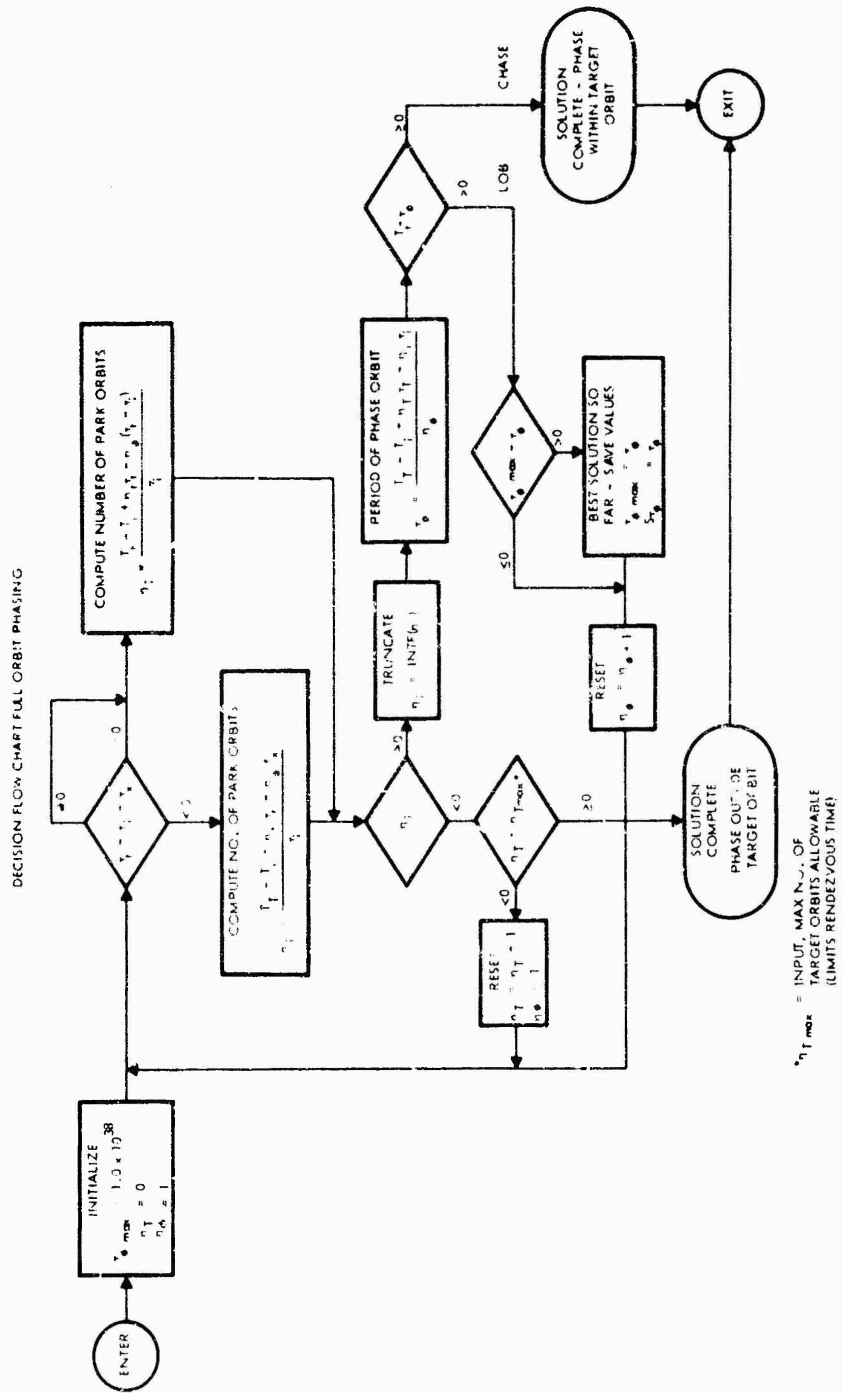
Figure 7. Decision Flow Chart Full Orbit Phasing

at different times. The decoupling between time of rendezvous and ΔV is possible because the burn at the high-altitude end of the transfer orbit can be split into two collinear sub-burns, performed an orbit apart, the sum of which is vectorially equal to the original single burn. The ΔV allotted to each sub-burn controls the size and period of the phasing orbit, hence the time of arrival of the interceptor at the specified rendezvous point. The logic which implements this phasing method solves the phasing problem first, and the plane-change problem second.

a. On-Orbit Tangent Transfer. The transfer trajectory is established as that which is tangent to the target orbit at the intersection of the target orbit with LN, and tangent to the circular parking orbit.

The parking orbit velocity vector at the node is:

$$\bar{V}_m = (\bar{1}_{HM} \times \bar{1}_{Ra}) \left(\frac{GM}{R_a} \right)^{1/2} \tag{III-5}$$

The tangent of flight path angle at the node and the radius vector at the nodes are computed for both the target orbit and the parking orbit. The tangent transfer (see Figure 8) is determined by finding range angle from the node on the target orbit to the tangent point on the parking. There is one such angle for each node defined by its inverse tangent half angle function.

$$Z = \frac{1}{\tan \frac{\Omega}{2}} = \frac{\tan \gamma_{Nt} - \dfrac{R_{Nt}}{R_{Nm}} \tan \gamma_{Nm}}{\dfrac{R_{Nt}}{R_{Nm}} - 1} \tag{III-6}$$

The trigonometric identity for the half angle gives the sine and cosine of the angle.

$$Z = \frac{\sin \Omega_{ij}}{1 - \cos \Omega_{ij}} \tag{III-7}$$

The sign and cosine of the angle is computed from

$$\sin \Omega_{ij} = \frac{2Z}{1 + Z^2} \tag{III-8}$$

and
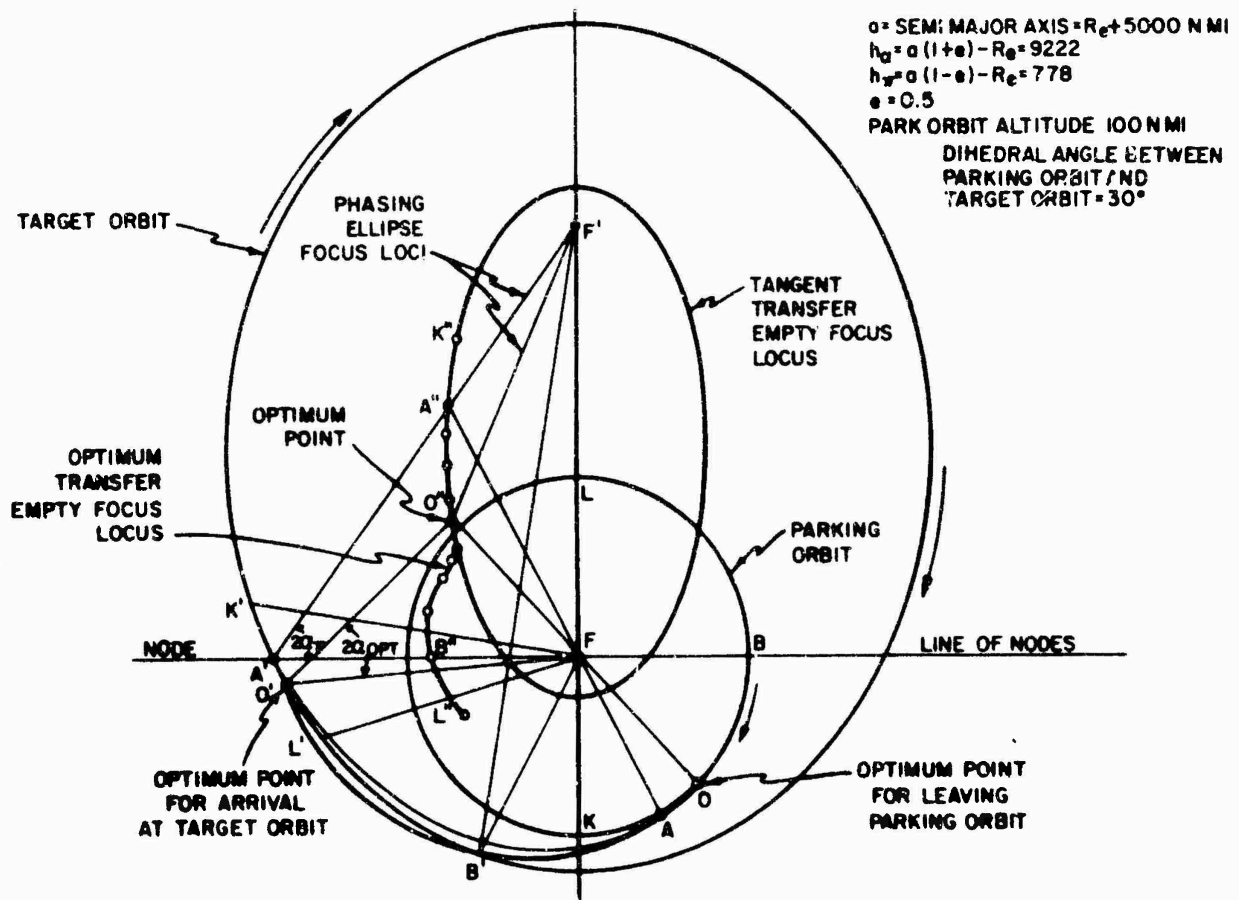
Figure 8. Transfers From Parking Orbit to Target Orbit

$$\cos \Omega_{ij} = 1 - \frac{2}{1 + Z^2} \tag{III-9}$$

The time at node is obtained as follows:

$$\frac{P}{R_m} = \frac{1 - \cos \Omega_{ij}}{\dfrac{R_m}{R_{Nt}} - \cos \Omega + \sin \Omega \tan \gamma_m} \tag{III-10}$$

$$\frac{R_m}{a} = 2 - \frac{P}{R_M} \left(1 + \tan^2 \gamma_n\right) \tag{III-11}$$

$$\frac{b}{a} = \left(\frac{P}{R_M} \frac{R_M}{a}\right)^{1/2} \tag{III-12}$$

$$\Delta E = \left[\pi - 2 \tan^{-1} \frac{b}{R_M} (Z - \tan \gamma_m)\right] \tag{III-13 prep}$$

$$T_{N1} = T_o + \left(\frac{a}{R_M}\right)^{3/2} \frac{R_M}{\left(\frac{GM}{R_M}\right)^{1/2}} \left[\Delta E - \frac{b}{a}(\tan \gamma_a - \tan \gamma_m)\right] \tag{III-13}$$

b. Optimal Plane Change Split. It was stated above that the rendezvous problem was solved by reducing to a planar case first, solving for the shape of trajectory legs to satisfy the time constraint, and then secondly determining the plane for each of these legs. A means to divide the total plane change to be made into optimally-sized portions is as follows:

$$\Delta V_T = \sum_{i=1}^{n} \Delta V_i \tag{III-14}$$

where ΔV_T is the total mission ΔV which is to be minimized. ΔV_i, the velocity increment at the ith impulse point, may be written as

$$\Delta V_i = \left(A_i - B_i \cos \alpha_i\right)^{1/2} \qquad \text{(III-15)}$$

where A_i and B_i are defined as:

$$A_i = V_{iE}^2 + V_{iL}^2 - 2V_{iE} V_{iL} \sin\gamma_{iE} \sin\gamma_{iL} \qquad \text{(III-16)}$$

$$B_i = 2V_{iE} V_{iL} \cos\gamma_{iE} \cos\gamma_{iL} \qquad \text{(III-17)}$$

and where:

$V_{iE(L)}$ = velocity entering (leaving) the impulse point

$\gamma_{iE(L)}$ = flight path angle entering (leaving) the impulse point

α_i = Plane change angle taken at that impulse point

Coefficients A_i and B_i are constants for the ith burn determined fully by the in-plane por-
tion of the rendezvous problem solution. The total plane change to be taken (α_T) is the
dihedral angle between the interceptor's initial plane and the target orbit plane. It can be
written as the sum of the plane change made at each burn:

$$\alpha_T = \sum_i \alpha_i \qquad \text{(III-18)}$$

The problem is stated as one of finding that set of α_i's which minimizes ΔV_T as given by
equations (III-14) subject to the constraint equation (III-18). The solution to this problem is
readily obtained by the method of Lagrange multipliers.

A necessary condition for an extremum is that the incremental ΔV for an increment of
plane change angle, $\dfrac{\partial (\Delta V)}{\partial \alpha}$, be a constant be a constant for each burn. That is:

$$\frac{\partial (\Delta V_i)}{\partial \alpha_i} = \frac{B_i \sin \alpha_i}{\Delta V_i} \qquad (i = 1, 2, \ldots n) \qquad \text{(III-19)}$$

31

Screening techniques have been developed to set up valid arrays of aim point conditions to be used by the plane change split routine. The objectives of screening are:

1.) To exclude points from plane change processing which would cause convergence of the routine to a maximum rather than a minimum

2.) To cut down computation time caused by slowly converging solutions

3.) To insure that parking orbit points that would produce a better solution if used are included in the plane change aim point arrays.

Figure 9 shows a block diagram of the plane-change subroutine which follows screening.

c. Ephemeris of the Target Orbit. The format for expressing target orbital parameters consists of a matrix of six orbital elements and their first three time derivatives. The parameters used are:

1.) Mean anomaly (M)

2.) Eccentricity (ε)

3.) Inclination (ι)

4.) Right Ascension of Ascending Node (Ω)

5.) Argument of Perigee (ω)

6.) Semi-major axis (a)

7.) The precise meaning of the elements is based on their use in the Variable Point Guidance and Targeting Program.

Within the program, prediction of future missile position for the aim point ahead of present position is made on the basis of a Keplerian orbit starting with the present position and velocity. This orbit is known as the osculating orbit. If the orbital perturbations, e.g., those due to earth oblateness, are appreciable, the true path will deviate from the predicted path. If the missile orbit differs little from the target orbit, as will certainly be true in the final stages of the rendezvous problem, the perturbative forces on the missile and target will be approximately equal. Therefore, if the target position is predicted on the basis of its current osculating elements, the relative error at rendezvous will be much smaller than the absolute deviation in predicted position. In the earlier portions of the rendezvous problem, the target and missile orbits will differ appreciably and small predic-reduced as the two orbits are brought into coincidence. For these reasons, osculating elements are used in the element matrix.

If the time over which the elements are to apply is short compared to the period of perigee rotation (which is a minimum of eighteen days), the long period terms may be expanded in a power series in time and included with the secular terms. Otherwise, the secular terms alone will be used.

d. Earth Oblateness. The derivatives of the elements due to the principal harmonic term in the expansion of the earth's field are given in many places. For reference, the

32

INPUT

1. OUT-OF-PLANE ANGLE (σ_T)
2. AIM POINT NUMBERS (i) AND TOTAL NUMBER OF BURNS (N) INVOLVED
3. VELOCITY AND FLIGHT PATH ANGLE ARRAYS
4. MIN BURN ΔV

START →

INITIALIZE
COMPUTE A_i, B_i & COPLANAR ΔV_i
COMPLETION INDICATOR = 1

SET ITERATION
COUNTER TO 1

SET $\sigma_i = \dfrac{\sigma_T}{N}$

COMPUTE
$$\sigma_i^* = \sin^{-1}\left(\frac{\Delta V_i}{B_i} \times \lambda^{-1}_{avg}\right)$$
$$\sigma_i^{**} = \frac{\sigma_T}{\Sigma\sigma_i^*}\,\sigma_i^*$$

COMPUTE
$$\lambda^{-1}_{avg} \sum_{i=1}^{N} \frac{\lambda_i^{-1}}{N}$$

= 1

COMPLETION INDICATOR   0

COMPUTE
ΔV_i
λ_i^{-1}

ITERATION LOOP

TEST
$|\sigma_i - \sigma_i| - \epsilon$
FOR ALL
i's

$\sigma_i = \sigma_i^{**}$
UPDATE ITERATION COUNTER

< MAX

> MAX

TEST
ITERATION
COUNT

≤ 0

= MAX

SET COMPLETION IND. TO 0

CLOSURE ROUTINE

ELIMINATE NON-BURN POINTS IF BOTH:

1. NO COPLANAR ΔV_i
2. ΔV_i BELOW INPUT MINIMUM

REDISTRIBUTE PLANE CHANGE PROPORTIONATELY IF A POINT IS ELIMINATED
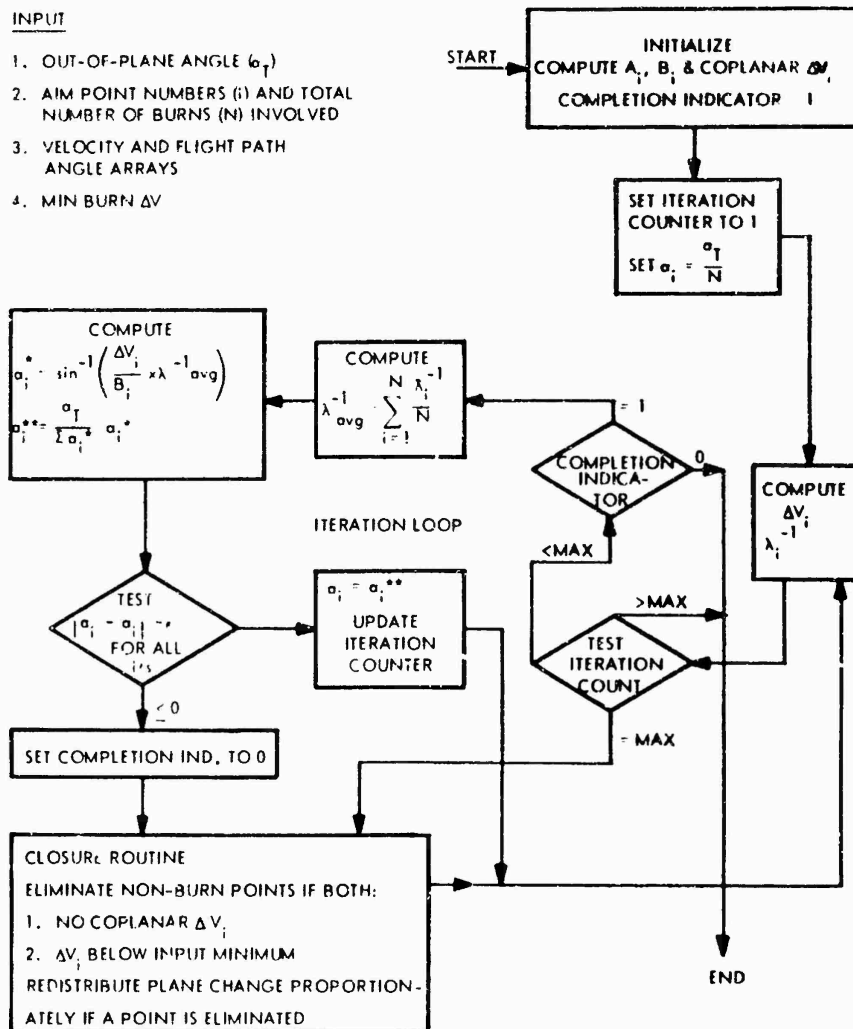
END

Figure 9.   Split P Block Diagram

33

article "Derivation of Nodal Period" by Kalil and Martikan, AIAA Journal, Volume 1 to No. 9, p 2041 (September 1963) is used here. Only secular terms are included.

$$\dot{a} = \dot{e} = \dot{i} = 0 \tag{III-20}$$

$$\dot{M} = n_0 \left[1 + \frac{J}{a^2 (1 - e^2)^{3/2}} \left(\frac{3 \cos^2 i - 1}{2} \right) \right] \tag{III-21}$$

$$\dot{\Omega} = -n_0 \frac{J}{a^2 (1 - e^2)^2} \cos i \tag{III-2?}$$

$$\dot{\omega} = +n_0 \frac{J}{a^2 (1 - e^2)^2} \left(\frac{5 \cos^2 i - 1}{2} \right) \tag{III-23}$$

where:

$$n_0 = \sqrt{\frac{GM}{a^3}} = \text{mean motion in osculating orbit} \tag{III-24}$$

$$\sqrt{GM} = 1.239443589 \times 10^{-3} \ \sec^{-1}$$

$$J = \frac{3}{2} J_2 = 1.62345 \times 10^{-3}$$

a = semi-major axis of osculating orbit in earth equatorial radii

The provision for changing targets was implemented by setting aside a storage register for the time at which a new ephemeris is to be read. If no change in target is to be made this register is set to a very large number. When the time of effectivity of a new ephemeris (as indicated by this register) is exceeded, the new ephemeris is read, inserted into the target ephemeris registers and processed to develop a new flight plan. The new ephemeris time register is then reset to the large number.

To relate this capability to a realistic situation where a change in target or in the final orbit of the interceptor is required it would be necessary to build into the guidance computer a provision from accepting 25 words of information through a ground data link or from some source internal to the vehicle. The read-a-new-ephemeris time register could be reset at any time through the mission.

This capability provides the following advantages to the vehicle once in flight:

        1.) The ability to receive better data on a present target

        2.) The ability to change targets completely

3.) The ability to start a rendezvous mission from a quiescent in-orbit state.

4.) The ability to handle multiple targets (or to inject multiple payloads) starting rendezvous n + 1 after completing rendezvous n

5.) The ability to adapt to a safe orbit if the rendezvous mission is aborted

6.) The ability to accept orbit change instructions from a human pilot.

The ephemeris of the target at any time is given by:

$$
\begin{bmatrix} M_t \\ \Omega_t \\ \omega_t \\ i_t \\ e_t \\ a_t \end{bmatrix}
=
\begin{bmatrix}
M & \dot{M} & \ddot{M} & \dddot{M} \\
\Omega & \dot{\Omega} & \ddot{\Omega} & \dddot{\Omega} \\
\omega & \dot{\omega} & \ddot{\omega} & \dddot{\omega} \\
i & \dot{i} & \ddot{i} & \dddot{i} \\
e & \dot{e} & \ddot{e} & \dddot{e} \\
a & \dot{a} & \ddot{a} & \dddot{a}
\end{bmatrix}
\begin{bmatrix}
1 \\
t - t_o \\
1/2\,(t - t_o)^2 \\
1/6\,(t - t_o)^3
\end{bmatrix}
\qquad (\text{III-25})
$$

e. **Ephemeris Conversion.** The ephemeris is converted to position and velocity vectors at any time by the following elliptical orbit relationships:

$$ M = E - e \sin E \qquad (\text{III-26}) $$

$$ R = a\,(1 - e \cos E) \qquad (\text{III-27}) $$

$$ R_\pi = a\,(1 - e) \qquad (\text{III-28}) $$

$$ P = R_\pi\,(1 + e) \qquad (\text{III-29}) $$

$$ b = (P\,a)^{1/2} \qquad (\text{III-30}) $$

$$ \tan \gamma = \frac{a\,e}{b}\,\sin E \qquad (\text{III-31}) $$

$$ \tan \frac{\nu}{2} = \frac{b}{R_\pi}\,\tan \frac{E}{2} \qquad (\text{III-32}) $$

$$
\overline{1}_R =
\begin{bmatrix}
\cos \Omega \cos (\nu + \omega) - \sin \Omega \sin (\nu + \omega) \cos i \\
\cos (\nu + \omega) \sin \Omega + \cos \Omega \sin (\nu + \omega) \cos i \\
\sin i \sin (\nu + \omega)
\end{bmatrix}
\qquad (\text{III-33})
$$

35

$$\overline{R} = R\,\overline{1}_R \tag{III-34}$$

$$\overline{1}_H = \begin{bmatrix} -\cos\Omega\sin(\nu+\omega) - \sin\Omega\cos(\nu+\omega)\cos i \\ -\sin\Omega\sin(\nu+\omega) + \cos\Omega\cos(\nu+\omega)\cos i \\ \cos(\nu+\omega)\sin i \end{bmatrix} \tag{III-35}$$

$$V_H = \left(\frac{P}{R}\ \frac{GM}{R}\right)^{1/2} \tag{III-36}$$

$$V_R = V_H\tan\gamma$$

$$\overline{V} = V_R\,\overline{1}_R + V_H\,\overline{1}_H \tag{III-37}$$

$$\overline{1}_V = \frac{\overline{V}}{|V|}$$

f. <u>Position and Velocity of the Launch Site.</u> Before the system is switched to the inertial mode the position and velocity of the launch pad in inertial space is computed from the latitude and longitude as follows:

$$\overline{R}_m = R_e \begin{bmatrix} \cos\phi\cos\left[\Omega_m + \dot\Omega_m\,(t_i - t_o)\right] \\ \cos\phi\sin\left[\Omega_m + \dot\Omega_m\,(t_i - t_o)\right] \\ \sin\phi \end{bmatrix} \tag{III-38}$$

$$\overline{V}_m = R_e\,\dot\Omega_m\cos\phi \begin{bmatrix} -\sin\left[\Omega_m + \dot\Omega_m\,(t_i - t_o)\right] \\ \cos\left[\Omega_m + \dot\Omega_m\,(t_i - t_o)\right] \\ 0 \end{bmatrix} \tag{III-39}$$

During the prelaunch phase, the primary function being performed by the on-board computer is targeting and flight planning. The line of nodes is defined 90 degree downrange from the launch site by the following equation:

$$\overline{1}_{NODE} = \overline{1}_{HT} \times \overline{1}_M / \left| \overline{1}_{HT} \times \overline{1}_M \right| \tag{III-40}$$

The first aim point is then set along the defined line of nodes 90 degree downrange from the launch site at a specified altitude. The missile angular momentum unit vector is defined as that instantaneously required to reach the first aim point:

$$\overline{1}_{HM} = \overline{1}_M \times \overline{1}_{a1} / \left| \overline{1}_M \times \overline{1}_{a1} \right| \tag{III-41}$$

The impulsive velocity (scalar) required to reach the first aim point at zero flight path angle is computed, along with the velocity of arrival. The time of arrival is computed, including a penalty (input) for losses during the first burn. The impulsive velocity-to-be-gained vector is computed. It is assumed that the first and second aim points lie on the parking orbit. Two complete flight plans are computed (rendezvous at both nodes) for each lift-off time, and the "better" of the two is chosen. (Following lift-off, only one flight plan is computed, corresponding to the "better" solution at lift off, except under special circumstances such as a major shift of the line of nodes or a new target ephemeris.)

During all non-thrusting mission phases after lift-off, the missile unit angular momentum vector is computed from:

$$\overline{1}_{HM} = \frac{\overline{1}_M \times \overline{V}_M}{\left| \overline{1}_M \times \overline{V}_M \right|} \tag{III-42}$$

The sine of the out-of-plane angle is computed from:

$$\sin OOP = \left| 1_{HT} \times 1_{HM} \right| \tag{III-43}$$

If this is less than the sine of 0.15 degree, the out of plane angle is set to zero and the target line of apsides is substituted as the line of nodes:

$$\overline{1}_{NODE} = \overline{1}_{\pi T}. \tag{III-44}$$

Otherwise, the nodal unit vector is set from:

$$\overline{1}_{NODE} = \frac{\overline{1}_{HT} \times \overline{1}_{HM}}{\left| \overline{1}_{HT} \times \overline{1}_{HM} \right|} \tag{III-45}$$

The position and velocity vectors in earth centered coordinates are computed while on the launch pad by the geometric relationship of the known latitude and longitude of the site on the rotating earth.

After lift-off the position and velocity determination (navigation) are computed by integration of accelerometer pulses derived from an inertial measuring unit.

3. Guidance and Navigation. Variable Point Guidance and Targeting includes navigation guidance and control subroutines to implement the flight plans generated by the targeting procedures. On the basis of inertial sensor inputs, the navigation subroutine continuously maintains the position and velocity of the vehicle over the oblate earth with respect to an inertial coordinate system. The guidance subroutines determine desired actions and convert these to steering commands and engine ignition and cut-off commands.

Guidance is conveniently discussed relative to the first burn, all later major burns included in the flight plan, and one or two minor burns. First burn guidance begins at lift-off, the latter being commanded by the launch director. After an initial rise and a roll to the azimuth determined by the flight plan, the vehicle begins an open-loop pitch program which steers the vehicle through the sensible atmosphere. Closed-loop guidance is initiated midway through the first burn. It operates to cause the vehicle to arrive at the next aim point (whose location may be fixed or variable) with the correct flight path angle. A velocity-to-be-gained vector is continuously computed as that which, if instantaneously achieved, would allow the vehicle to free-fall to the aim point on the specified trajectory. Steering drives two components of this velocity vector to zero. Cut-off is commanded when the third component passes through zero.

The essence of the guidance problem for the on-orbit burns is to convert from an impulsive flight plan to a finite-burn flight plan accomplishing the same results. Each on-orbit burn is handled in the same way. The start of the burn is timed so as to locate the centroid of the predicted acceleration-time profile at the time of the equivalent impulsive maneuver. That this is an element of a finite-burn trajectory optimally approximating an impulse is described in Reference 3. The attitude of the vehicle prior to the start of the burn directs the nominal thrust direction along the required ΔV vector. Once the burn is started, the guidance computes a velocity-to-be-gained as the difference between the required velocity (that which allows the vehicle to follow the current flight plan) and the actual velocity. Steering and cut-off are based on the velocity-to-be-gained vector exactly as in the first burn.

One minor burn, typically requiring no more than a few feet per second, is introduced between nodes to take up the accumulated inaccuracies from control tolerances or other perturbations. In a vehicle typical of the near future, a minor burn may be accomplished by other than the main engine, perhaps by the attitude control system in a translational mode. The guidance steering for this mode would be the same as that described above.

38

a. **Position and Velocity (Navigation) After Start of Inertial Mode.**

$$\frac{d^2\overline{R}}{dt^2} = \overline{g} + \frac{\overline{F}}{M}$$
<div align="right">Acceleration   (III-46)</div>

$$\frac{d\overline{R}}{dt} = \overline{V} = \overline{V}_0 + \int_0^t \frac{d^2\overline{R}}{dt^2} \, dt$$
<div align="right">Velocity   (III-47)</div>

$$\overline{R} = \overline{R}_0 + \int_0^t \overline{V} \, dt$$
<div align="right">Position   (III-48)</div>

where:

$$\overline{g} = \overline{I}_x \, g_x + \overline{I}_y \, g_y + \overline{I}_z \, g_z$$
<div align="right">Gravity Vector   (III-49)</div>

and

$$g_x = \zeta' \, \frac{GM}{R^3} \, x$$

$$g_y = \zeta' \, \frac{GM}{R^3} \, y$$

$$g_z = \left(\zeta' + 2\frac{J}{R^2} \right) \frac{GM}{R^3} \, z$$

<div align="right">Components of Gravity   (III-50)
(including first harmonic
oblateness effect)</div>

where:

$$\zeta' = 1 + \frac{J}{R^2} \left[1 - 5 \left(\frac{z}{R}\right)^2 \right]$$
<div align="right">(III-51)</div>

b. **Angular Momentum Vector of Target.**

$$\overline{I}_{HT} = \overline{I}_{RT} \times \overline{I}_{\theta T} = \frac{\overline{I}_{RT} \times \overline{I}_{VT}}{\left| \overline{I}_{RT} \times \overline{I}_{VT} \right|}$$
<div align="right">(III-52)</div>

c. **Aim Point One.** From launch site the node will be placed

$$\overline{1}_{NODE} = \frac{\overline{1}_{HT} \times \overline{1}_{RM}}{\left|\overline{1}_{RT} \times \overline{1}_{RM}\right|} \tag{III-53}$$

The radius vector of the first aim point is then:

$$\overline{R}_{a1} = R_{a1}\,\overline{1}_{NODE} \tag{III-54}$$

Angular momentum vector of guided vehicle on pad define:

$$\overline{1}_{HM} = \frac{\overline{1}_{RM} \times \overline{1}_{a1}}{\left|\overline{1}_{RM} \times \overline{1}_{a1}\right|} \quad \text{in orbit} \quad \overline{1}_{HM} = \frac{1_{RM} \times 1_{VM}}{\left|\overline{1}_{RM} \times \overline{1}_{VM}\right|} \tag{III-55}$$

d. **Launch Azimuth.** The launch azimuth is used to define the required roll maneuver. Range safety requirements may limit the allowable launch azimuth.

$$\tan A_Z = \frac{\overline{1}_{vg} \cdot \overline{1}_E}{\overline{1}_{vg} \cdot \overline{1}_N} \qquad 0° < A_Z < 360° \tag{III-56}$$

where:

$$\overline{1}_E = \frac{\overline{1}_R \times \overline{1}_Z}{\left|\overline{1}_R \times \overline{1}_Z\right|} \quad \text{(East vector)} \tag{III-57}$$

and

$$\overline{1}_N = \overline{1}_E \times \overline{1}_R \quad \text{(North vector)} \tag{III-58}$$

e. **Velocity to be Gained.** Having computed the initial position vector $\overline{R}_i$ and the radius vector of the final point R_j the sine and cosine of down range angle between these points is computed

$$C = \cos \Omega_{ij} = \overline{1}_{Ri} \cdot \overline{1}_{Rj} \tag{III-59}$$

$$S = \sin \Omega_{ij} = \left| \overline{1}_{Ri} \times \overline{1}_{Rj} \right| \tag{III-60}$$

$$\text{sign of s} = \text{sign of } (\overline{1}_i \times \overline{1}_j) \cdot \overline{1}_{HT}$$

$$\tan \gamma_i = \frac{s}{1 - c} \left(1 - \frac{R_i}{R_j} \right) - \frac{R_i}{R_j} \tan \gamma_j \tag{III-61}$$

$\tan \gamma_j$ is known by phase of mission in tangent transfer.

$$\frac{P_j}{R_j} = \frac{1 - C}{\dfrac{R_i}{R_i} - C - s \tan \gamma_j} \tag{III-62}$$

$$V_{req} \cos \gamma_{req} = \left(\frac{P}{R_m} \frac{GM}{R_m} \right)^{1/2} \tag{III-63}$$

$$V_{req} \sin \gamma_{req} = V_{req} \cos \gamma_{req} \tan \gamma_{req} \tag{III-64}$$

$$\overline{V}_{req} = \overline{1}_r V_{req} \sin \gamma_{req} + \overline{1}_\Theta V_{req} \cos \gamma_{req} \tag{III-65}$$

$$\overline{V}_g = \overline{V}_{req} - \overline{V} \tag{III-66}$$

f.   Steering During Thrust

$$\left[\overline{V}_g \right] \text{Steering} = \left[\text{ECI to Steering} \right] \left[\overline{V}_g \right] \text{ECI} \tag{III-67}$$

$$\omega_{Xbci} = \frac{K_2}{f_i} \left[V_{g \zeta i} - K_1 V_{g \zeta (i-1)} \right] \tag{III-68}$$

$$\omega_{Ybci} = 0$$

$$\omega_{Zbci} = \frac{K_2}{f_i} \left[V_{g \eta i} - K_1 V_{g \eta (i-1)} \right]$$

41

$$f_i = \frac{1}{\Delta t_i} \sqrt{(\Sigma \Delta V_X)_i^2 + (\Sigma \Delta V_Y)_i^2 + (\Sigma \Delta V_Z)_i^2} \qquad \text{(III-69)}$$

$$\left[\text{ECI To Steering}\right] = \begin{bmatrix} \overline{1}_\xi \\ \overline{1}_\eta \\ \overline{1}_\zeta \end{bmatrix} \qquad \text{(III-70)}$$

where:

$$\overline{1}_\zeta = \frac{\overline{V}_g}{V_g}$$

$$1_\eta = \frac{\overline{1}_\eta \times \overline{1}_{Rm}}{\overline{1}_\eta \times \overline{1}_{Rm}} \qquad \text{(III-71)}$$

$$1_\zeta = \overline{1}_\zeta \times \overline{1}_\zeta$$

g. __Reorientation Steering (During Coast).__

Line up vehicle nominal thrust axis (y_b) with $\overline{V}_g(t)$

$$\left[\overline{1}_{V_g}\right]^{ECI} = \frac{\overline{V}_g^{\,ECI}}{\left|\overline{V}_g\right|} \qquad \text{(III-72)}$$

$$\left[\overline{1}_{V_g}\right]^B = \left[\text{Platform to body}\right]\left[\text{ECI to platform}\right]\left[\overline{1}_{V_g}\right]^{ECI} \qquad \text{(III-73)}$$

42

is

$$\left(\overline{1}_{V_g}\right) yb \quad \text{positive?}$$

yes;

$$\omega_{xbci} = \frac{K_{xi}}{\Delta t_i} \; (\overline{1}_{Vg}) \, zb$$

$$\omega_{ybci} = 0 \qquad\qquad\qquad\qquad\qquad\qquad \text{(III-74)}$$

$$\omega_{zbci} = \frac{K_{zi}}{\Delta t_i} \; (\overline{1}_{Vg})$$
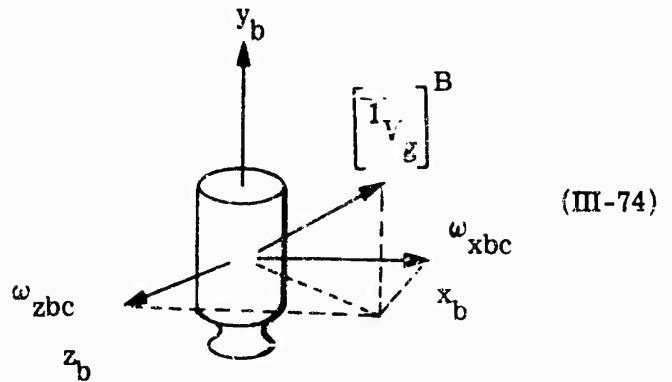
No, then is:

$$\left| (\overline{1}_{Vg}) \, xb \right| < \epsilon_{zi} \qquad\qquad\qquad\qquad\qquad\qquad \text{(III-75)}$$

and is

$$\left| (\overline{1}_{Vg}) \, zb \right| < \epsilon_{xi} \quad ? \qquad\qquad\qquad\qquad\qquad\qquad \text{(III-76)}$$

yes then:

$$\omega_{xbci} = \pm q \qquad\qquad\qquad\qquad\qquad\qquad \text{(III-77)}$$

$$\omega_{ybci} = 0$$

$$\omega_{zbci} = -K_{zi} \, \overline{(1}_{Vg}) \, xb \Big/ \Delta t_i$$

where:

the sign of q = sign of $(\overline{1}_{Vg})_{zb}$

No then repeat Equation (III-74)

43

h. Time to Start the Burn (Two Stages). The calculation of time to start the on-orbit burns cover the possibility that two stages will be required, because of the imminent fuel-depletion of one. The equations for this are based on a constant thrust, constant mass-flow rate vehicle. In the present version, once a burn is started, the requisite number of stages needed to complete the burn will be properly called for.

$$T = T_A - \frac{V_{gx}^2}{2AV_g'} \left[1 - \frac{1}{3} \frac{V_{gx}}{C'} + \frac{1}{12} \left(\frac{V_{gx}}{C'}\right)^2 - \frac{1}{60} \left(\frac{V_{gx}}{C'}\right)^3 \right] - t_{2.7} + \frac{S_1}{V_g} \quad \text{(III-78)}$$

Test for Fuel Remaining in Last Stage to Complete the Next Burn

$$\Delta V_{c3} = \text{Velocity Capability Remaining in Core 3}$$

(1) If Either Stage will Complete the Burn.

$$V_{gx} = |\overline{V}_g|$$

$$A = \text{Thrust to Mass Ratio of Stage} \qquad\qquad \text{(III-79)}$$

$$C' = \text{Exhaust Velocity of Stage}$$

$$t_{2.7} = 0$$

$$S_1 = 0$$

(2) If Both Stages Complete the Burn:

$$V_{gx} = |V_g| - \Delta V_{c3} \qquad\qquad \text{(III-80)}$$

$$t_{2.7} = \frac{C'_{c3}}{\dfrac{T_{c3}}{M_i - M_f}}$$

$$S_1 = \frac{C'^2_{c3}}{A_{c3}} \left[1 - \frac{W_{c30}}{W_{c3}} \left(1 + \frac{\Delta V_{c3}}{C'_{c3}}\right) \right]$$

44

i. __Time to Cut Off Engine.__ The time to cut off is based upon the component of $\overline{V}_g$ along the $\overline{1}_\xi$ steering axis. The other two components, $V_{g\zeta}$ and $V_{g\eta}$ are continually driven to zero by the pitch and yaw steering commands. As $V_{g\xi}$ diminishes, the time of zero crossing is predicted, taking into account the predicted tail off effects of the engine. A discrete is issued at the correct time.
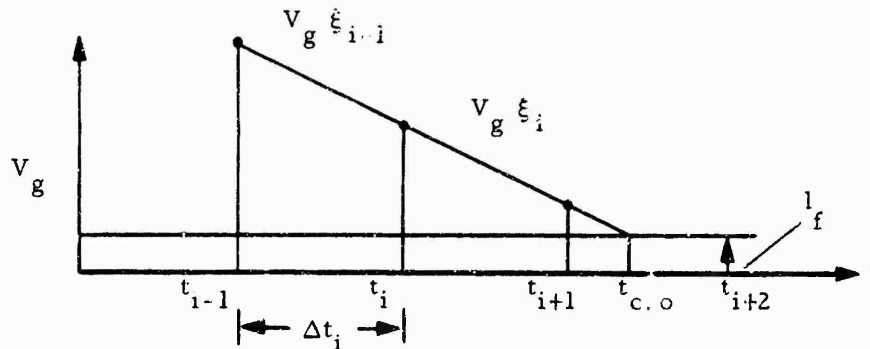
$$t_{c.o} = t_i + \frac{(V_{g\xi i} - I_f)\,\Delta t_i}{V_{g\xi (i-1)} - V_{g\xi i}}$$

$$f = 1, 2, 3....$$

where:

$$I_f = \frac{\text{ENGINE TAILOFF IMPULSE}}{\text{NOMINAL CUTOFF MASS}}$$

Is:

$$t_{co} \leq t_{(i+2)}?$$

Yes: Issue Cutoff Discrete at t_{co}

No: Exit

SECTION IV

RENDEZVOUS MISSION SIMULATION STUDIES

Task 4 of Contract AF04(695)-946 requires that several typical rendezvous missions be simulated and their results plotted and tabulated. Twelve simulation runs were made against the various targets specified by contract (Paragraphs 3.4.1 through 3.4.4) and the results obtained in these runs are shown and discussed in this section.

The particular targets specified were the following:

Target 41 (Paragraph 3.4.1) "A satellite in a circular orbit at an altitude of 150 nautical miles inclined 35 degrees".

Target 42 (Paragraph 3.4.2) "A satellite in a circular orbit at 1000 nautical miles inclined 49 degrees".

Target 43 (Paragraph 3.4.3) "A synchronous satellite in an orbit whose perigee is 500 nautical miles at an inclination of 65 degrees".

Target 44 (Paragraph 3.4.4) "A satellite in an elliptical polar orbit with a 200 nautical mile altitude of perigee and a 300 nautical mile altitude of apogee and 90 degree inclination".

The target definitions given above do not completely specify the rendezvous situation for these targets since no initial conditions are given. In order to make the runs required a set of initial conditions was selected for each target. An attempt was made to make this selection on a rational basis which will be discussed below with the results for each target.

1. General Discussions of Simulation and Cases Studied. Prior to making the simulation runs, extensive changes were made to the Variable Point Simulation Program to conform to Task 1 (Paragraph 3.1) of AF04(695)-946. These changes fall into the following four categories:

   a. Category 1 - Program Improvement and Cleanup. The effort performed in this category was primarily in reducing the number of subroutines required in the program. This was done by eliminating routines whose functions had been superseded and by consolidating functions of several routines. The number of subroutines (after all changes discussed below had been made) was changed from 96 to 78. During the cleanup process about 3000 words of required storage were eliminated. These savings were realized even after the addition of the routines necessary to generate a data tape for the SC4020 plot output.

47

Also, in this category, the simulation program was completely converted from Fortran II to Fortran IV. This change required more effort than simply examining the language of the program and making appropriate changes. The 7090 Fortran II system allows division by zero and square roots of negative numbers without a machine stop. The 7094 Fortran IV system does not. This led to a review of each routine during which major sections of routines were redesigned. Fortran IV options such as name list and data were also incorporated. Results obtained indicated that the conversion was successful.

b. Category 2 - Incorporation of Tangent-Tangent Transfers and Full Orbit Phasing. This change required a redesign of the targeting routines that existed at the initiation of the contract. The major subroutines resulting from this redesign were PLAN, which contains the targeting functions for the major part of the trajectory, and GAME which contains the logic to solve the time constraint for rendezvous using full orbit phasing. The changes made were essentially those described in Reference 9. No real problems were encountered in this phase of contract effort and no failures of the program in these subroutines have been encountered. The combination of PLAN and GAME performs the functions of generating complete rendezvous trajectories from the present location of the missile to an internally generated rendezvous point in the future. The output of these subroutines is an array of aim points on this trajectory through which the missile must fly. The data stored for each of these aim points include the position vectors, radii, velocities and flight path angles entering and leaving, the plane change to be executed and the time at which the missile must pass through each. This data fully defines the planned missile trajectory to rendezvous.

c. Category 3 - Further Refinement in Accuracy of Closure. The effort involved in this portion of Task 1 resulted in subroutine PLANCM which is described in Part 2, Volume I of this report. The solution chosen was essentially that described in Paragraph 4.1.2.2 of Reference 9.

Previously bi-elliptic transfers over a simulated oblate earth were used. The range and relative velocity conditions observed at the end of a mission were marginally acceptable. The resulting miss distance and velocity deviation was a result of the method used for generating the aim point parameters. Aim points were generated as vectors that were on the true target orbit accounting for oblateness effects. In contrast, the missile's flight path between aim points was predicted on a Keplerian basis over a spherical earth. The result was that during the coast time between aim points the missile was acted on by the simulated earth oblateness and consequently its real position deviated from the desired position (3.7 nmi in one case) from its predicted position as the rendezvous aim point was approached.

A two part solution was attempted for increasing the accuracy and performance in the closure mode or terminal phase of the mission. The first part of the solution was very effective while the second appeared to cause difficulty in the terminal phase of the simulation runs against Target 43, the highly elliptical synchronous target, though it was effective against the other three lower targets.

The first portion of the solution consisted of changing the method by which aim points are generated. The change from the method described above was to predict future positions of both vehicles consistently (eliminated using ephemeris oblateness terms in computing future target positions). The present position is continuously computed by the corrected navigation equations but the future positions are computed by a more simple means.

The updated orbital parameters are projected ahead with Keplerian-spherical earth equations to determine the position of the node between the two orbit planes and the conditions with which the target will arrive at the nodal points. The justifying assumption for this change is that the orbits of the target and missile become very close as both approach the rendezvous point where each will be equally affected by earth oblateness. Thus, the rendezvous point is predicted by projecting the orbits of both the target and missile without considering oblateness effects in the projection process. The actual intercept aim point may drift slightly from the predicted rendezvous point, but since the target and missile are affected in a nearly identical manner by earth oblateness, they will both arrive at the drifted point at the same time. At that time the error in predicting future aim points will approach zero, since after adaptation at the rendezvous point the missile and target orbits are nearly identical.

The second part of the solution was to use a variation of the Phase A bi-elliptic phasing scheme (see Reference 9) as a "closure guidance" mode. In closure guidance, which is entered as the missile approaches the last half orbit of the phasing trajectory, a new set of aim points is set up for vernier adjustments to the trajectory. These aim points are located at the rendezvous point (aim point no. 5) and 22.5, 45, 90 and 180 degrees uprange from the rendezvous point (aim point numbers 4 through 1, respectively). This new set of aim points is then used to guide the missile through the last stages of the trajectory. As the missile approaches each of the first, second or third aim points the altitude of the aim point halfway between the missile and the rendezvous point is adjusted to solve the time constraint for rendezvous. The missile then executes the upcoming burn aiming for the adjusted aim point.

The object of this scheme is to further improve the accuracy of arrival of the missile at the rendezvous point. Any differential oblateness errors that may filter through the early phases of the mission are successively attenuated by the shorter downrange angles used in trajectory prediction.

The two methods for reducing the errors in rendezvous due to oblateness have worked quite well in all cases except the highly elliptical synchronous target. As an example for comparison a table of results of runs made with the same set of initial conditions against Target 42 is included as Table V to show the improvement in rendezvous conditions achieved. The first two runs shown in this table are taken from data shown in Reference 9. The first is made without simulation of earth oblateness while both of the others have oblateness effects included; the deviations in range and relative velocity from the spherical case are shown in parenthesis. In this example the changes described above have cut the deviation in relative velocity by 50 percent and practically eliminated the deviation in range.

In the case of the highly elliptical synchronous target orbit, termination or rendezvous was not achieved in making the simulation runs when using oblateness effects. The principle symptoms encountered were failures in the closure mode targeting section when it is first used about 180 degrees from the planned rendezvous point. These failures were of two general types. The first type was a program stop due to the computation of a "negative semi-major axis", an indication that a hyperbolic trajectory is required by the missile to satisfy the rendezvous time constraint. No capability for flight time computation in the hyperbolic range has been built into the program, therefore this stop has been set up for debugging purposes. The second type of stop encountered was the "NOGO, rendezvous not achieved within fuel budget". This stop is actuated when the predicted ΔV to finish the mission has exceeded the ΔV remaining. Since all liftoffs were made with a ΔV margin over and above the computed ΔV required, the error stop indicated that some major change had taken place. The diagnosis of these error stops is discussed more fully in Paragraph 4.

Table V. Comparison of Runs Against Target 42 (Lift-Off at 8.33 hrs)

	Flight Time	Total ΔV	Range at Rendezvous Burn Completion (nmi)	Relative Velocity at Rendezvous Completion (ft/sec)
Phase A* Spherical Earth	4.432	33,005	1.01	5.65
Phase A* Oblate Earth	4.418	33,927	4.71 (+4.70)	16.98 (+11.33)
Run No. 101	5.416	33,320	1.26 (+0.24)	11.62 (+5.36)

*Run Under Contract AF04(695)-633

d. Category 4 - Use of Reference Velocity Vectors for Reorientation During Coast Periods. This change in the method of orienting the vehicle for upcoming burns is contained almost completely in subroutine GUIDON described in Part 2 of the volume.

Prior to this contract reorientation for on-orbit burns was begun at the time the vehicle approached a specific time increment, 225 seconds, prior to the upcoming aim point time. As an example as the vehicle approached the nth aim point, whose computed time of arrival was 1200 seconds, computation of the velocity-to-be-gained vector ($\overline{V}_g$) would begin at 975 seconds. $\overline{V}_g$ would be based upon a trajectory from the missile position at that time, 975 seconds, to the next aim point downrange, $n + 1$. The vector components of $\overline{V}_g$ would then be processed and attitude rate commands computed and issued to align the vehicle for the upcoming burn. This scheme was effective in almost all cases. In cases where very long on-orbit burns were encountered, the vehicle could not reorient quickly enough to a proper attitude prior to the start of the burn.

The approach used was to begin the computation of a $\overline{V}_g$ vector for the next burn immediately after completion of the previous burn. The parameters of missile arrival at the next aim point are computed and compared with the stored parameters leaving that aim point (velocity, flight path angle and plane change) to compute an "impulsive" $\overline{V}_g$ vector. This $\overline{V}_g$ is then used for reorientation during coast. The calculation is repeated every 100 seconds during coast periods (see subroutine CONTROL) to update the $\overline{V}_g$ vector whose magnitude is also used to compute the time to start the next burn. As the time to start the burn is approached the calculation reverts to the previous method of computing $\overline{V}_g$ and vernier corrections to attitude are commanded. Using the example above, a typical sequence would be to compute an impulsive $\overline{V}_g$ and time to start a burn at 800 seconds. These values would be updated at 900, 1000 and 1100 seconds reissuing attitude commands at each computation. For a burn starting at 1150 seconds, switchover would occur at 1120 seconds to the previous method of $\overline{V}_g$ computation.

2. Launch Trade-Off Charts. Prior to running the full simulation program in most cases, a "launch trade-offs" analysis is usually made to determine the parameters of the rendezvous situation. Program PHIBOP, an impulse program which incorporates the essential ideas of the flight planning part of Variable Point Guidance and Targeting is particularly suited to this purpose. The inputs to this program are target ephemeris, launch site location and time period to be investigated. The program computes various parameters of the rendezvous situation such as total ΔV, flight time, out-of-plane angle and launch azimuth as a function of lift-off time relative to some epoch clock time. From these parameters lift-off times of interest may be chosen and the full Variable Point Guidance and Targeting simulation program used at these lift-off times to obtain complete information. Program PHIBOP was modified prior to this contract to be consistent with the inputs for program SCPLOT, the SC4020 plotting program described in Section IV of Part 2, Volume I. The output data of interest from PHIBOP was plotted and used in many cases to select lift-off times. Other data useful as input to the simulation program is also obtainable from these plots, i.e., from flight time output a maximum simulated flight time (TFINAL) may be selected.

3. Guided Multi-Stage Vehicle and Environmental Simulation Results. Paragraphs a. through d. discuss the initial conditions used for the various ephemerides and compare results with previous results where available. A tabular summary of results obtained in the twelve contractually required demonstration runs is included as Table IV. All runs, except those for the synchronous ellipse, were made with earth oblateness simulated. These results will be discussed in the following sections.

Table VI. Variable Point Guidance and Targeting Demonstration Run Results

Target No.		Angle out-of Plane	Lift-Off Time (hrs)	Run No.	Total ΔV (ft/sec)	Flight Time (hrs)	Range (nmi)	Wt. In Orbit (lbs)	Relative Velocity (ft/sec)	Flight Time to 100 nmi Range (hrs)	WADC Output Tape No.	Relative Velocity Prior to Final Burn (ft/sec)
41	150 nmi Circular 35 degrees	6.13	3.0	131	38,411	2.763	3.72	8,617.7	13.98	2.627	2630	1319.4
		6.0	3.15	132	33,011	4.83	3.63	21,000	12.76	3.402	2640	452.3
		1.2	4.7	133	30,530	3.833	3.77	27,000	12.54	2.557	2641	113.1
42	1000 nmi Circular 49 degrees	0.2	8.25	101	33,320	5.416	1.40	20,600	0.84	5.125	2627	632.5
		18.8	3.0	102	39,264	9.060	1.71	8,000	8.60	8.224	2628	23.8
		2.90	0.33	109	32,942	7.998	1.74	21,180.7	4.90	7.382	2626	486.7
43	Synchronous* Ellipse at 65 degrees 500 nmi Perigee	19.73	1.50	121	43,572	46.71	0.01	5,165.6	0.22	45.07	2634	42.7
		15.00	1.00	122	42,463	46.97	0.78	5900.	11.48	44.28	2629	171.8
		8.00	0.33	123	41,533	47.82	1.17	6500.	4.62	45.38	2639	93.1
44	Polar Ellipse 200-300 nmi	5.70	2.2	111	33,742	3.526	1.80	19,000	6.48	2.883	2620	189.4
		23.83	0.7	112	41,118	5.044	2.00	6,588.3	4.92	4.976	2642	553.7
		14.04	3.8	113	38,785	5.055	1.15	8,314.5	5.53	4.951	2643	179.3

*Spherical Earth Simulation – All Others are Oblate Earth Results

52

In all of these runs a parking orbit altitude of 100 nmi was specified. Therefore, in each case, the simulated vehicle flew to a first aim point at 100 nmi altitude, 90 degrees down range from the launch point. The following group of plots, Figure 10 through 16, represent a time history of the first burn of a simulated Titan IIIC launch vehicle. The particular mission flown was a rendezvous mission against Target 42; this run, number 100, was later repeated with oblateness to become run number 109. The launch azimuth involved was 48.8 degrees. The parameters plotted as functions of time include:

1.) Altitude
2.) Velocity
3.) Mach number
4.) Dynamic pressure
5.) Body rate commands in radians/second
6.) Alpha - angle of attack of pitch
7.) Beta - angle of attack in yaw.

Mach number, dynamic pressure, alpha and beta are set to zero after core 2 cut-off when the atmospheric calculations are discontinued. The plot of body rate commands (Figure 14) shows various phases of the first burn very clearly. This plot is a 3 ordinate plot in which the star (*) represents pitch commands and the cross (X) roll commands. Lift-off occurs at 8 seconds. The yaw command (represented by a straight line) and roll commands are both zero throughout the mission except between 10 and 16 seconds where the roll program is invoked. The commands for the pitch program can be seen between 8 and 120 seconds and the new pitch command sequence can be seen starting as each new core is initiated. One yaw command was issued at 486 seconds, probably to provide a yaw vernier as the transtage was started.

The dynamic pressure and angle of attack were found to be well within maximum safe values for the Titan IIIC specified in Paragraph 3.5.1 of Reference 10.

a. Target in Circular Orbit at 150 nmi, i = 35 degrees. The initial conditions selected for this target were based on the hypothetical case of a satellite launched from AMR into a 35 degree inclination orbit. The emphemeris is written so that at time zero the satellite is about 20 degrees downrange from its launch point. The ephemeris inputs computed for this situation are:

$$M = 68.3 \qquad \dot{M} = +5759.9488$$
$$\Omega = 53.36 \qquad \dot{\Omega} = -7.0281238$$
$$\omega = 0.0 \qquad \dot{\omega} = +10.115821$$
$$i = 35°$$
$$e = 0.0$$
$$a = 1.0435548$$

The first derivative terms are computed from Appendix IV of Part 2 of this volume. The hypothetical interceptor vehicle is based at AMR and the rendezvous situation is to be investigated through a 10 hour period.

Program PHIBOP was run using this data and used to generate the six plots shown in Figure 17 through 22. Each of these shows a time history of one item of interest as a function of rendezvous time throughout the 10 hour period. As an example, a lift-off at 1.0 hours would result in a flight time of 7.6 hours (Figure 17) a total ΔV of 32,200 FPS (Figure 18), an out-of-plane angle of 4.5 degrees (Figure 19) and a launch azimuth of

77 degrees (Figure 20). Figure 21 displays one of the intermediate quantities used in the calculation, the ΔV required for the rendezvous aim point burn. This quantity is equivalent to the relative velocity between the missile and target satellite prior to the rendezvous burn (terminal maneuver). Figure 22 displays another of the intermediate quantities used showing the period of the phasing orbit in hours. This value is about 1.5 hours. The comparatively brief periods when the plot flattens out below this value indicates the times when the missile may launch and stay completely below the target orbit altitude up to the rendezvous point.

Three simulation runs (131, 132, 133) were made against this target. The summary results are shown in Table VI. The range and relative velocity figures shown at the end of the rendezvous burn are about the worst shown for any of the four targets averaging about 3.7 nmi and 13 ft/sec. All of these runs were continued beyond the nominal rendezvous point to determine if the range and relative velocity errors would improve. The range and relative velocity results of a half orbit after the nominal rendezvous burn are shown in Table VII with reductions in errors shown for comparison. Range error is not improved significantly but relative velocity error is cut an average of 25 percent for the three runs by the extra pass through the closure mode guidance scheme. Further extra passes did not reduce the error beyond this value indicating that a steady state condition had been reached. It is suspected that input ephemeris inconsistencies may account for some portion of the range and relative velocity errors as well as affecting the closure guidance scheme itself.

b. Target in Circular Orbit at 1000 nmi, Inclined 49 Degrees. This target had been used as a demonstration case in two previous Variable Point Guidance and Targeting contracts. Initial conditions used were the same as these used in the previous Variable Point Guidance and Targeting final reports (References 9 and 11). At time zero the target is placed at its ascending node and the target plane passes through the launch site (OOP = 0) at Cape Kennedy. A PHIBOP run was made for this situation over a 10 hour period and the results are shown in Figure 23 through 28. These plots are read in the same manner as those of Figure 7 through 22.

$$M = 0.0 \qquad \dot{M} = 4186.5437 \, °/day$$
$$\Omega = -28.145330 \qquad \dot{\Omega} = 2.6776274 \, °/day$$
$$\omega = 0 \qquad \dot{\omega} = 2.3510173 \, °/day$$
$$i = 49°$$
$$\nu = 0$$
$$a = 1.2903656$$

Three simulation runs were made to fulfill the demonstration requirements of the contract. The results of these runs are shown in Table VI. All runs were made with earth oblateness simulated. The runs were made with closure criteria settings (range = 15,000 feet and relative velocity = 15 ft/second) that caused the program to stop at the end of the nominal rendezvous burn. Two cases are available from Reference 9 for comparison with runs made on this target. The first of these has been previously shown in Paragraph 1 to illustrate improvement in accuracy of closure. It should also be noted from Table V that the total ΔV required for this mission has been reduced by 600 feet per second by incorporation of the tangent-tangent transfer scheme.

The second comparison case available can be made with runs that did simulate oblate earth conditions. Run No. 100 (109 without oblateness) is directly comparable to the run shown in Table VI, Reference 9. Various parameters from these runs are shown in Table VIII

Table VII. Improvement in Rendezvous Conditions

Run No.	Nominal Range (nmi)	Rendezvous Relative Velocity (fps)	1/2 Orbit After Nominal Rendezvous		Improvement	
			Range (nmi)	Relative Velocity (fps)	Range (nmi)	Relative Velocity (fps)
131	3.72	13.98	3.62	9.81	0.10	4.17
132	3.63	12.76	3.63	9.90	0.00	2.86
133	3.77	12.54	3.55	9.13	0.22	3.41

Table VIII. Comparison of Spherical Earth Runs

Target 42, Lift off at 0.33 hours

	Flight Time (hrs)	Total ΔV (fps)	Range at Rendezvous (nmi)	Relative Velocity at Rendezvous (fps)
Phase B (Run 100)	7.66	32,924	0.07	0.85
Phase A	1.46	33,972	0.78	5.78

which shows an improvement of over 1000 feet per second in total ΔV for the mission at a cost of 6.2 hours of flight time. These results were better than those expected at the writing of Reference 9 and the initiation of this contract.

Run 100 was also used to generate several samples of SC4020 plots of the type required. These are included as Figure 29 through 32 and show time histories of range, relative velocity, range rate and line of sight from the time range goes through 100 nmi until rendezvous. The slight step functions in the relative velocity range rate time histories at 26,610 and 27,075 seconds represent the midcourse correction burns at closure mode aim points Number 3 and 4. The ramp between 27,535 and 27,565 shows the relative velocity being driven toward zero by the rendezvous burn of transtage.

c. Target in Elliptical Syn Chronous (24 Hour) Orbit Inclined 65 Degrees With Specified Altitude of Perigee. The initial conditions selected for this target were based on the hypothetical case of a satellite launched northerly from Tyura-Tam (45.6 degrees N Latitude, 63.2 degrees E Longitude) into an elliptical orbit with its perigee about 12 degrees downrange from the launch site. Using an earth rotation rate of 0.72921155 radians per second, or 360.98562 degrees per day, results in a semi-major axis of 6.6107069 earth radii. Using the perigee altitude of 500 nmi results in an eccentricity of 0.82676697 (and an apogee altitude of over 38,000 nmi). The other inputs were selected so that the target was at perigee and the ascending node at 20 degrees west of the launch site.

$$M = 0.0 \qquad\qquad \dot{M} = 360.96863 \text{ °/day}$$
$$\Omega = -20.0 \qquad\quad \dot{\Omega} = -0.055031037 \text{ °/day}$$
$$\omega = 0.0 \qquad\qquad \dot{\omega} = -0.0069644605 \text{ °/day}$$
$$i = 65.0$$
$$e = .82676697$$
$$a = 6.6107070$$

These inputs were used to run program PHIBOP and to generate the plots included as Figure 33 through 36.

Figures 35 and 36 show an interesting situation that is troublesome in terms of launch geometry. At the time that the launch azimuth is within the normal AMR boundaries 44 degrees to 110 degrees (from Reference 12) the out-of-plane angle is high (over 22 degrees); this is caused simply by the 65 degrees inclination of the target plane and results in high ΔV requirements for rendezvous in this lift-off time period. Figure 34 shows that the shortest flight times are also within this range of lift-off times.

Three simulation runs were made against this target using a spherical earth simulation. The results of these are shown as runs 121, 122 and 123 of Table VI. An illustration of the relative positions of the rendezvous points is shown as Figure 39.

Several unsuccessful attempts were made to complete these runs using the oblate earth effects of the simulation program. In each case program stops were encountered during the last 180 degrees of the mission. These stops are built into the simulation program to avoid unrealizable and undesirable situations. The two messages encountered were "Nogo, Rendezvous Not Achieved With Fuel Budget" and "Semi-Major Axis Negative"; these are explained below.

Since no provision has been built into Variable Point Guidance and Targeting for computing flight times for parabolic and hyperbolic conic segments an error stop has been built in to terminate the program whenever such a segment is encountered. Up to this time the Variable Point Guidance and Targeting Program had not been required to rendezvous with a target of this type, and no acceptable flight plans used had involved hyperbolic or parabolic flight plan segments. Since such segments require high ∆V injections and "de-injections" it is doubtful that they would be desirable in earth satellite rendezvous missions. In addition this particular stop has indicated that the flight plan sensitivity to deviation is too high.

The fuel budget stop is included to indicate that the predicted ∆V to finish the mission has exceeded the ∆V capability remaining in the interceptor vehicle at that time. The maximum fuel budget for the simulated rendezvous mission is an input to the Variable Point Guidance and Targeting Program. The ∆V required for the rendezvous mission is reasonably well known from program PHIBOP. The fuel budget is usually set slightly above that amount. When the fuel budget error stop is printed out, it generally indicates that a major change has occurred in the flight plan.

Investigation of the stops that occurred during attempts at making oblate earth runs indicated a problem in the design of the closure mode guidance technique for targets of this severe eccentricity. The results of these investigations and probable reasons for inadequate terminal mode targeting are discussed fully in Paragraph 4.

   d. Target in Elliptical Polar Orbit With Altitude of Perigee of 200 Nautical Miles
      and Altitude of Apogee of 300 Nautical Miles. The initial conditions selected for
this target were such that the perigee was at the equator and the target was at perigee. Figure 39 illustrates the initial geometric relationship between the target and the launch site. A six hour time scan was set up for PHIBOP with the ascending node placed such that a series of southerly launches would be obtained from the flight plan generator. The input ephemeris is as follows:

$$M = 0 \text{ degrees} \qquad \dot{M} = 5522.5555 \text{ °/day}$$
$$\Omega = 220 \text{ degrees} \qquad \dot{\Omega} = 0.0$$
$$\omega = 0 \text{ degrees} \qquad \dot{\omega} = 3.900739$$
$$i = 90 \text{ degrees}$$
$$e = 0.01353572$$
$$a = 1.0725914 \text{ earth radii}$$

The plots resulting from this PHIBOP run are shown in Figure 41 through 45. Three lift-off times were selected for simulation and the results obtained are listed in Table VI under run numbers 111, 112 and 113.

The launch site used in these runs was PMR (34.8 degrees N. Latitude). The only change required to the simulation program for this launch site was to change the launch azimuth computation. The computation was changed to quadrant azimuth from 0 degrees to 360 degrees rather than from -180 degrees to +180 degrees. The change was made to insure that the launch vehicle would roll in the shortest direction during the vertical rise "roll to azimuth" maneuver. This change will not affect simulation of AMR launches.

This target was also used to generate the terminal phase plots shown in the following section.

57

4. Terminal Conditions. The following grouping of SC4020 plots, Figures 41 through 59 are included to show compliance to Paragraphs 3.1.4 and 3.2 of contract AF04(695)-946. The plots were made using program SCPLOT with the output tape of run 111.

The plots cover the time span in the flight during which relative range between the vehicle and target was less than 100 nmi. Table IX is a tabular representation of the major events that occurred within that time span for run 111.

In run 111 Figures 33 through 37 are plots of the time histories of the various position and velocity vectors of the target and chase vehicle as well as the relative position (range) and relative velocity between them. Since the simulation program operates with different integration time intervals in coast periods (10 seconds) and burn periods (2 seconds) the times when the burns are occurring are readily recognizable from these plots by the point grouping.

Figure 38 shows the body rate reorientation commands being issued to the chase vehicle. The comparatively large "humps" in pitch and yaw occurring after each burn illustrate the missile's reorientation to the reference velocity vector for the next burn. This effect is also apparent in a plot of range vector in body coordinates included as Figure 54.

Range rate time history is shown in Figure 55.

The next two plots 56 and 57 show the relative angular position of the missile in target centered coordinates. The center axis for this coordinate system is the target forward horizontal direction. As an example at 11,400 seconds the missile is 55 degrees to the right and 45 degrees below the target forward direction.

re 58 is a multiple plot of line of sight rate and its horizontal and vertical components. magnitude and vertical component appear equivalent while the horizontal component is very near zero. Note that each burn drives line of sight rate down significantly and that the final burn drives it from its maximum value of about 2 degrees per second to zero.

Figure 59 is an example of one of the many cross plot combinations available using SCPLOT with the Variable Point Guidance and Targeting simulation program output. A listing of the 68 quantities available for plotting is shown in Table III of Appendix IV, Part 2.

5. Oblateness Effects. During the two previous contracts in which Variable Point Guidance and Targeting was developed, little emphasis was placed on making simulation runs with earth oblateness effects. The few runs that were made demonstrated that the simulation worked correctly and showed range and relative velocity errors at rendezvous that were greater than those encountered in spherical earth runs but were considered as marginally acceptable. A more thorough look at the effects of oblateness on Variable Point Guidance and Targeting was initiated to improve the overall accuracy. In addition the requirement for full orbit phasing introduced longer nominal coast periods between burns and this would tend to increase the miss distance. All runs shown in Table VI were attempted with earth oblateness in effect. Not all of these runs were successful in the terminal phase. Because of the effect of earth oblateness in combinations with the high eccentricity and period of target 43 the oblate earth runs against this target did not terminate due to the high velocity requirement generated by the closure mode guidance and were rerun using a spherical earth model. The error stops encountered were discussed in more detail in Paragraph 1 and 2.c and the conditions under which they occurred are described below.

58

A typical situation for the type of failures encountered was the first entry into closure mode guidance PLANCM. This was evidenced by approximately five unsuccessful attempts to terminate "oblate earth" rendezvous missions against the synchronous elliptical target orbit.

Since Target 43 has such a large period, phasing orbits within it will also have large periods leading to long coast periods between aim points. During these long coast periods the orbits tend to drift slightly with respect to each other in space. The high eccentricity of Target 43 compounds the effect of drift by introducing a secondary effect. As the orbit planes move relative to each other, the nodal intersection line moves along the orbits in a toggle-type motion. Because the nodal intersection is at a point on the target orbit different than that originally designated for rendezvous the radius, velocity and flight path angle are also changing. PLANCM attempts to fit a new trajectory through the aim points which it has set up. This trajectory, which solves for rendezvous under the new nodal conditions, includes an aim point at an adjusted altitude to form a two segment flight plan rather than the single segment flight plan. The use of a large constrained flight path angle at rendezvous tends to result in a two segment flight plan that is different enough in shape from the original phasing orbit to require excessive velocity change. This difference in shape always results in a total ΔV larger than that originally planned; the added ΔV was large enough to cause activation of the fuel budget error stop. When the shape change was more pronounced it indicated that an hyperbolic type trajectory was required activating the semi-major axis error stop.

Table IX. Final Phase of Run 111

Time (sec)	Range (nmi)	Event
10,379.5	100	Range less than 100 nmi
11,249.5	34.4	Start transtage (16,000 lb thrust) for midcourse correction at closure mode aim point 2 (90 degrees to go)
11,259.2	33.8	Cut-off (ΔV was 244.1 fps)
11,966.3	17.1	Start transtage for midcourse correction at closure mode aim point 3 (45 degrees to go)
11,968.2	17.1	Cut-off (ΔV was 45.4 fps)
12,326.2	12.1	Start transtage for midcourse correction at closure mode aim point 4 (22.5 degrees to go)
12,329.5	12.1	Cut-off (ΔV was 102.3 fps)
12,685.5	1.90	Start transtage for rendezvous burn (thrust = 16,000 lbs, total weight = 19,941)
12,692.7	1.80	Cut-off (ΔV was 211.9 fps)

59

The situations encountered show a high sensitivity in the closure mode to condition changes produced by oblateness in rendezvous runs against Target 43. This high sensitivity is considered a fault in the engineering design of the closure mode PLANCM. A recommendation for the improvement of PLANCM is included in the following section.

An investigation was made to determine whether or not the methods of computing the absolute locations of the target satellite and chase vehicle were compatible. In the simulation program, the chase vehicle position and velocity are determined by integration of the equations of motion. The target position and velocity are found by a Taylor series expansion of the input target ephemeris in UPDATE and mathematical conversion of that ephemeris in GEOM to the required vectors and orbital parameters. The two methods were compared and a more exact and consistent procedure for generating oblate earth first derivative terms was derived. The refined ephemeris terms resulting from using this procedure with Target 43 were used as input to the simulation. The results of these runs on the synchronous ellipse gave further indication that the closure mode requires further improvement or at least a simple back up mode in order to assure that any general rendezvous mission will be successfully and reliably completed.

6. Conclusions Derived from Simulation Results. The results included in Section 4 show the present version of Variable Point Guidance and Targeting to be more effective, efficient and flexible than the version that existed at the completion of the previous contract, AF04(695)-633. The improvements made to Variable Point Guidance and Targeting were in the areas of fuel efficiency (evidenced by lower ΔV requirements), lower computer storage requirements and better closure conditions.

The twelve simulation runs required by contract AF04(695)-946, Paragraph 3.4, have been successfully completed and demonstrate the effectiveness of Variable Point Guidance against a variety of targets. Limitations to the present design of the terminal mode (last half orbit) guidance laws were discovered in the case of extremely eccentric targets.

Several solutions to the limitations encountered are possible. A simple solution is to continue with the prior working plan until sensor lock-on occurs. From here better data is available for the closure mode. The use of the two point explicit guidance solution for the closure burns where trajectory shaping by flight path angle iteration would be employed to solve the time constraint for rendezvous is another possibly better way to terminate the mission. Revising the equations for such a scheme to include valid hyperbolic trajectory solutions would extend the capability of Variable Point Guidance and Targeting to more effectively rendezvous with targets of extreme eccentricity. Another alternative would be to return to the primary targeting mode and updating the flight plan by slipping the rendezvous point further downrange until sensor lock-on occurs.
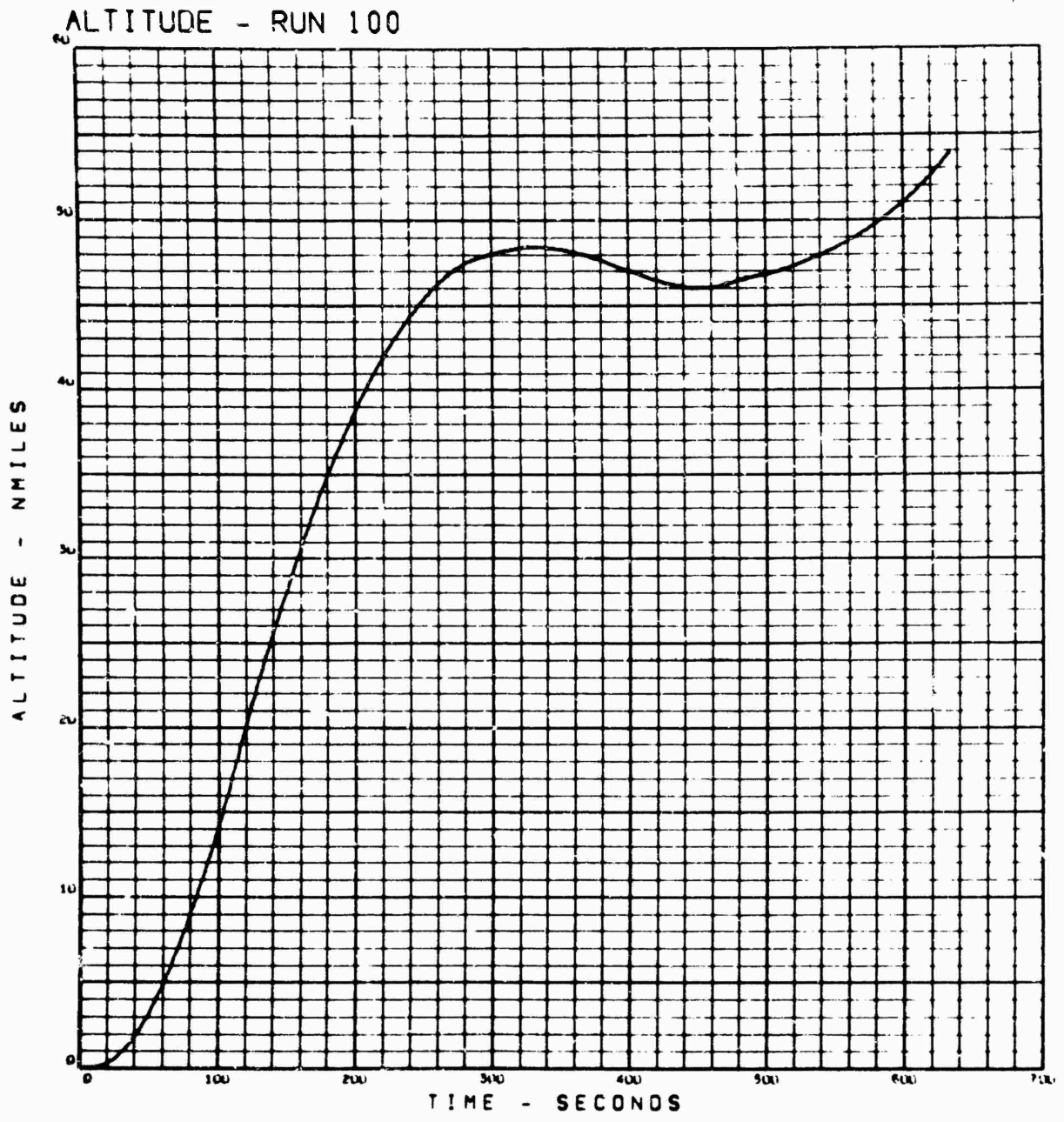
Figure 10. Altitude During First Burn as a Function of Time

61
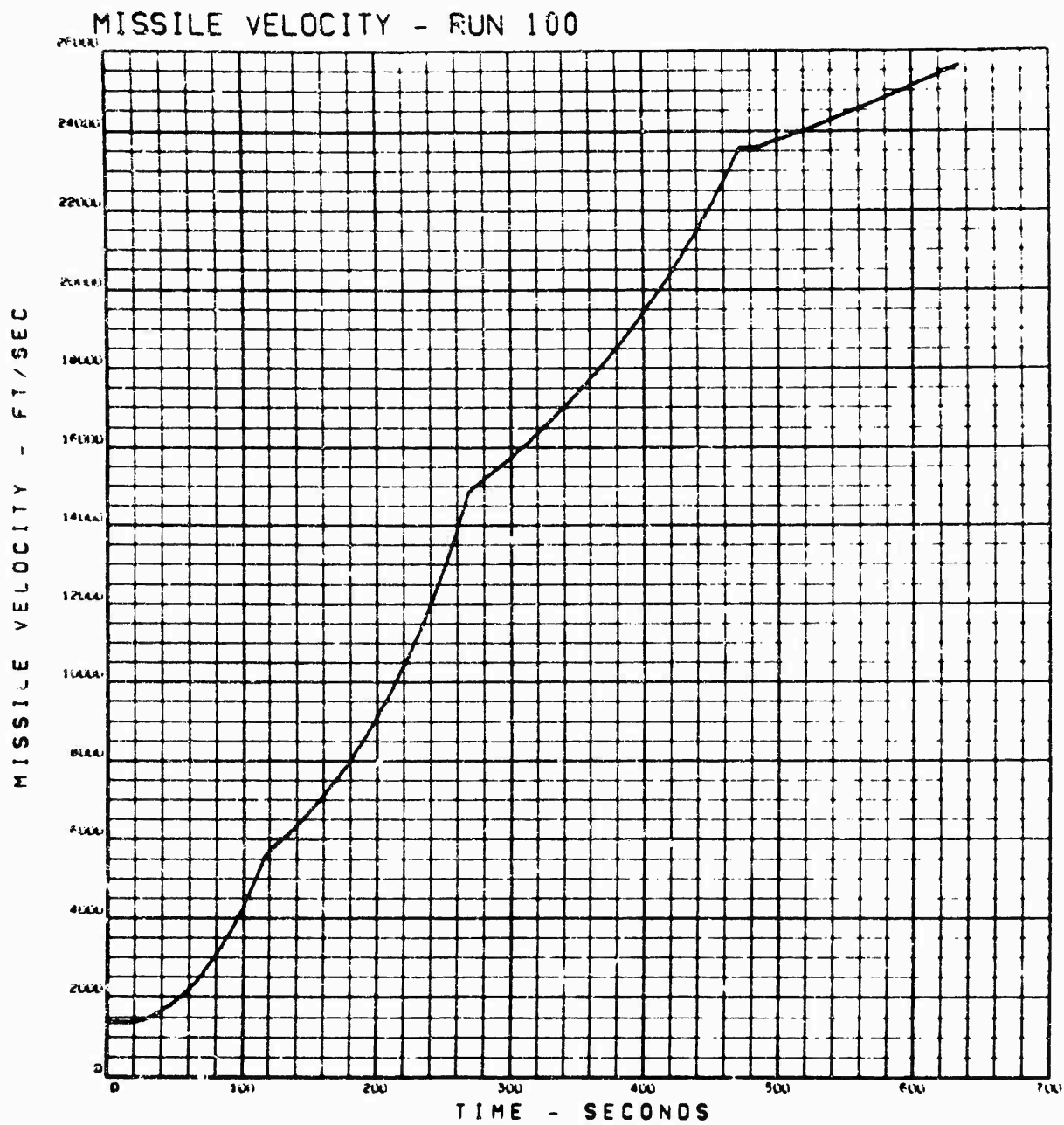
Figure 11. Velocity During First Burn as a Function of Time

62
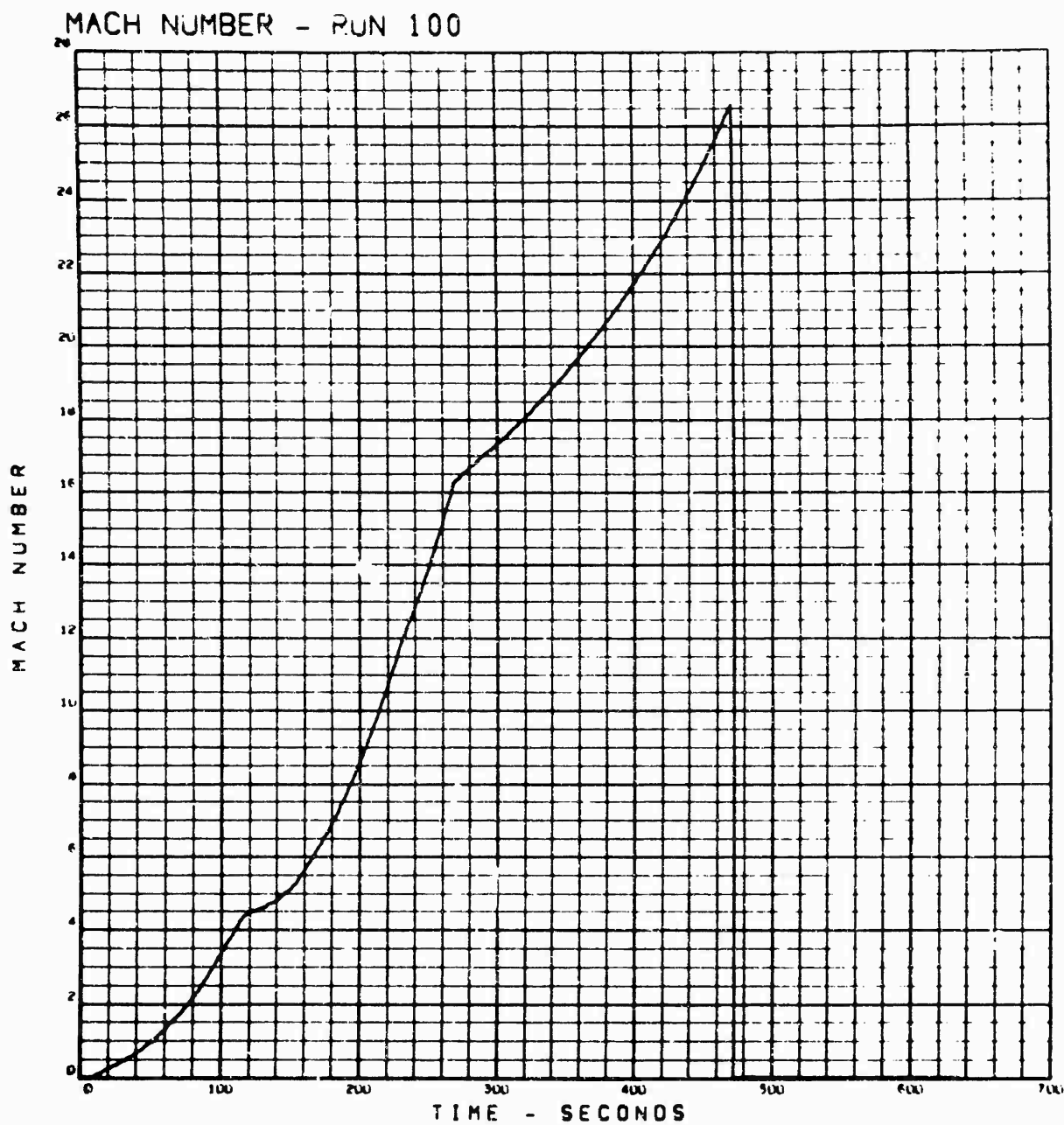
Figure 12. Mach Number as a Function of Time
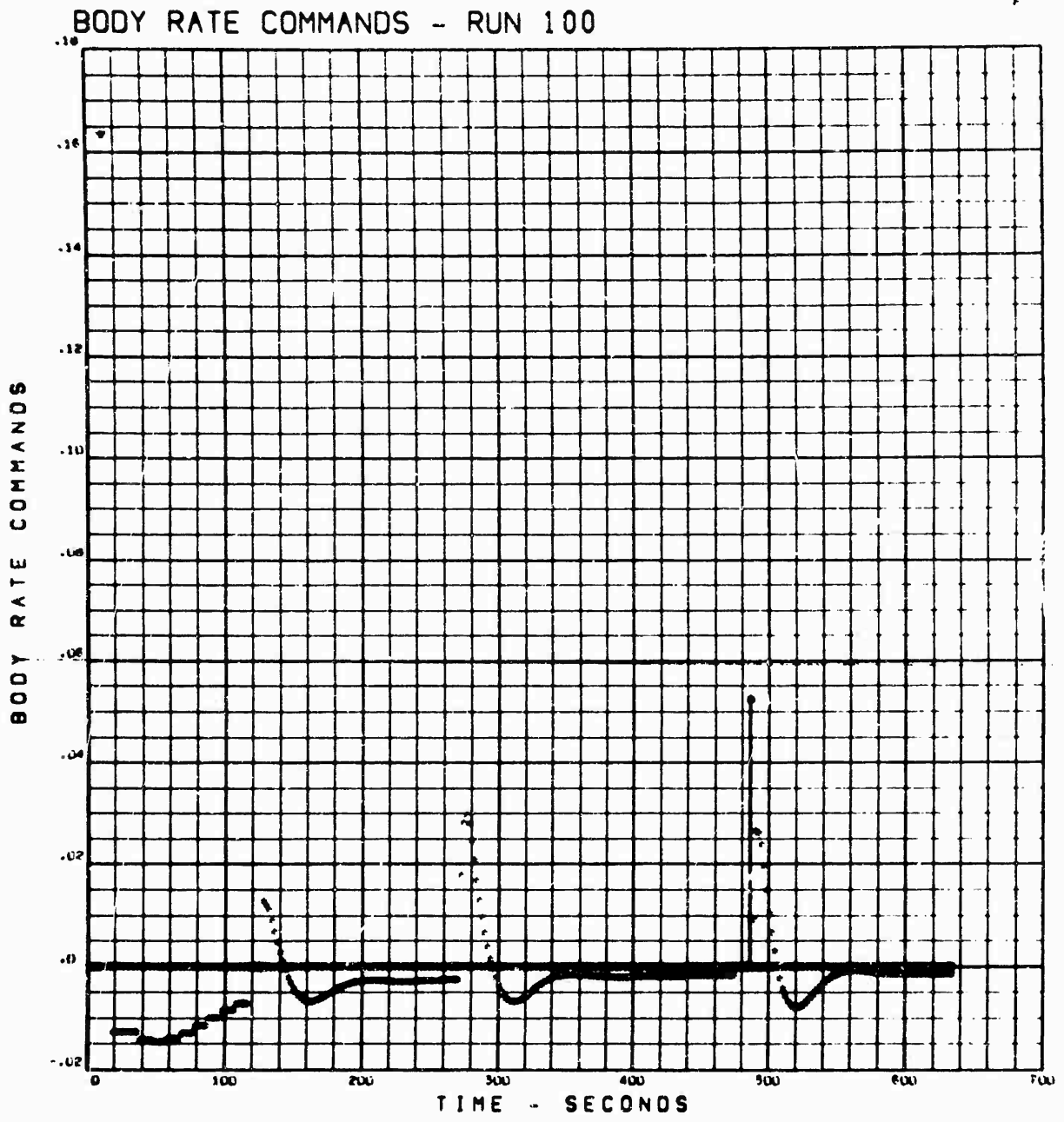
63
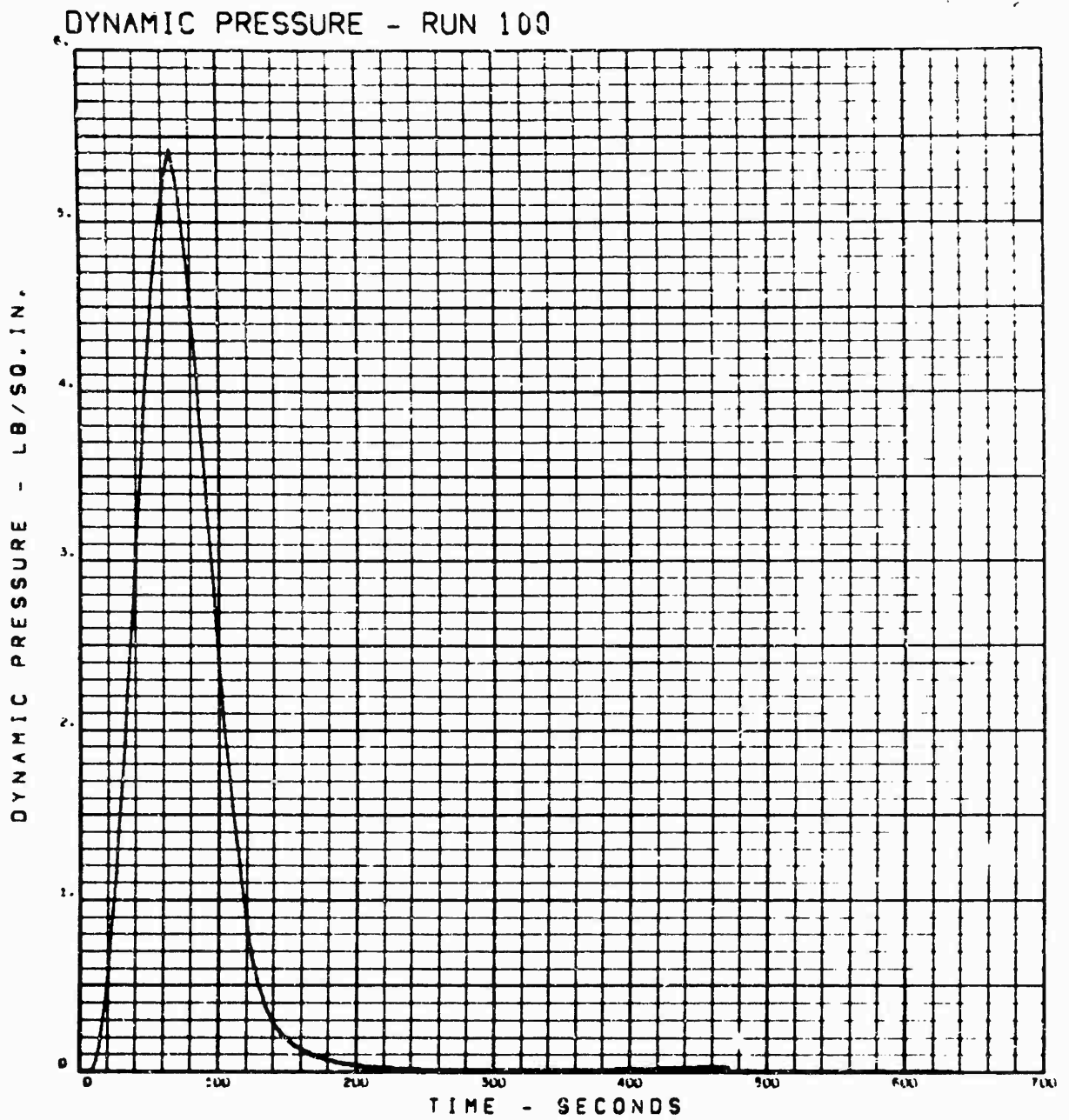
Figure 13. Dynamic Pressure as a Function of Time

64

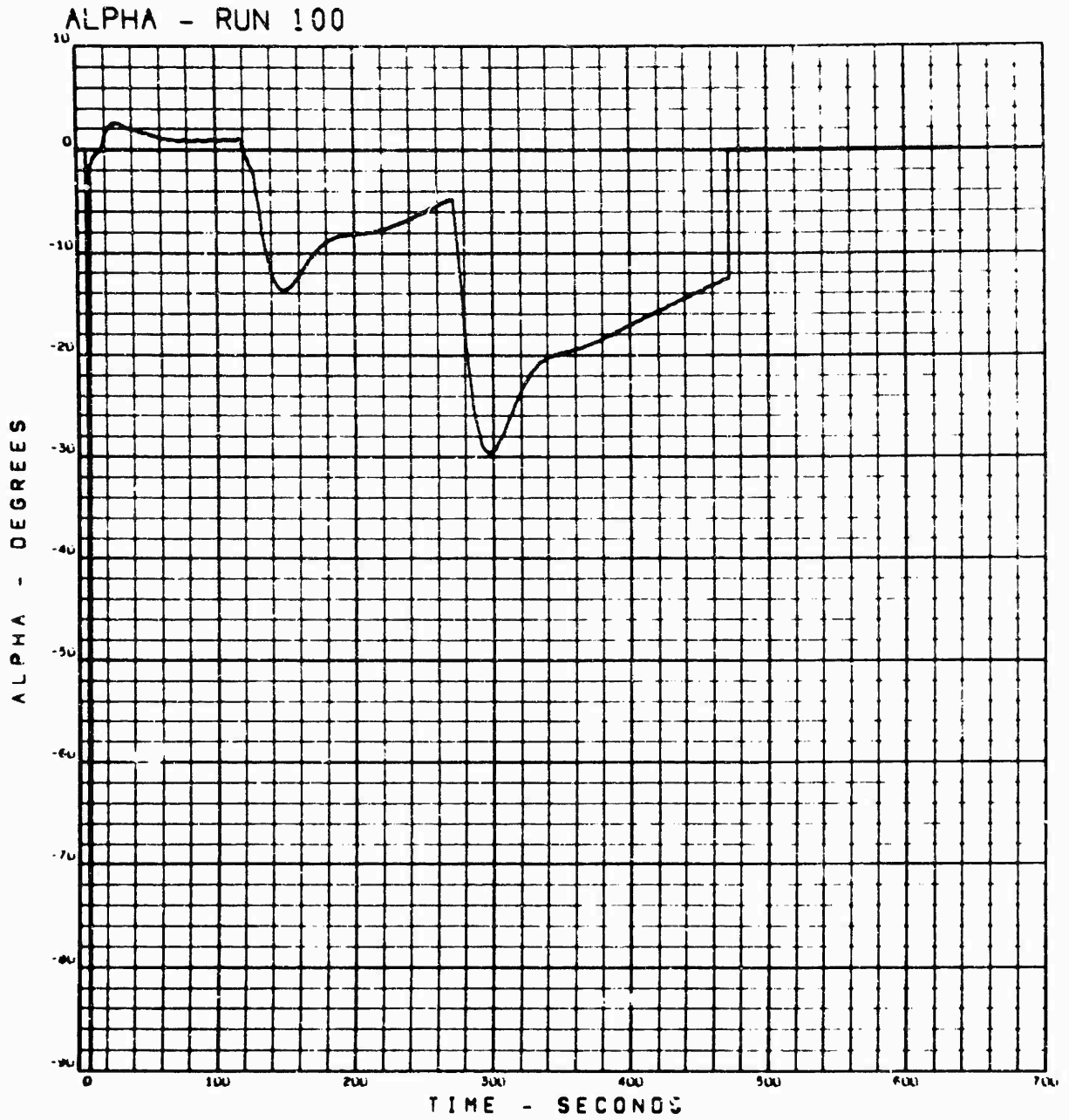Figure 14.   Body Rate Commands as a Function of Time

65

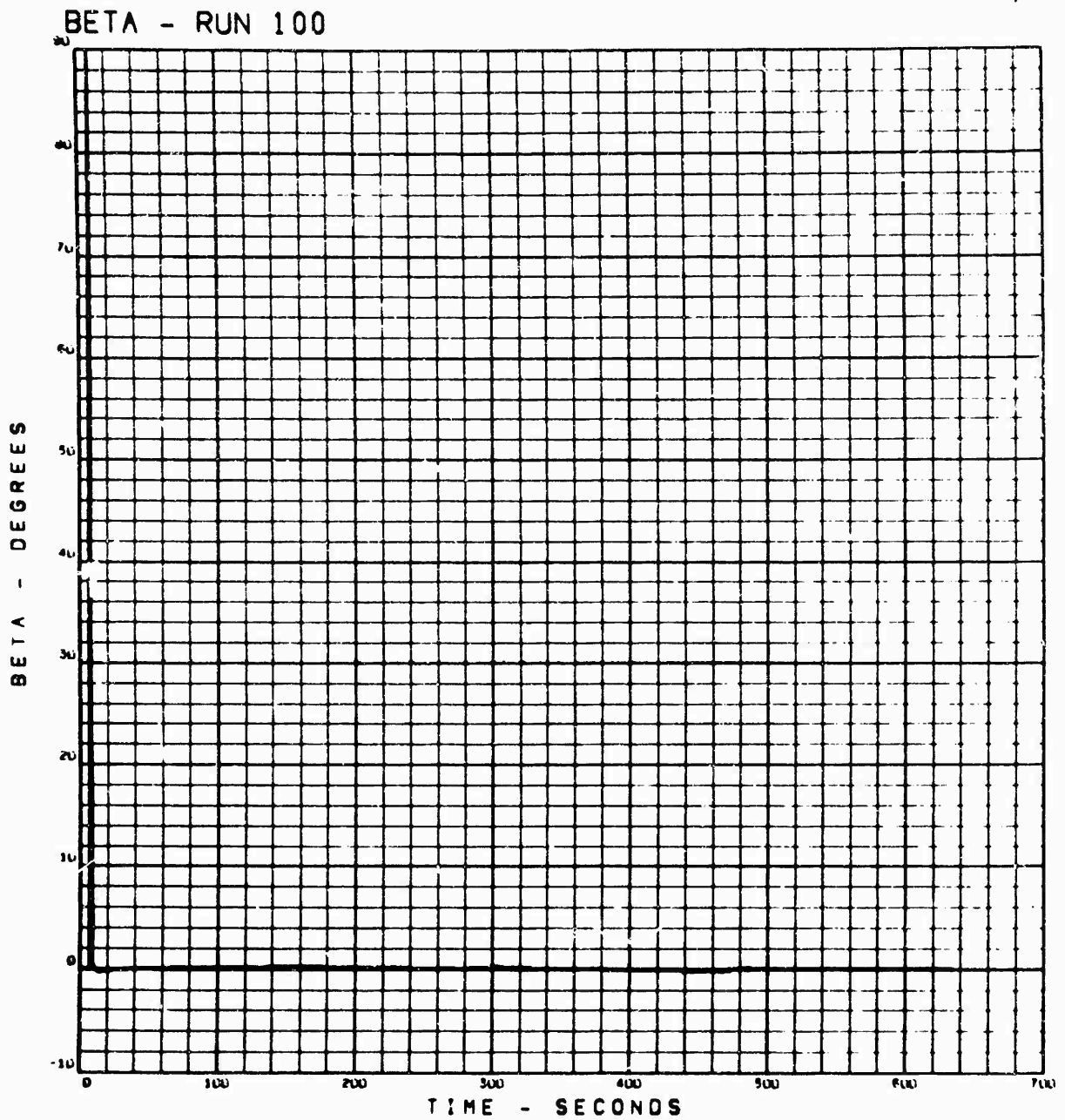Figure 15. Angle of Attack in Pitch as a Function of Time

66

BETA - RUN 100

BETA - DEGREES

TIME - SECONDS

Figure 16. Angle of Attack in Yaw as a Function of Time

67

Figure 17. Time of Flight as a Function of Lift-Off Time

68

TIME VS DELTA V - RUN 41 150 NMI CIRCULAR TARGET ORBIT
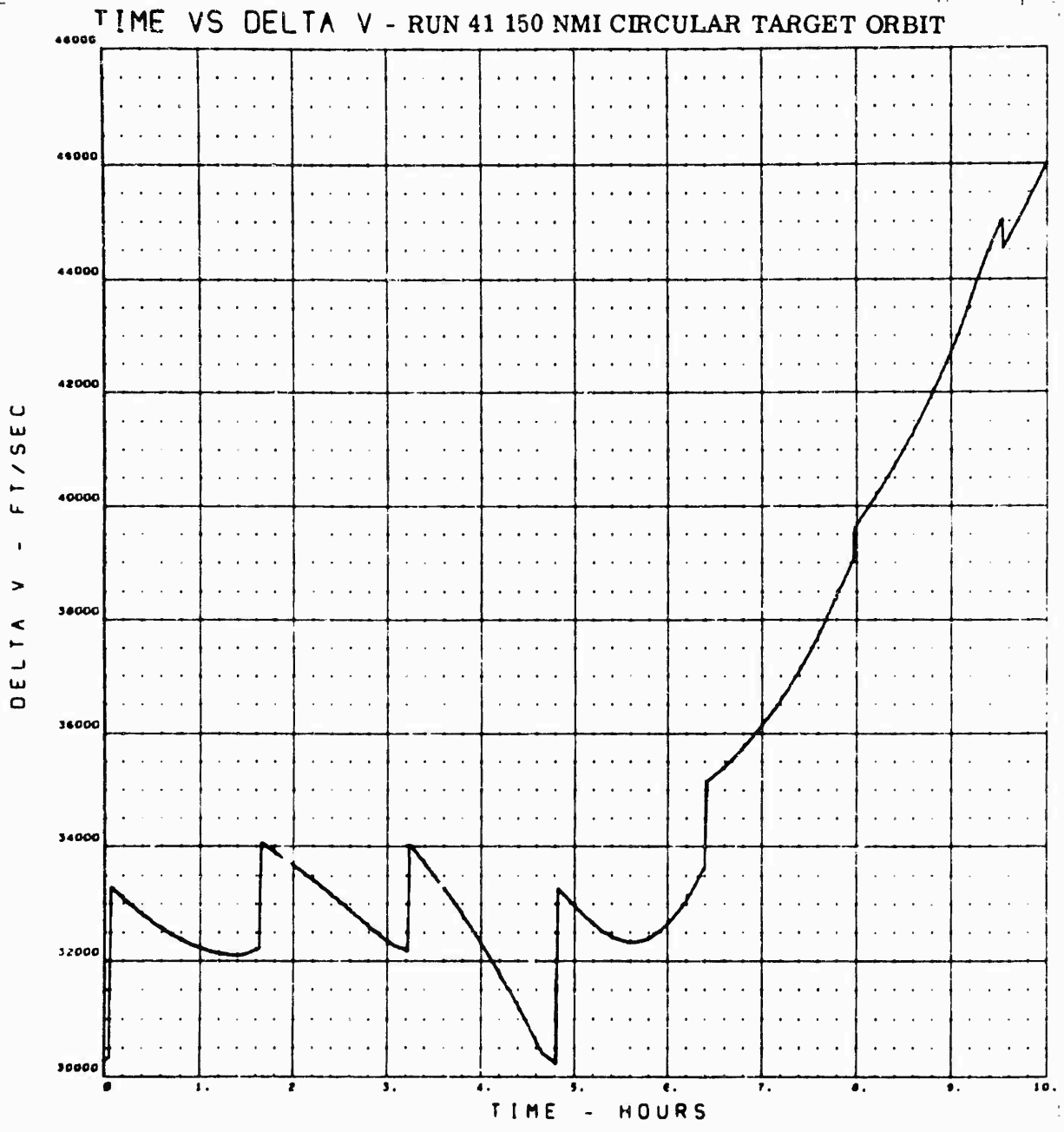
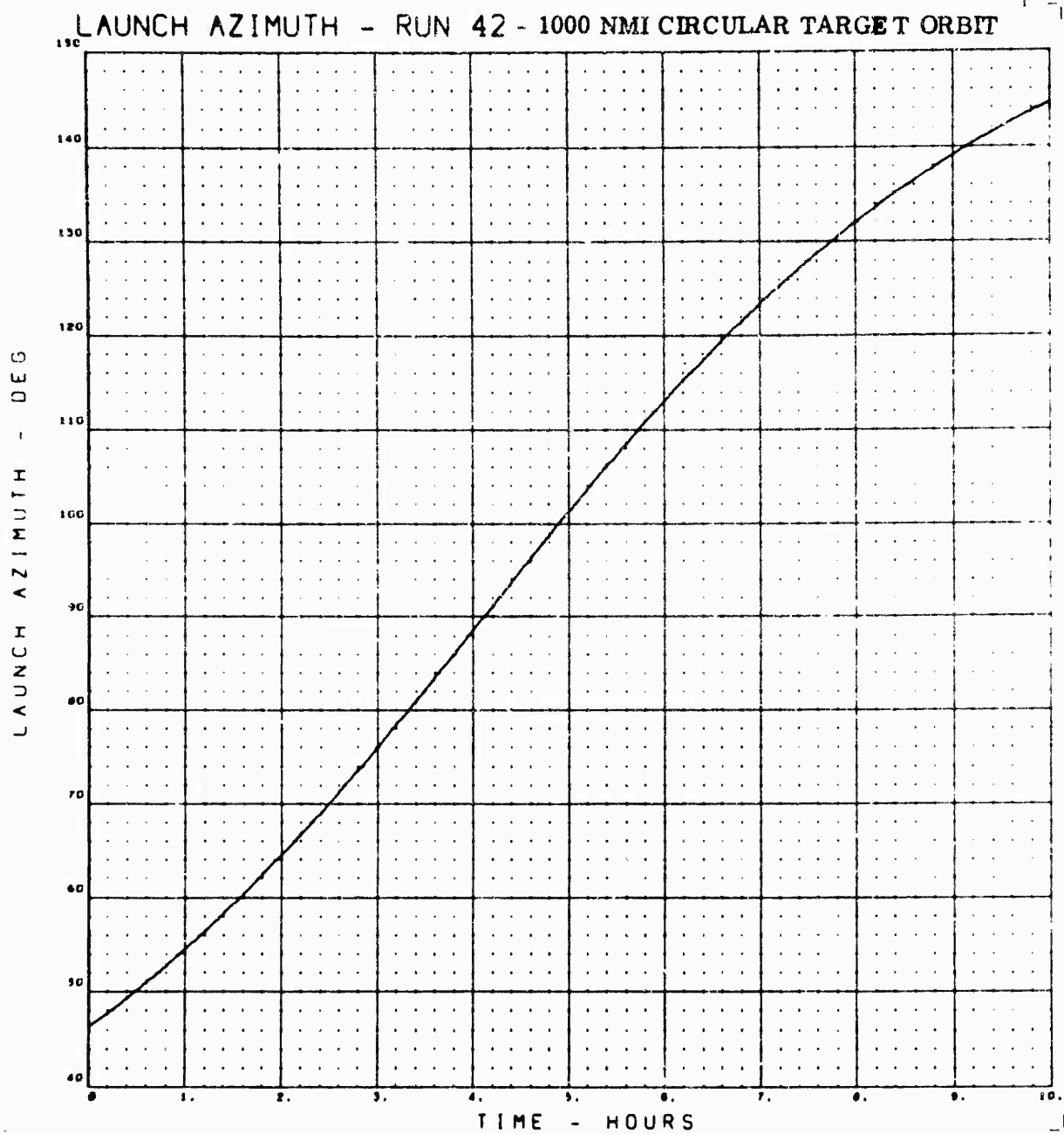Figure 18.   Total Velocity Change as a Function of Lift-Off Time

69
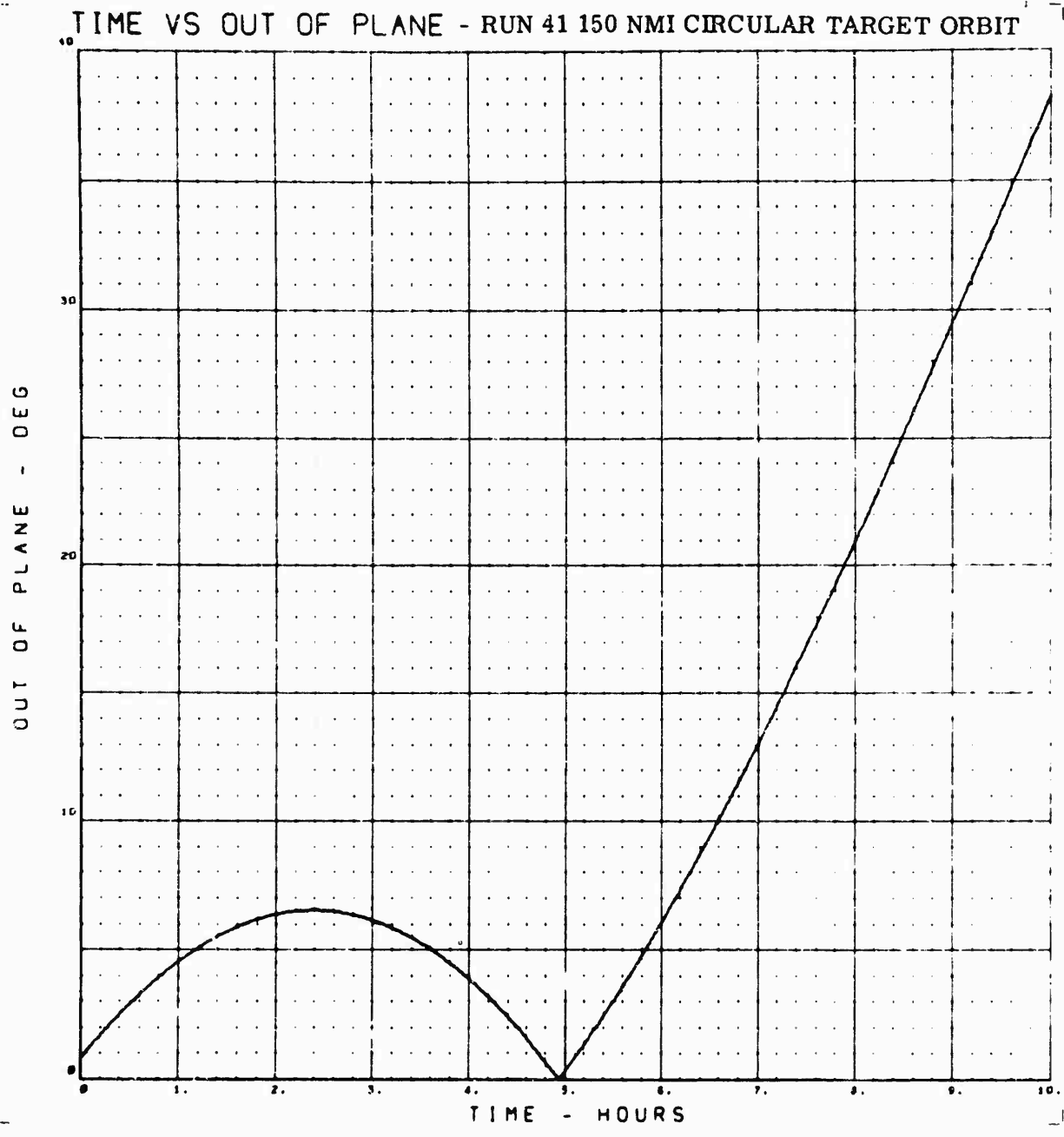
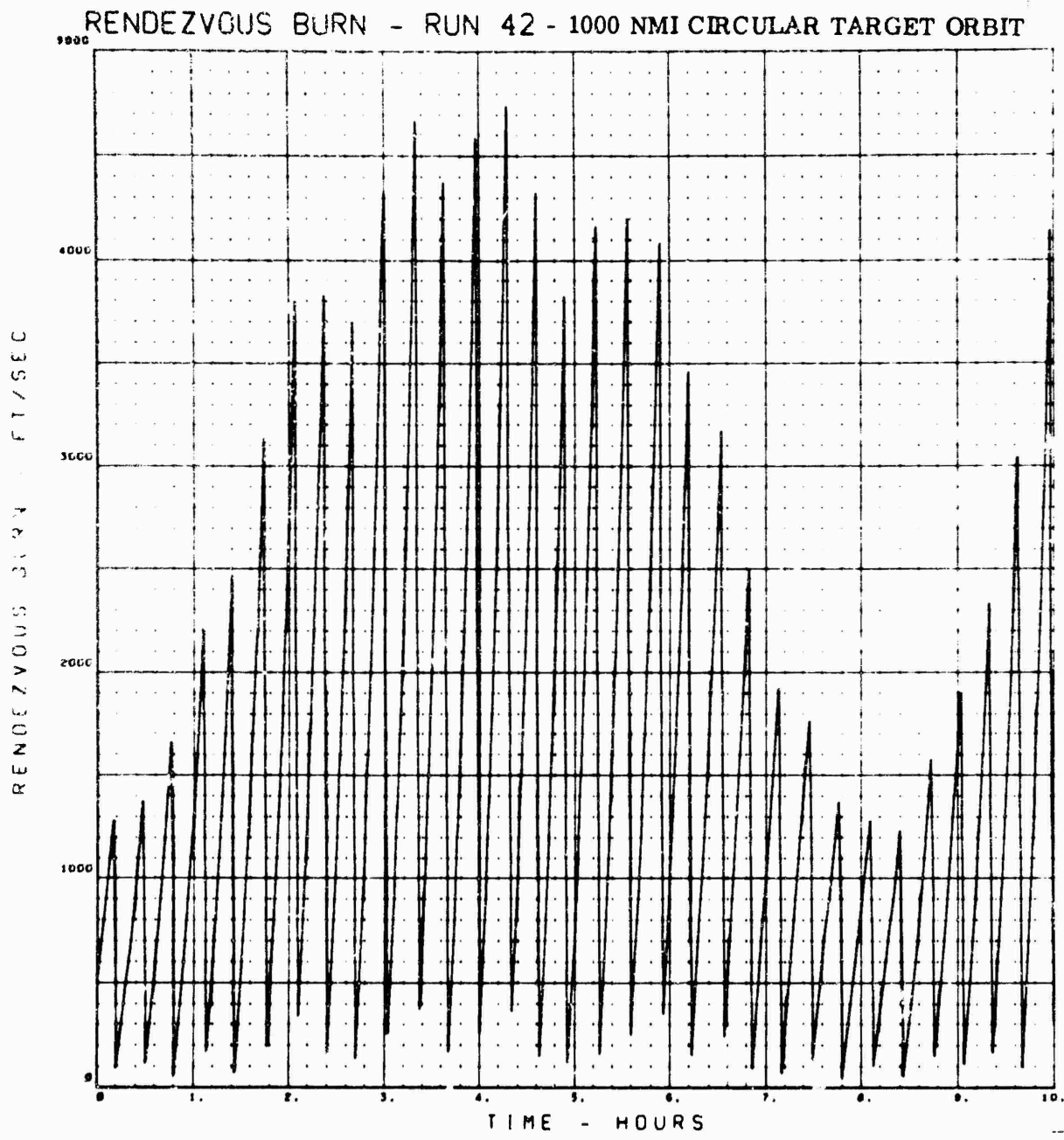Figure 19. Angle Out of Plane as a Function of Lift-Off Time

70
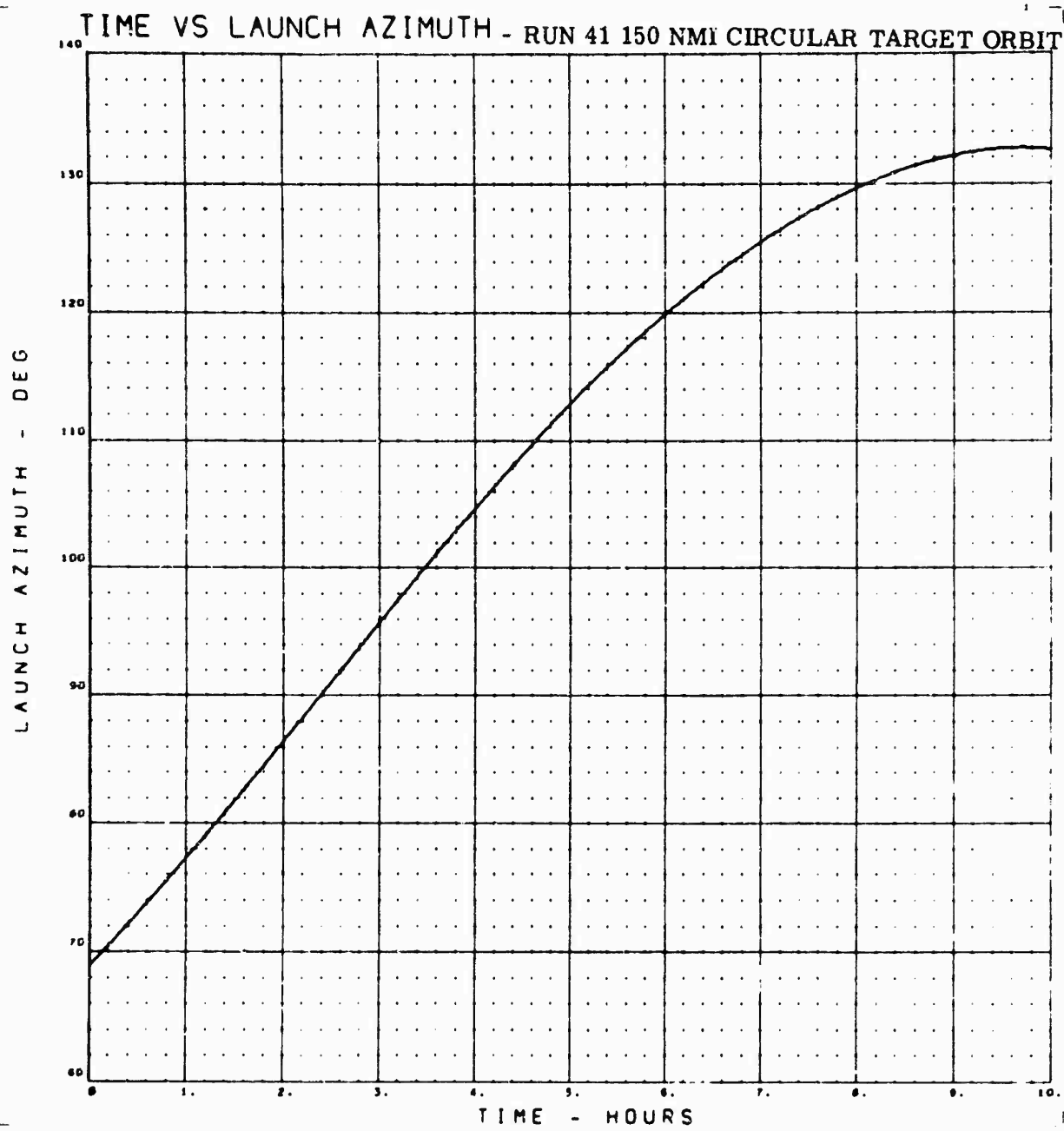
Figure 20. Launch Azimuth as a Function of Lift-Off Time

71
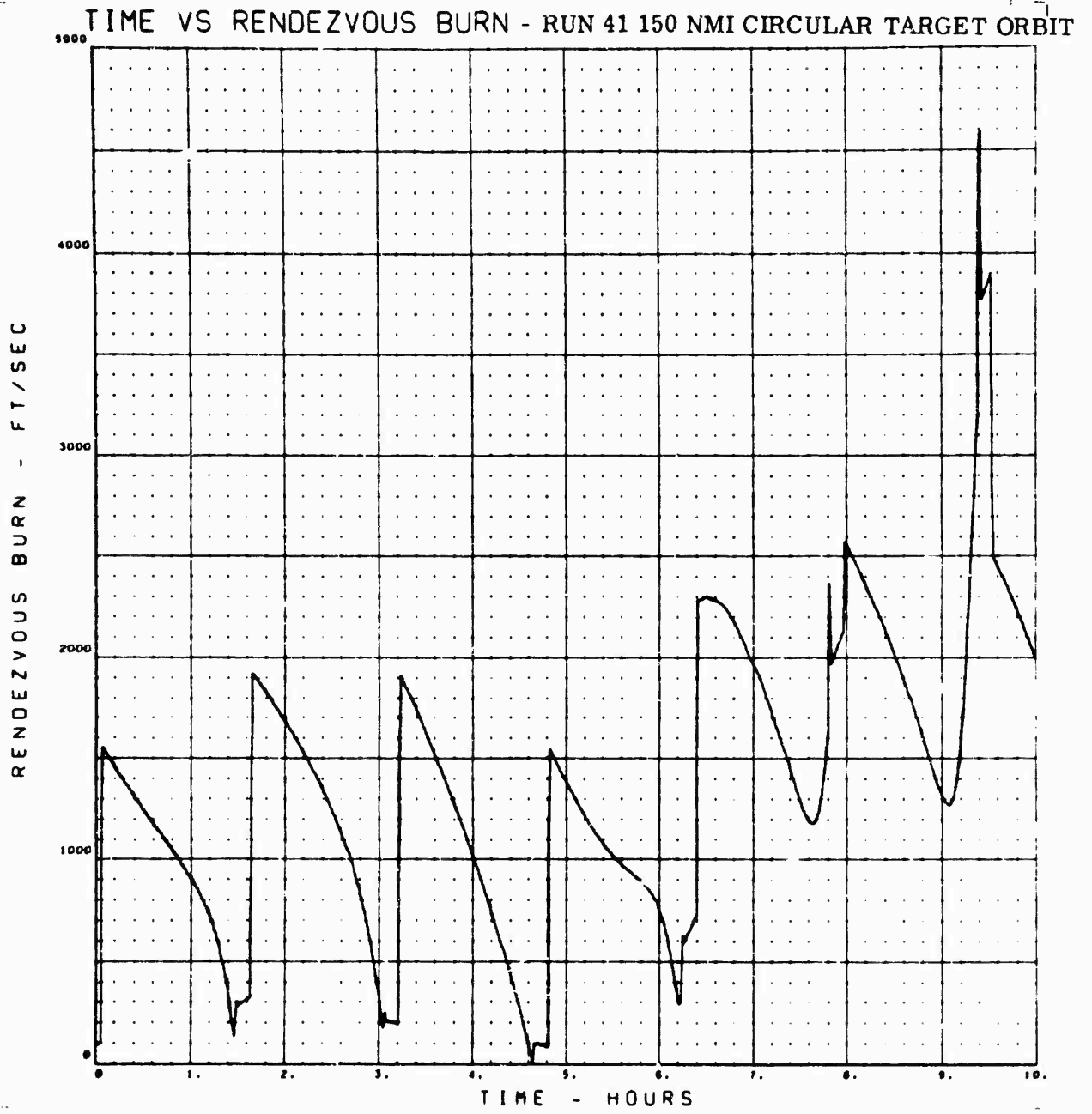
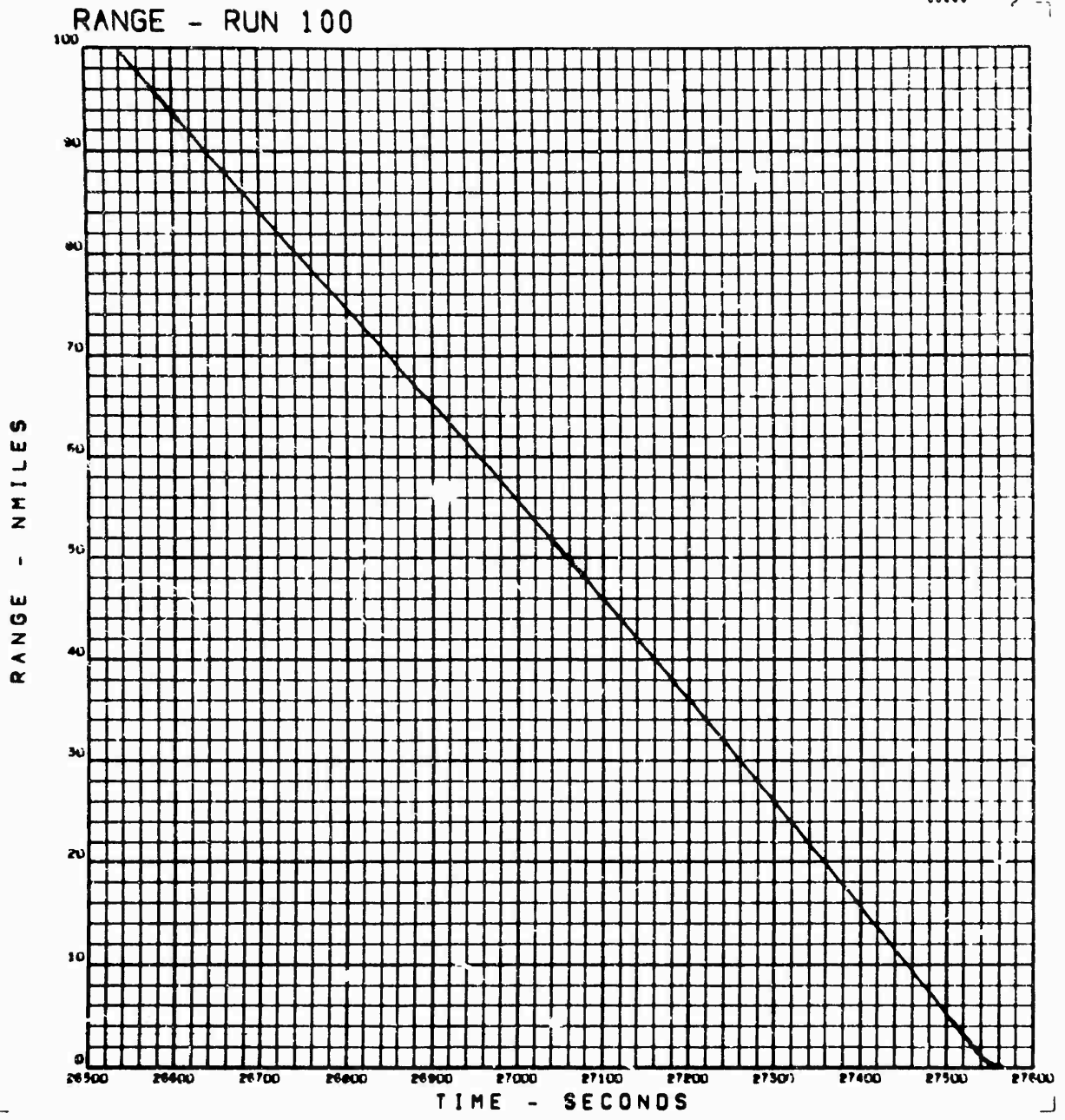Figure 21. Velocity Change in the Rendezvous Burn as a Function of Lift-Off Time

72
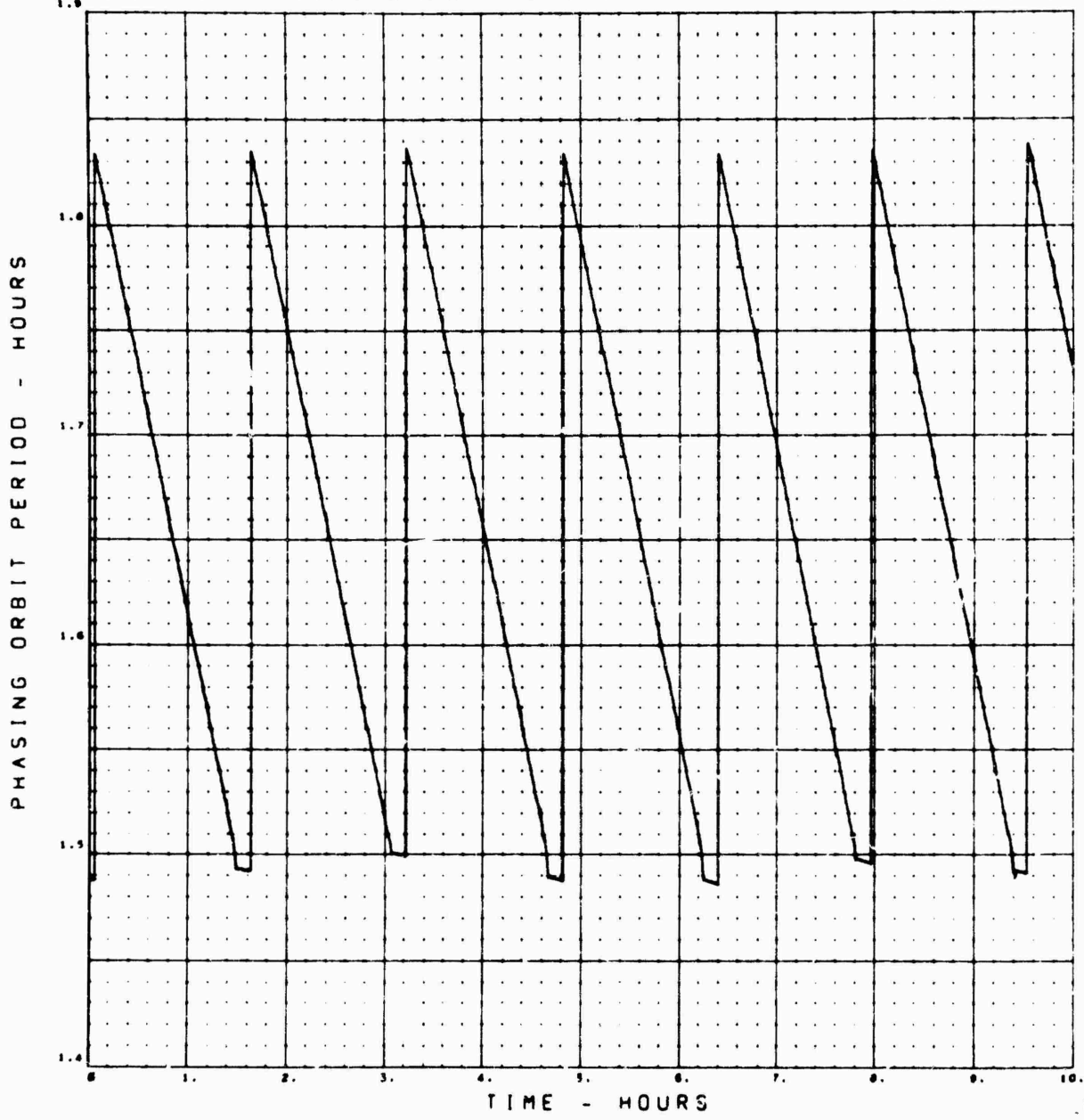
Figure 22. Phasing Orbit Period as a Function of Lift-Off Time

73

FLIGHT TIME - RUN 42 - 1000 NMI CIRCULAR TARGET ORBIT
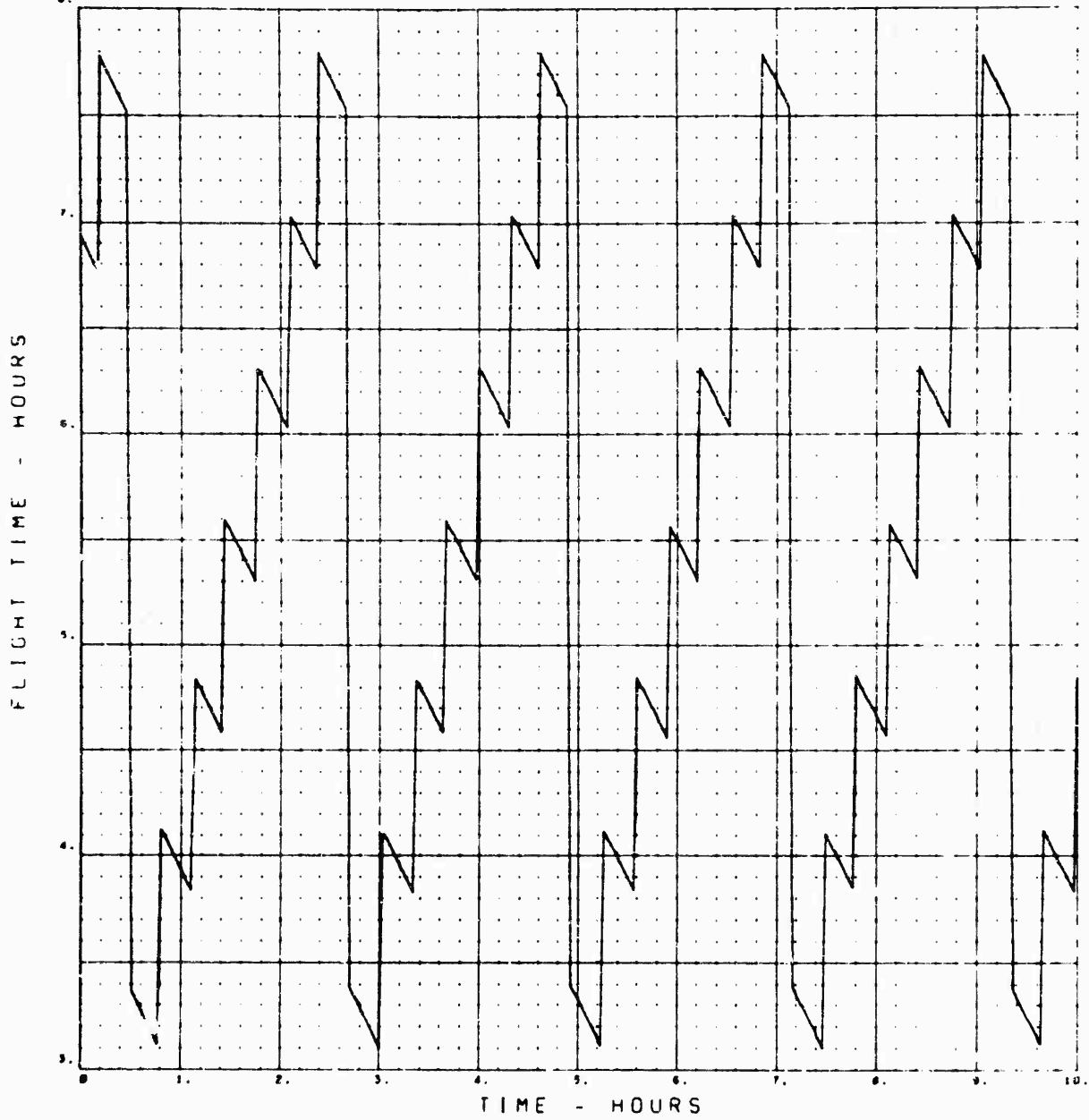
Figure 23.   Flight Time as a Function of Lift-Off Time

74
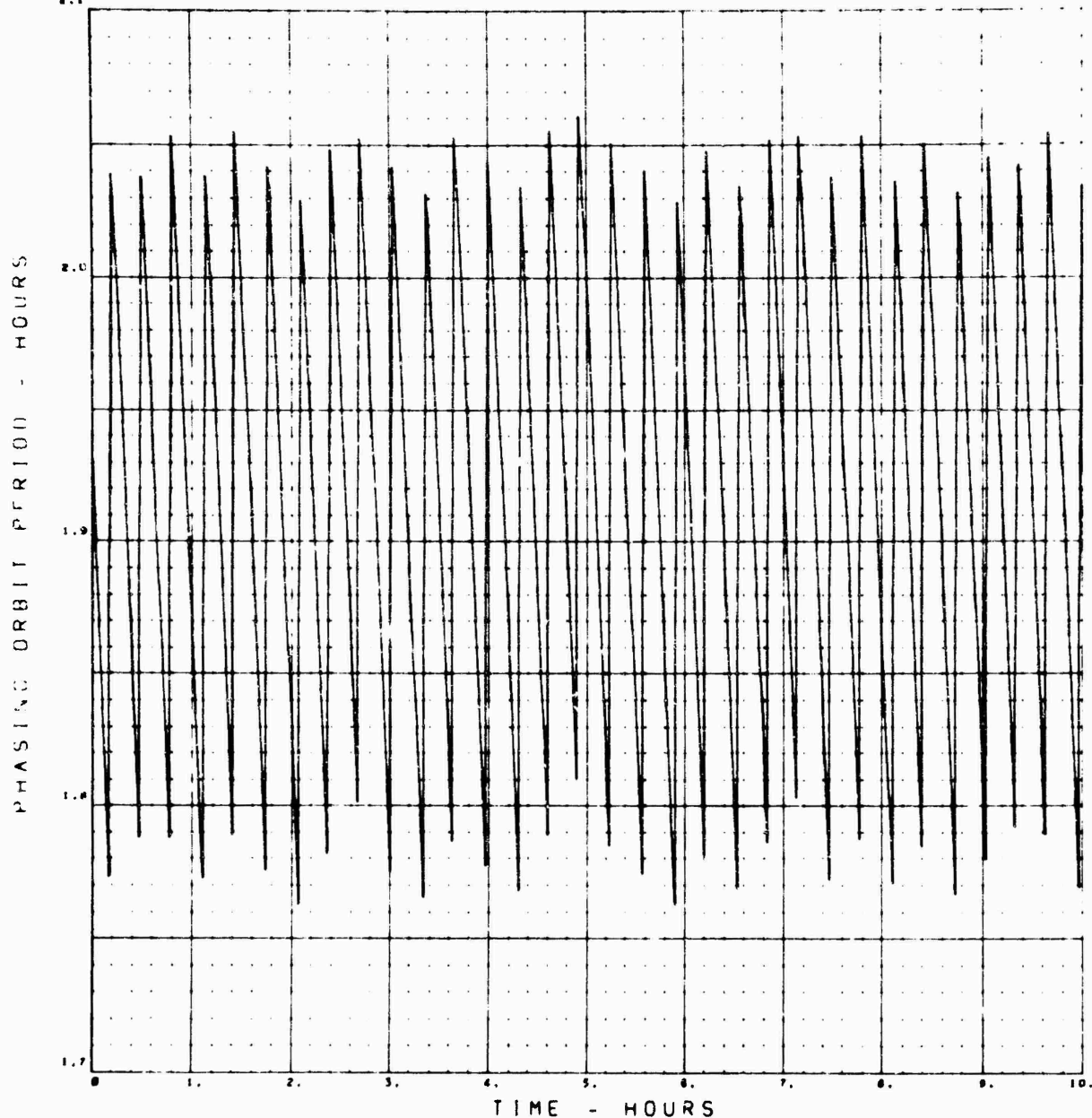
Figure 24. Phasing Orbit Period as a Function of Lift-Off Time

75
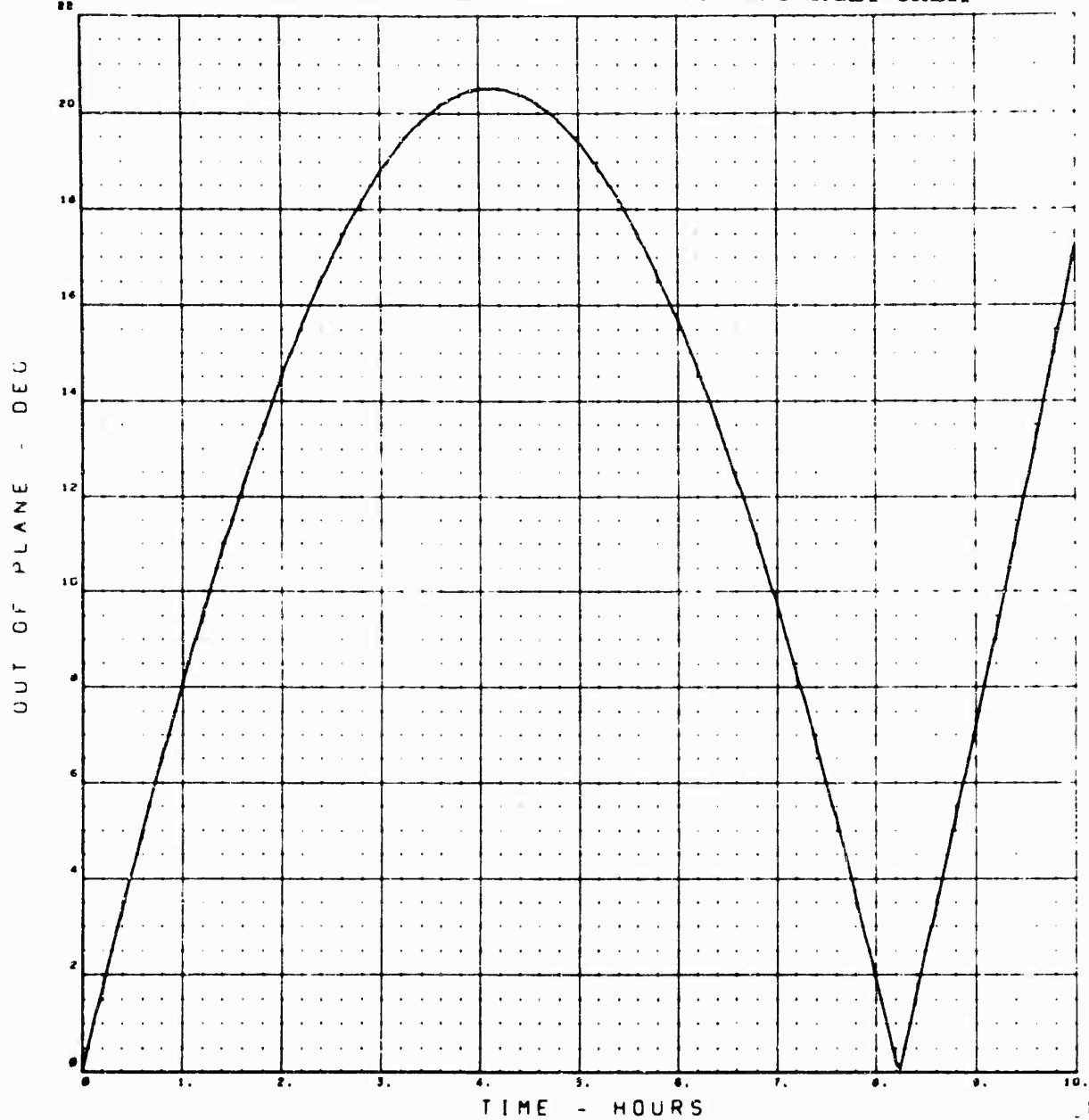
Figure 25. Angle Out of Plane as a Function of Lift-Off Time

76
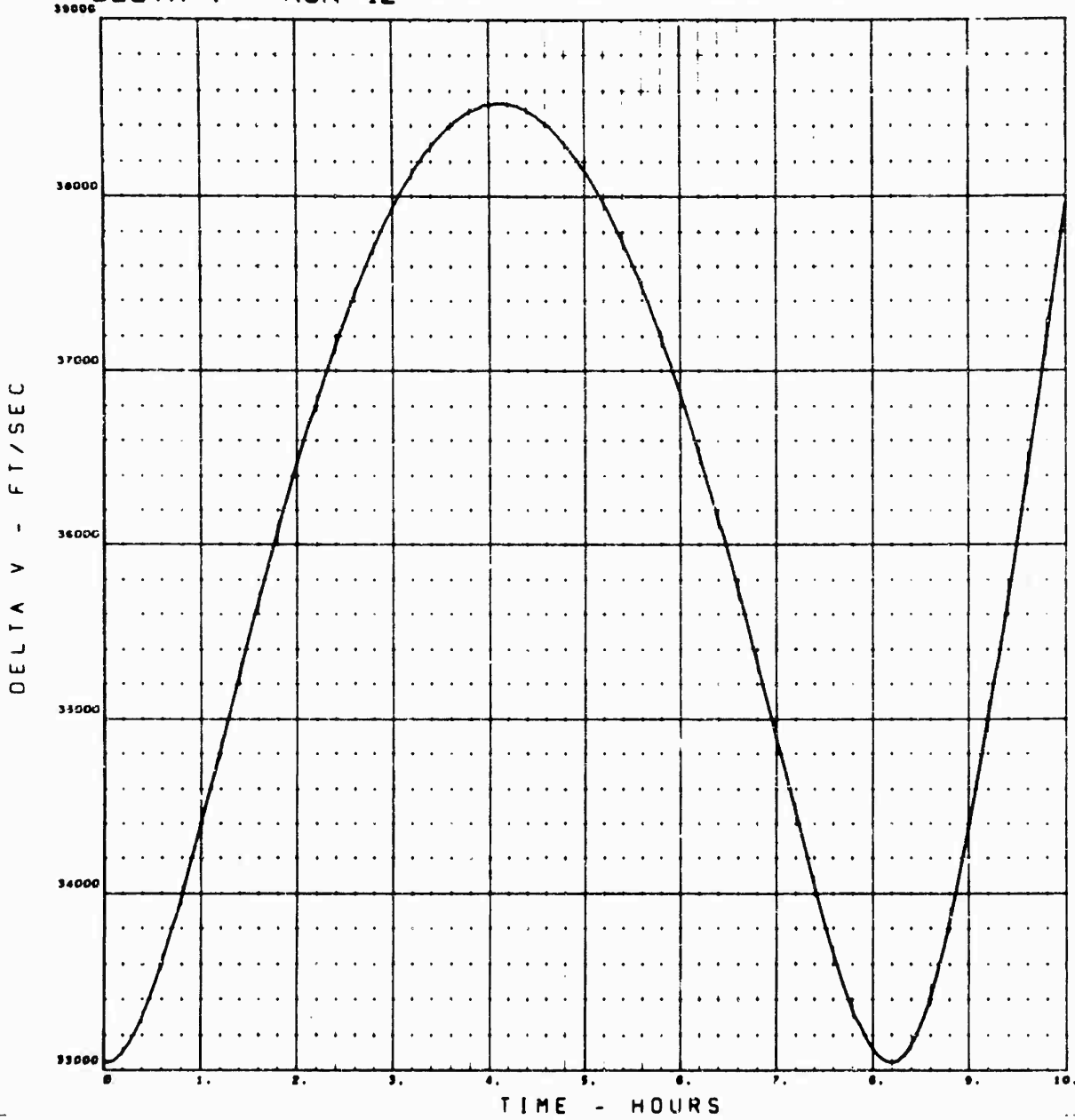
Figure 26. Total Velocity Change as a Function of Lift-Off Time

77

Figure 27. Launch Azimuth as a Function of Lift-Off Time

78

RENDEZVOUS BURN - RUN 42 - 1000 NMI CIRCULAR TARGET ORBIT

Figure 28. Velocity Change in the Rendezvous Burn as a Function of Lift-Off Time

79

Figure 29. Range as a Function of Time
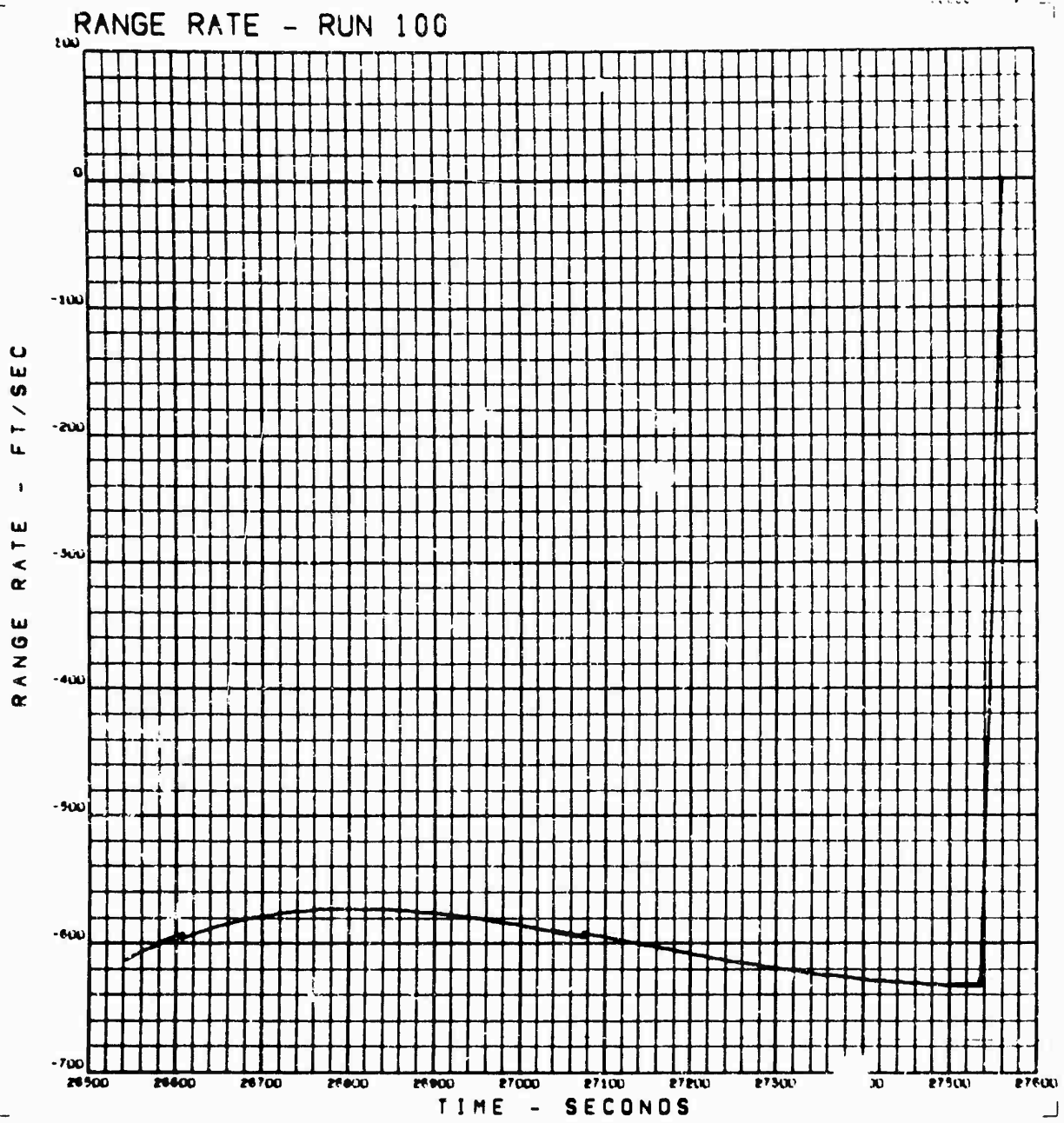
80
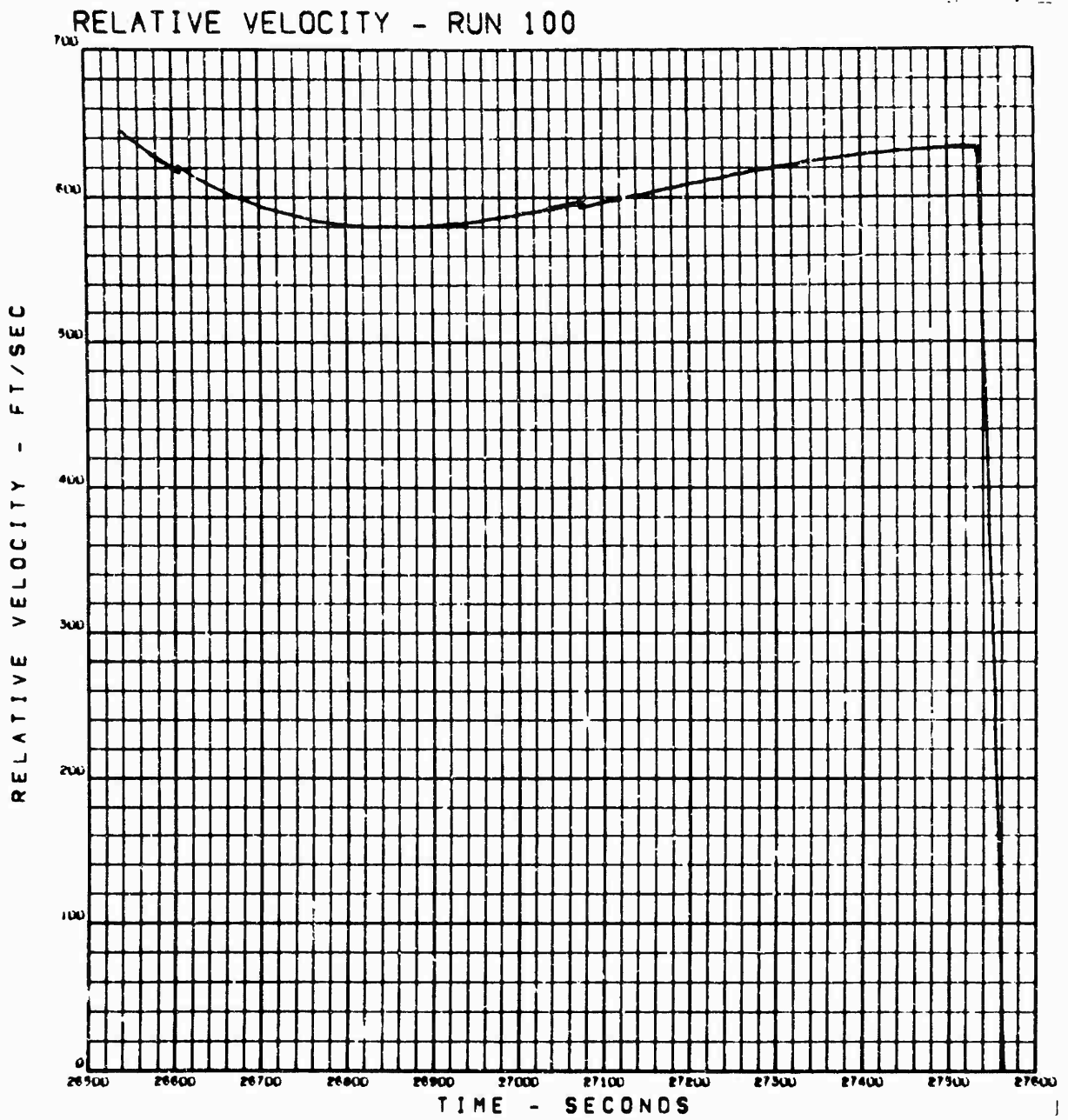
Figure 30. Relative Velocity as a Function of Time

81

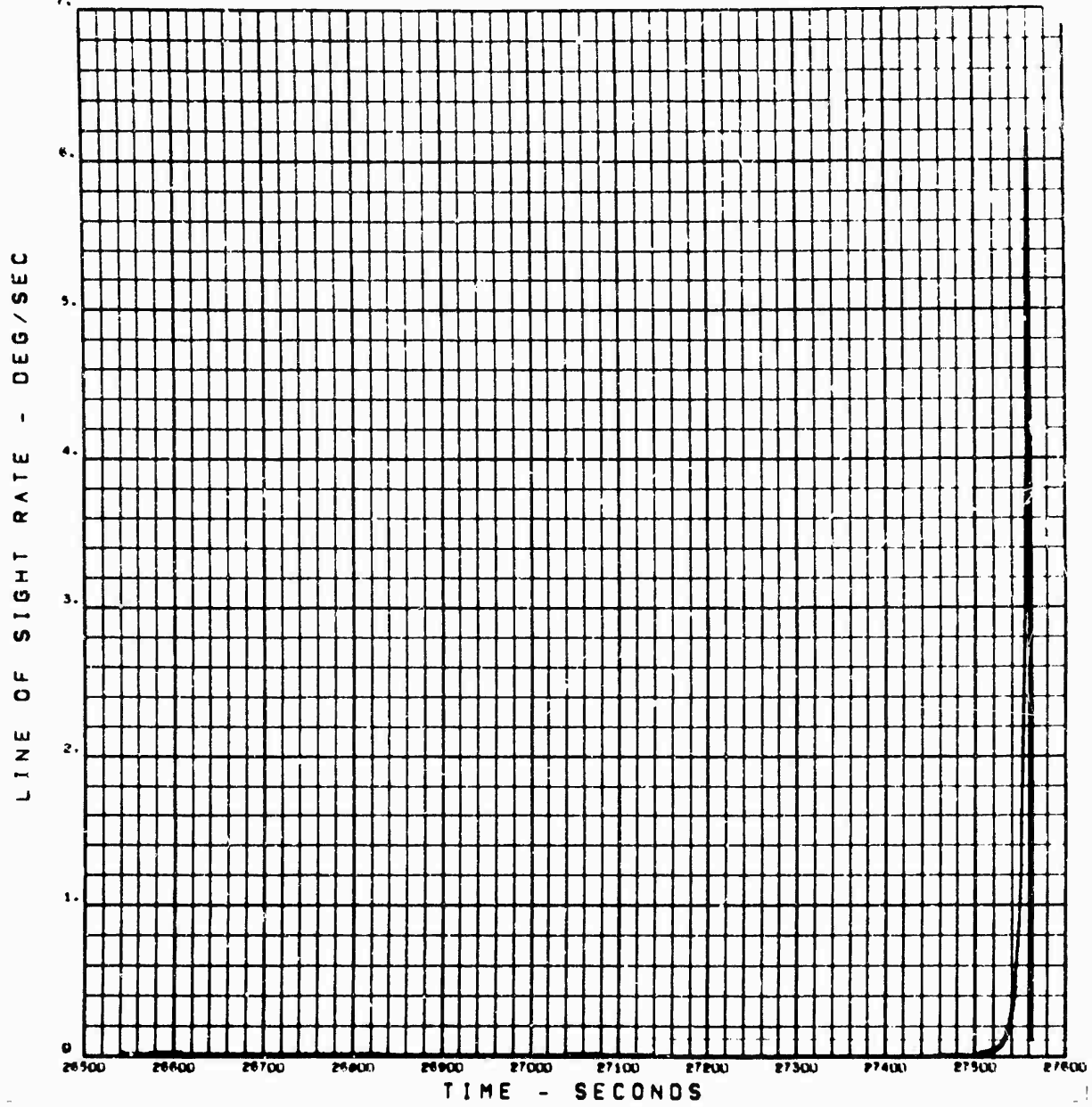Figure 31. Range Rate as a Function of Time
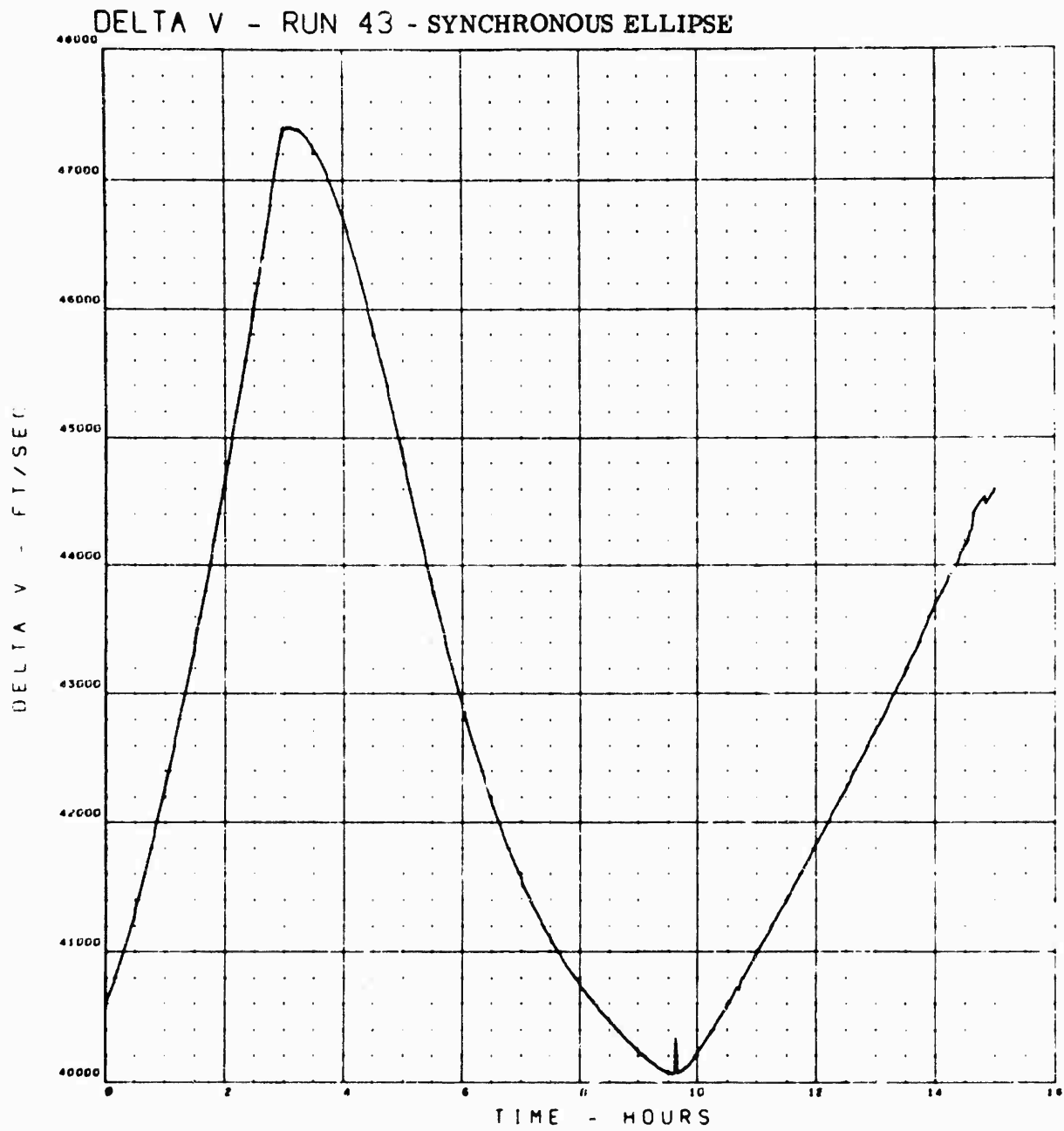
82

Figure 32. Line of Sight Ratio as a Function of Time

83

Figure 33. Total Velocity Change as a Function of Lift-Off Time

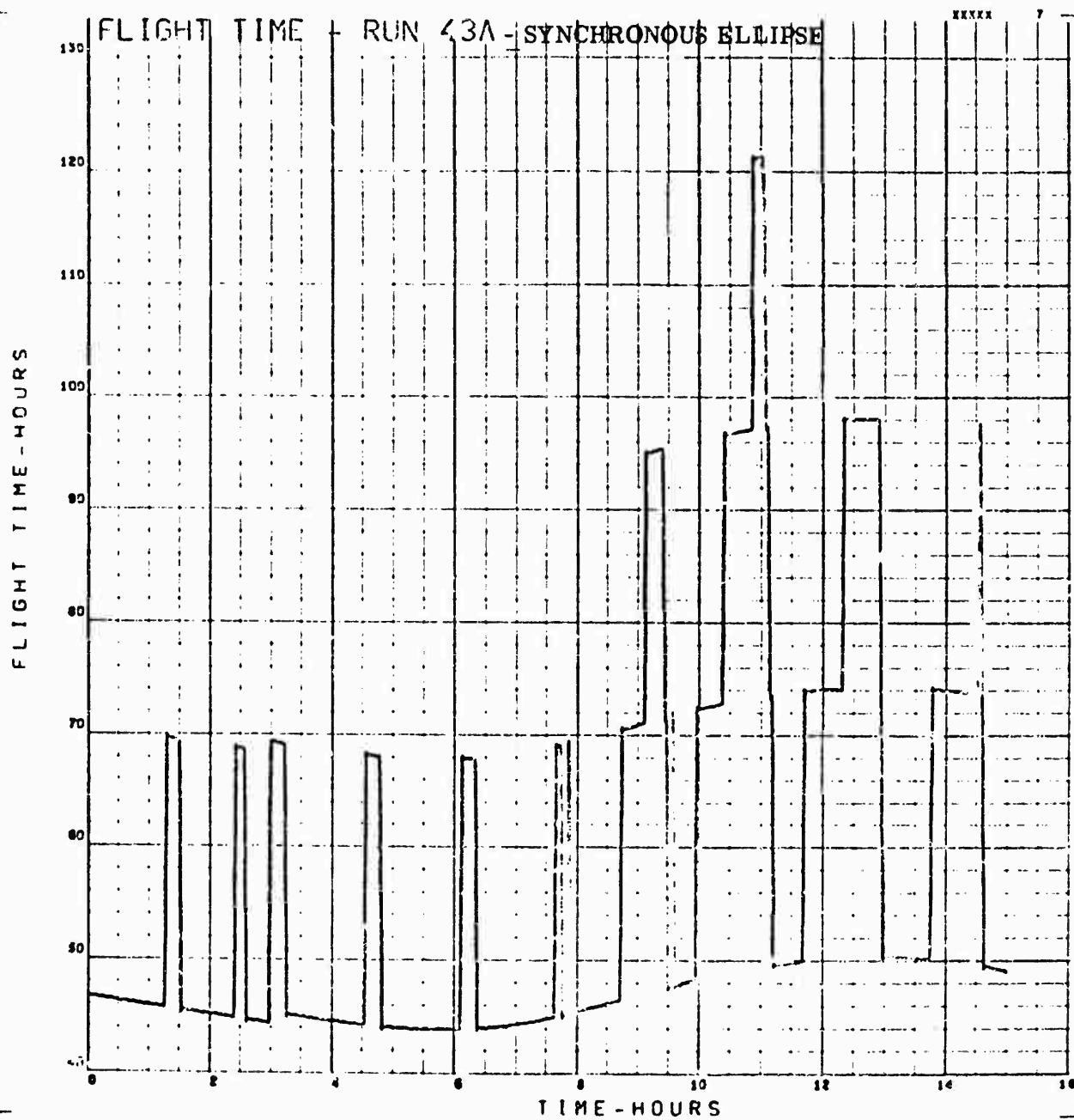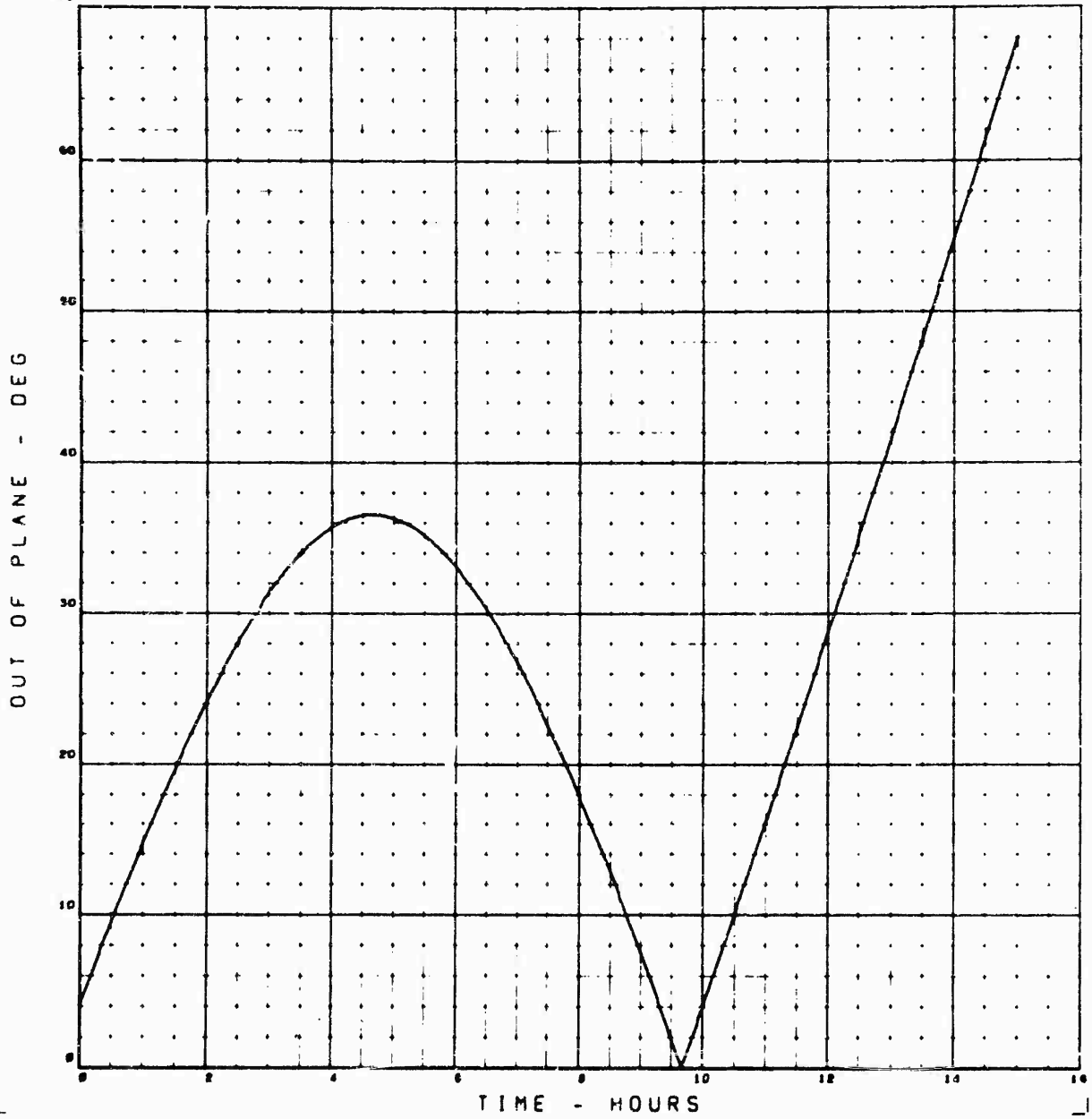Figure 34. Flight Time as a Function of Lift-Off Time

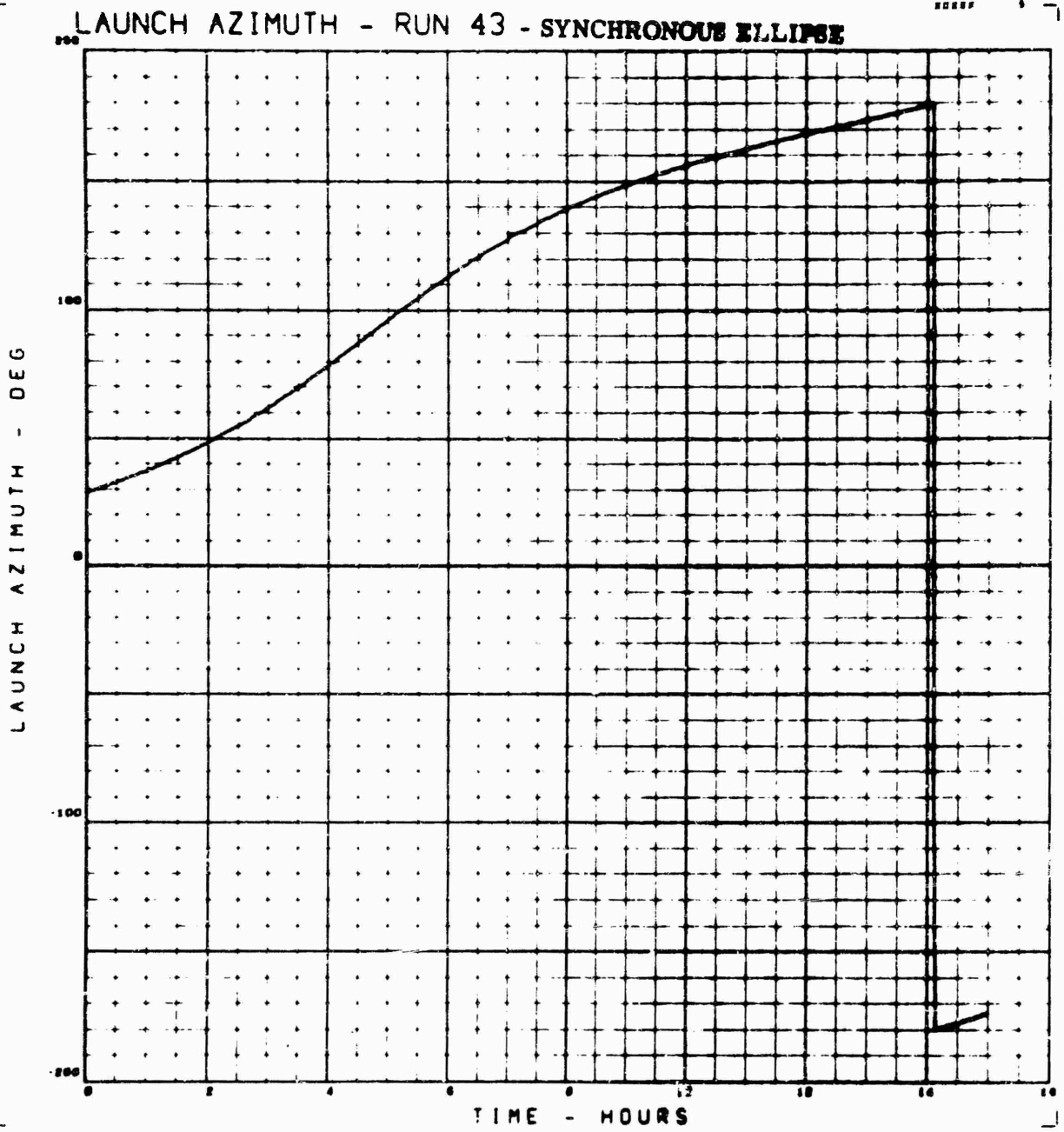Figure 35. Angle Out of Plane as a Function of Lift-Off Time

Figure 36. Launch Azimuth as a Function of Lift-Off Time

87

Figure 37. Rendezvous Burn as a Function of Lift-Off Time

88
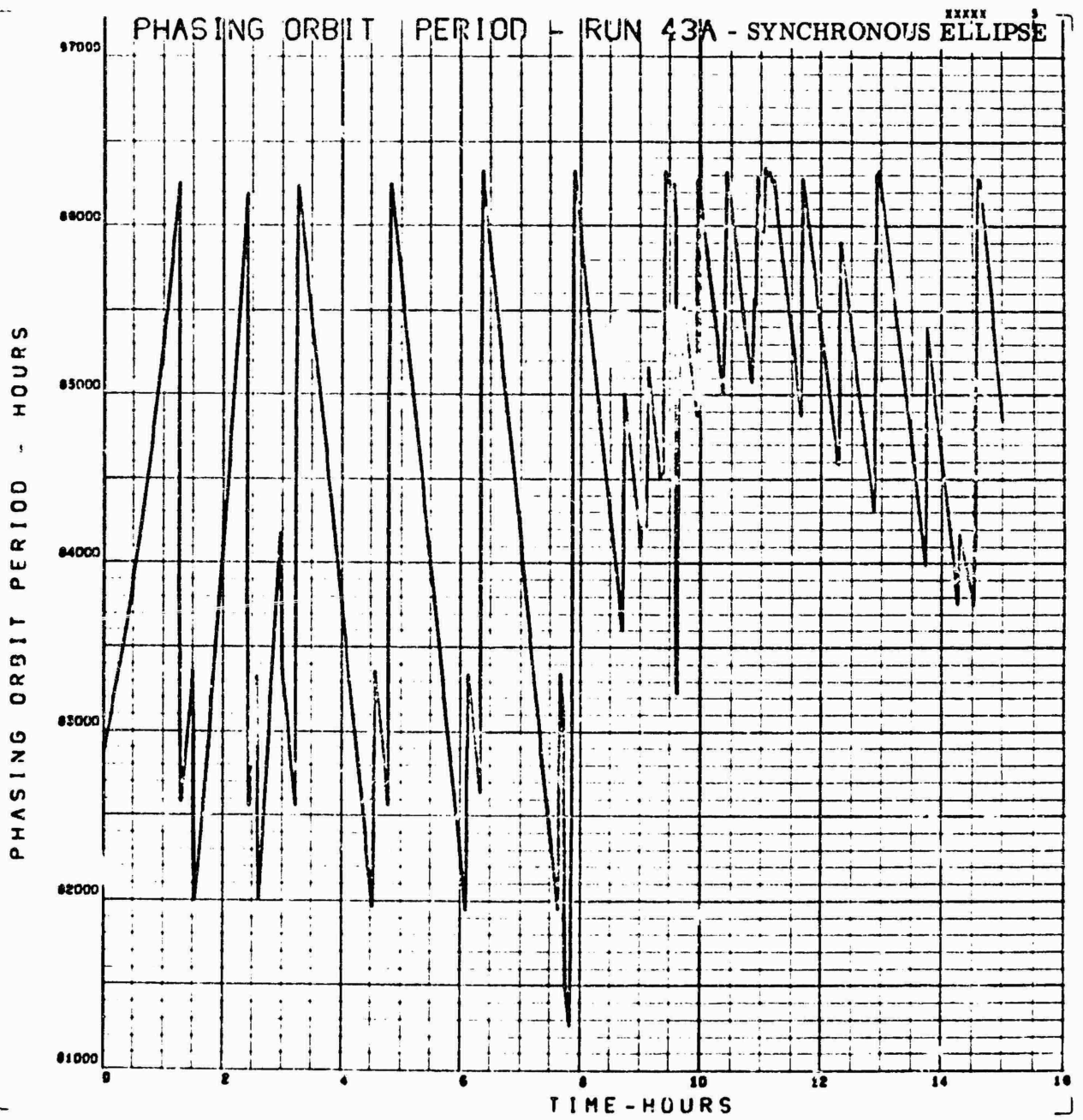
Figure 38. Phasing Orbit Period as a Function of Lift-Off Time

89

RENDEZVOUS POINTS

122

123   121

TARGET AT PERIGEE
AT TIME ZERO

LAUNCH
SITE

$\vec{We}$

PARKING ORBIT

SYNCHRONOUS
ELLIPTICAL ORBIT
PERIGEE AT 500NMI

a = 6.61 EARTH RADII
e = 0.827
i = 65°

Figure 39. Geometry of the Synchronous Elliptical Orbit

90
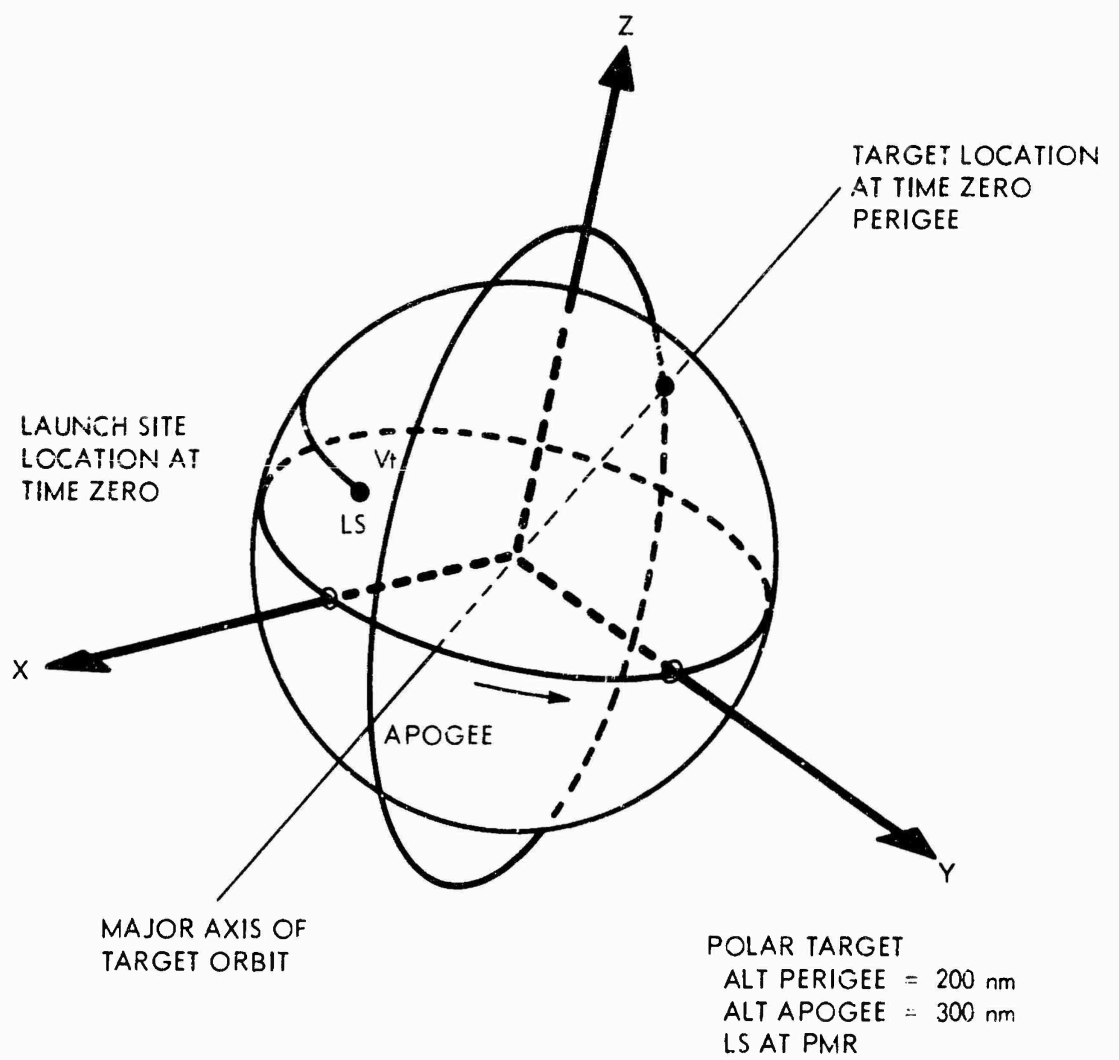
Figure 40. Geometry of the Elliptical Polar Satellite Orbit

91

FLIGHT TIME - RUN 44 - POLAR ELLIPSE
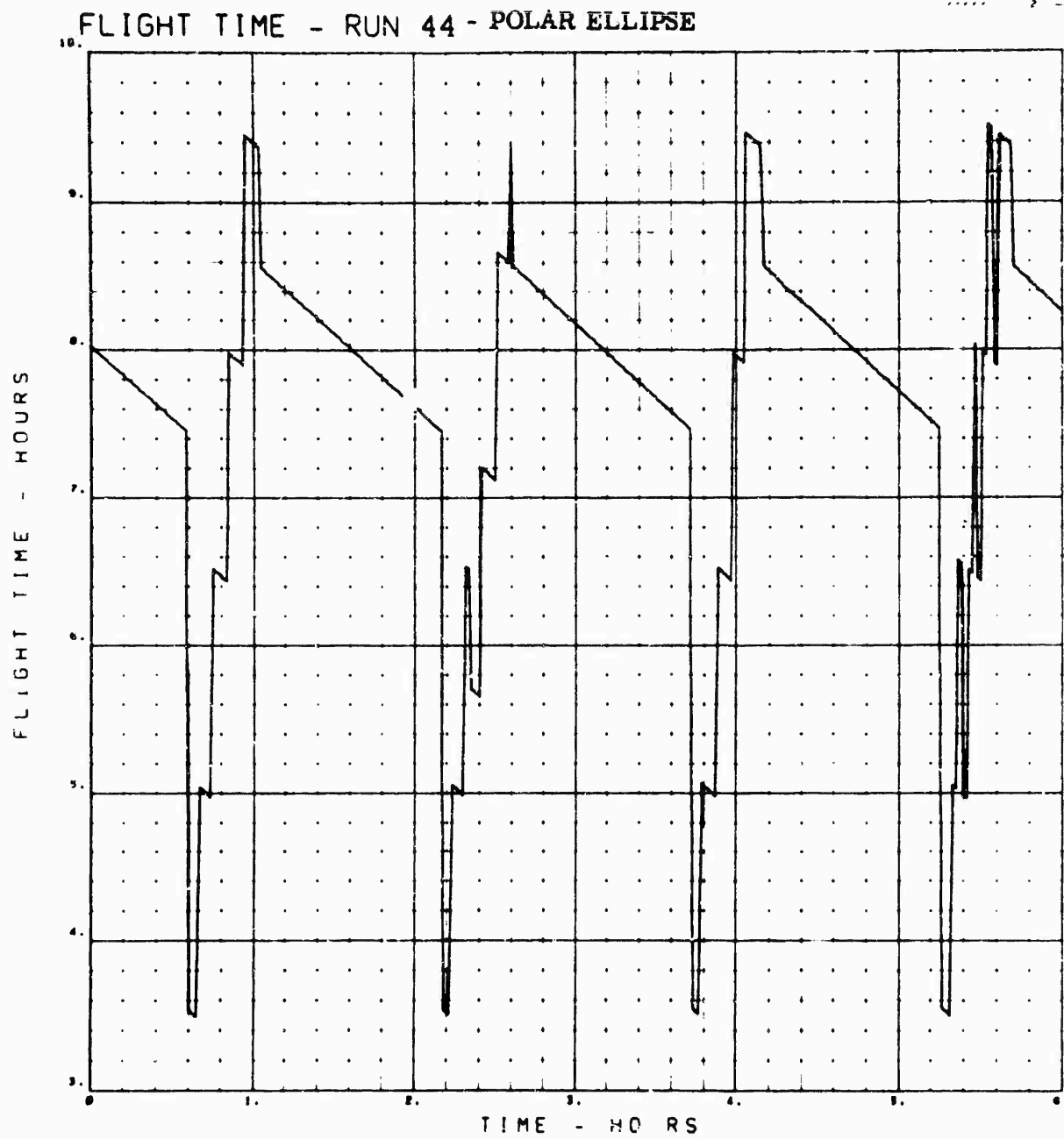
Figure 41. Flight Time as a Function of Lift-Off Time

92
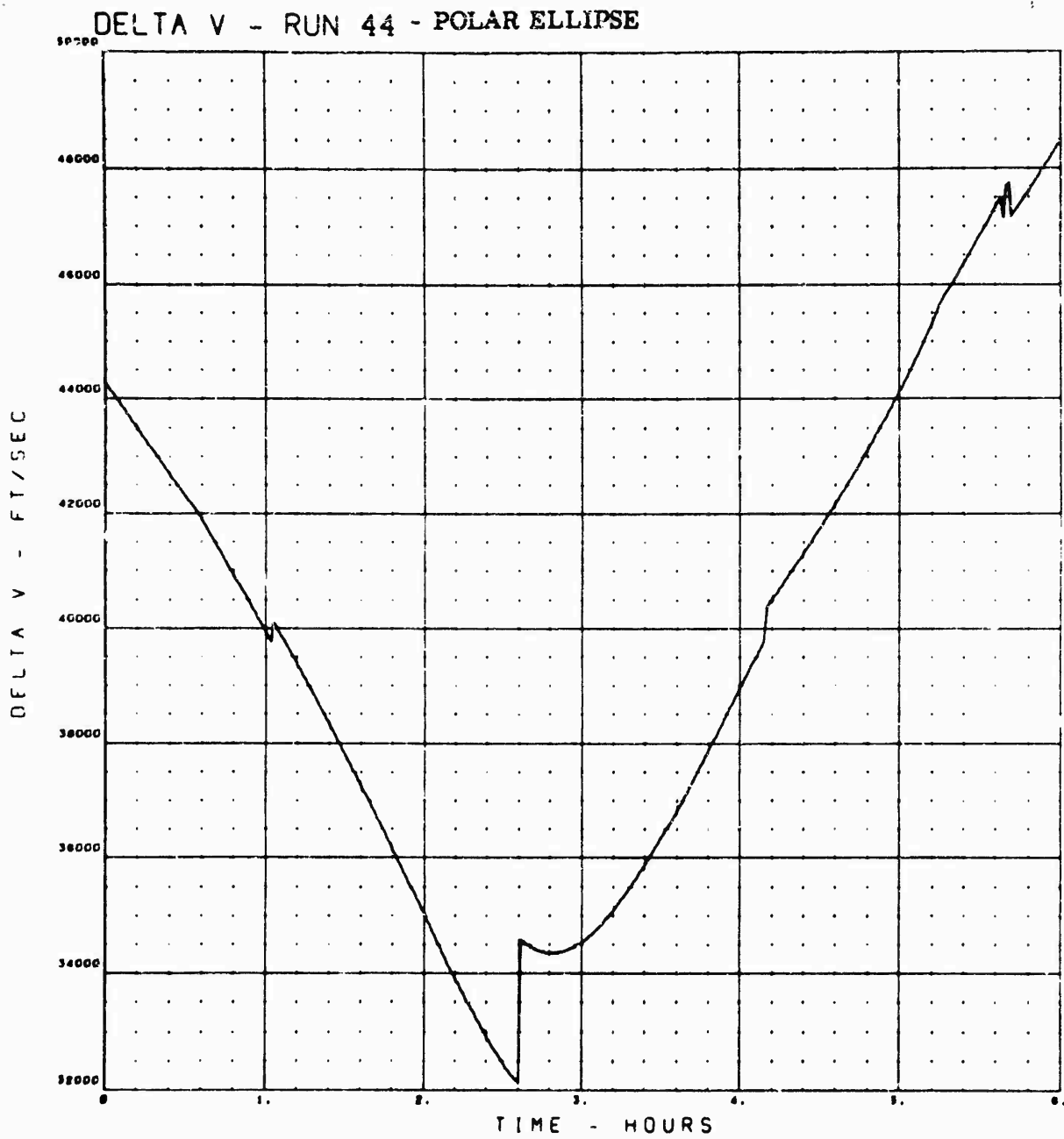
Figure 42. Total Velocity Change as a Function of Lift-Off Time

93

OUT OF PLANE - RUN 44 - POLAR ELLIPSE
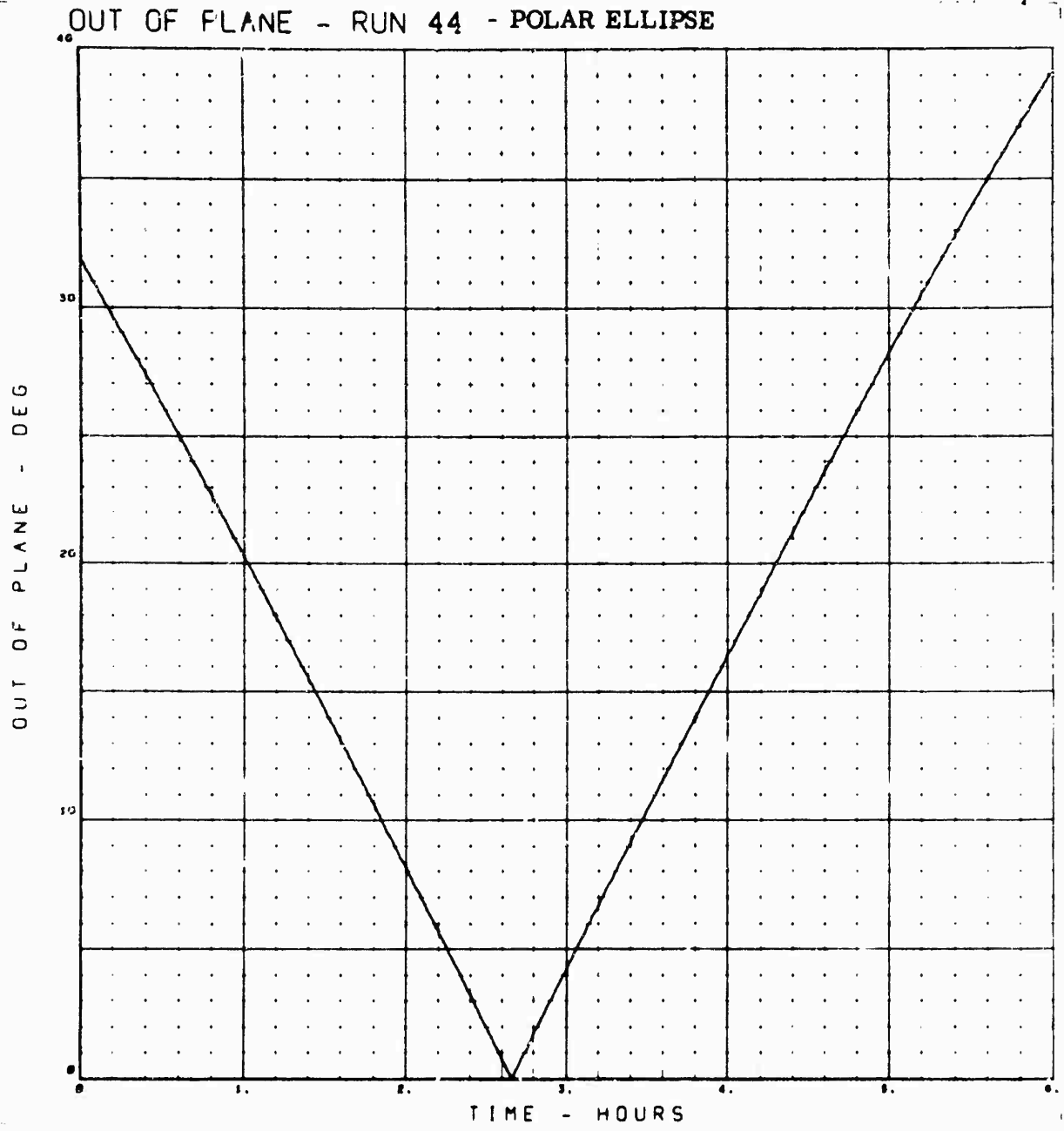
Figure 43. Out of Plane as a Function of Lift-Off Time

94
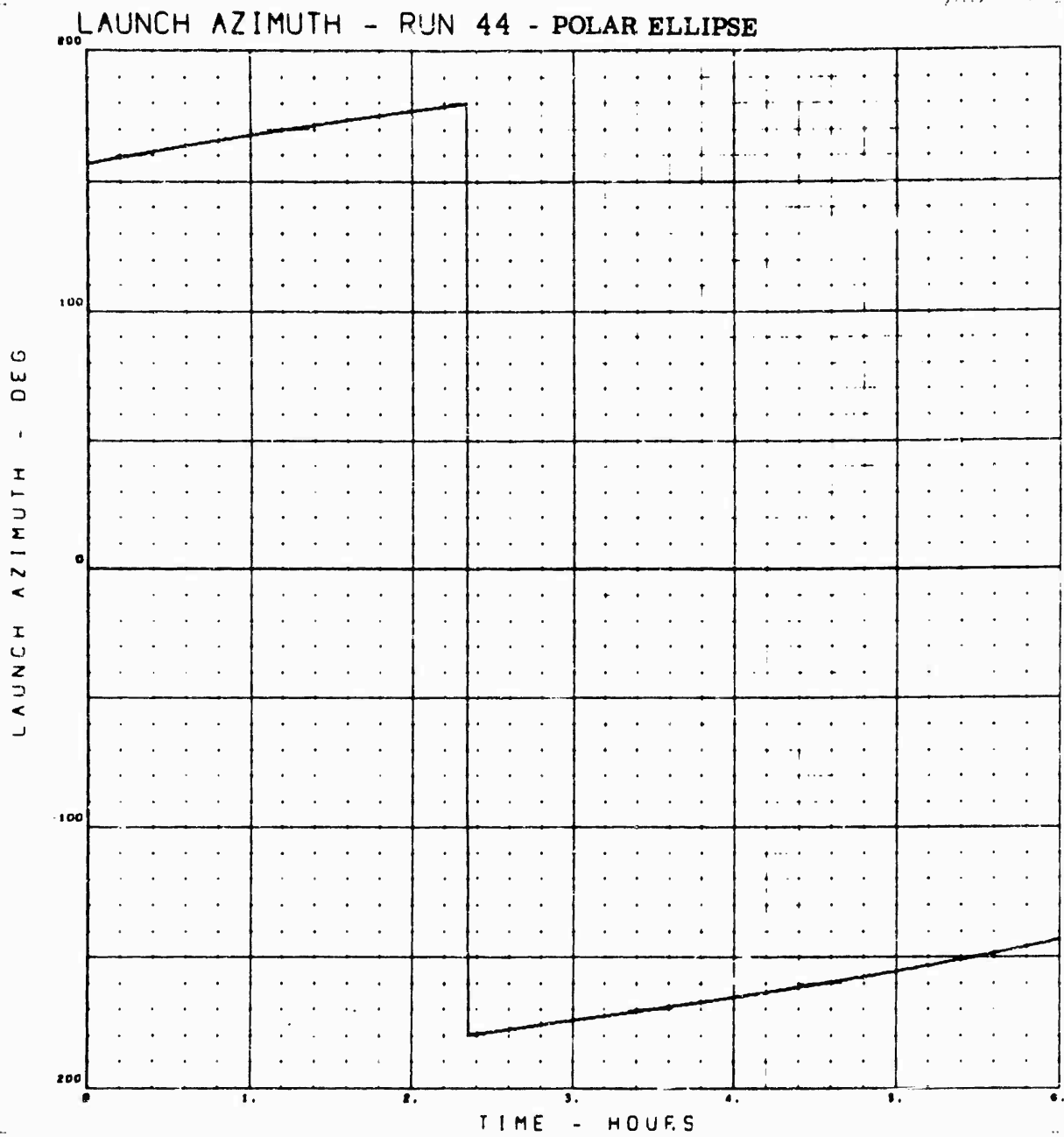
Figure 44. Launch Azimuth as a Function of Lift-Off Time

95
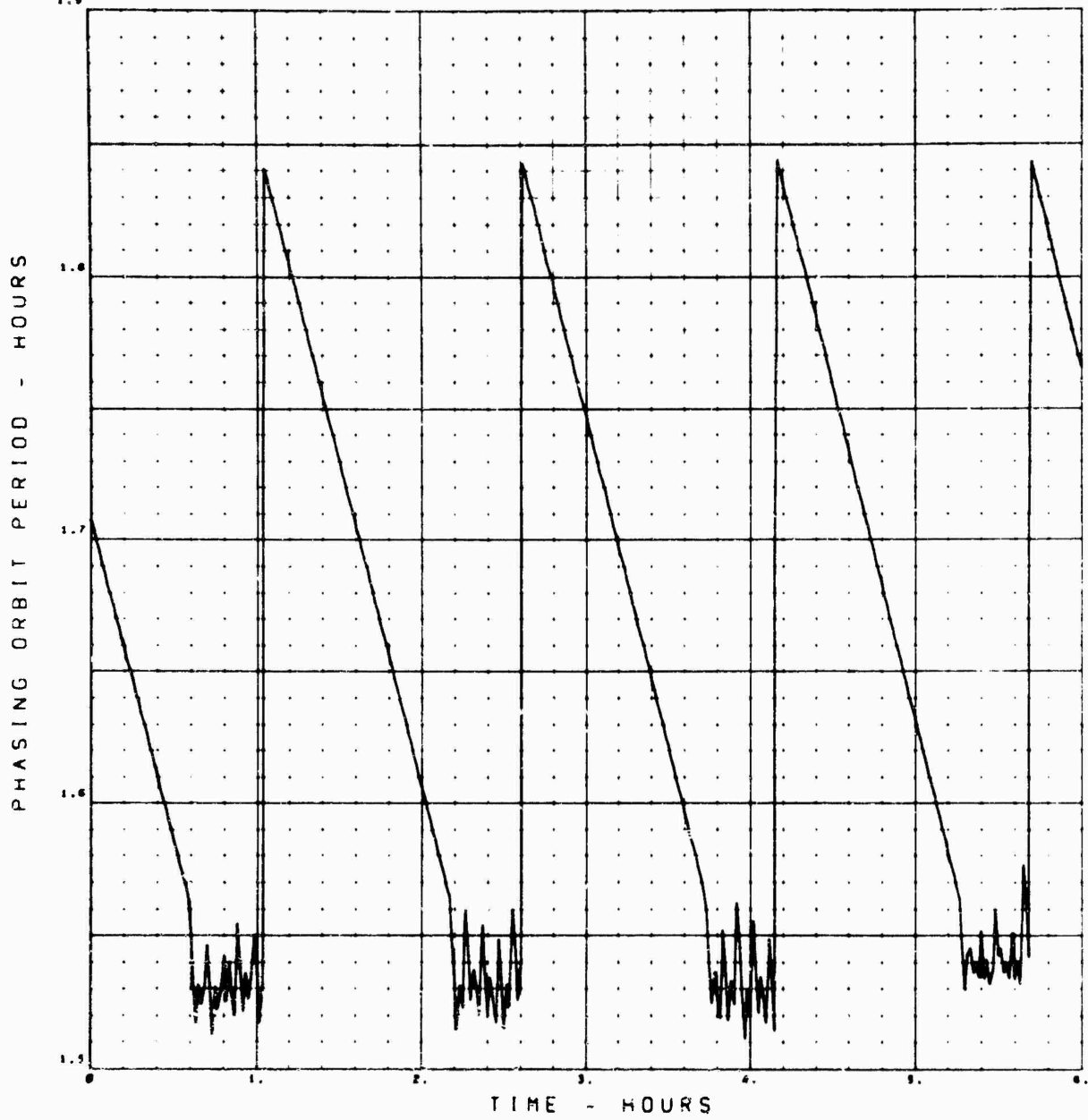
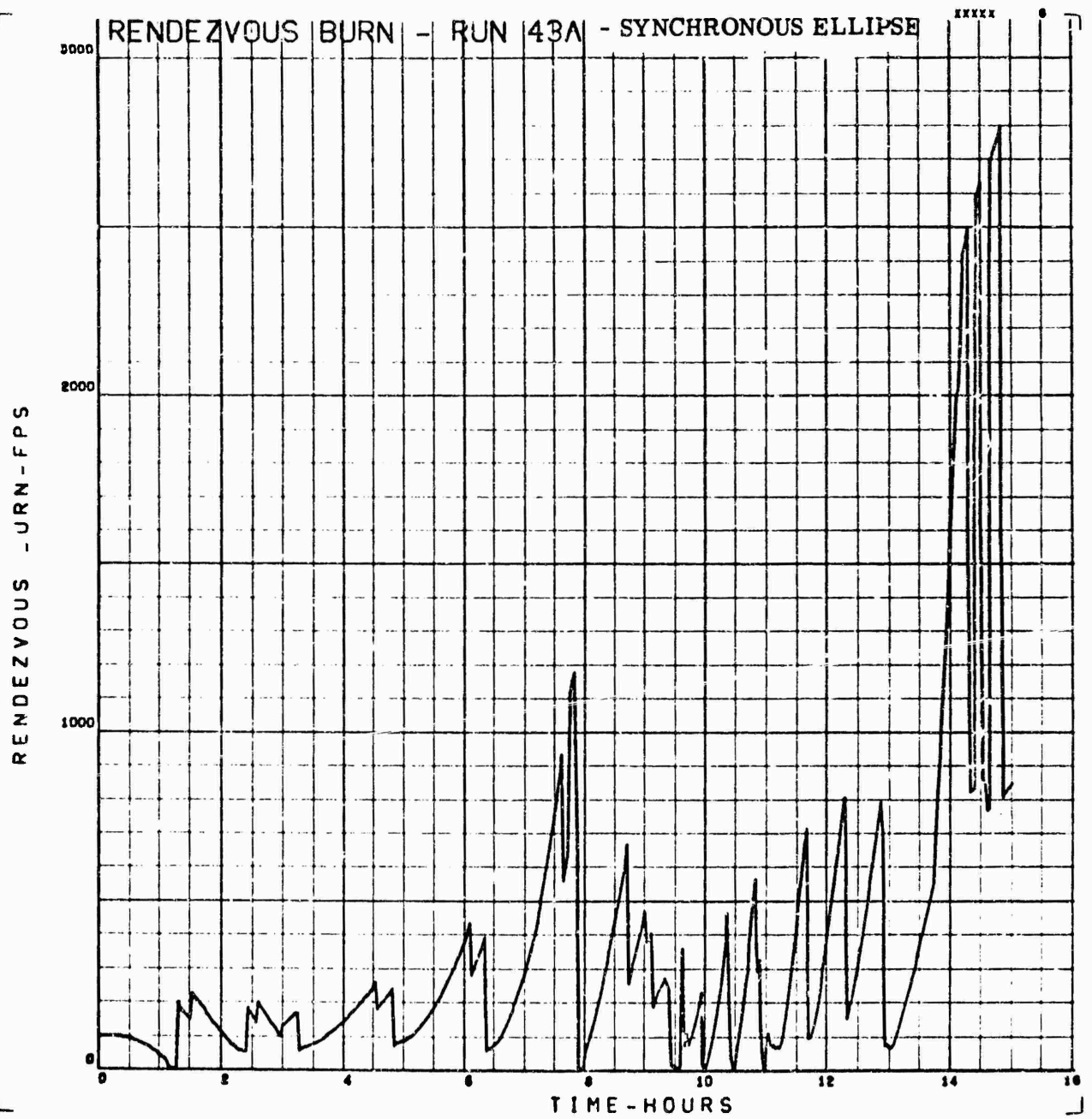Figure 45. Phasing Orbit Period as a Function of Lift-Off Time

96

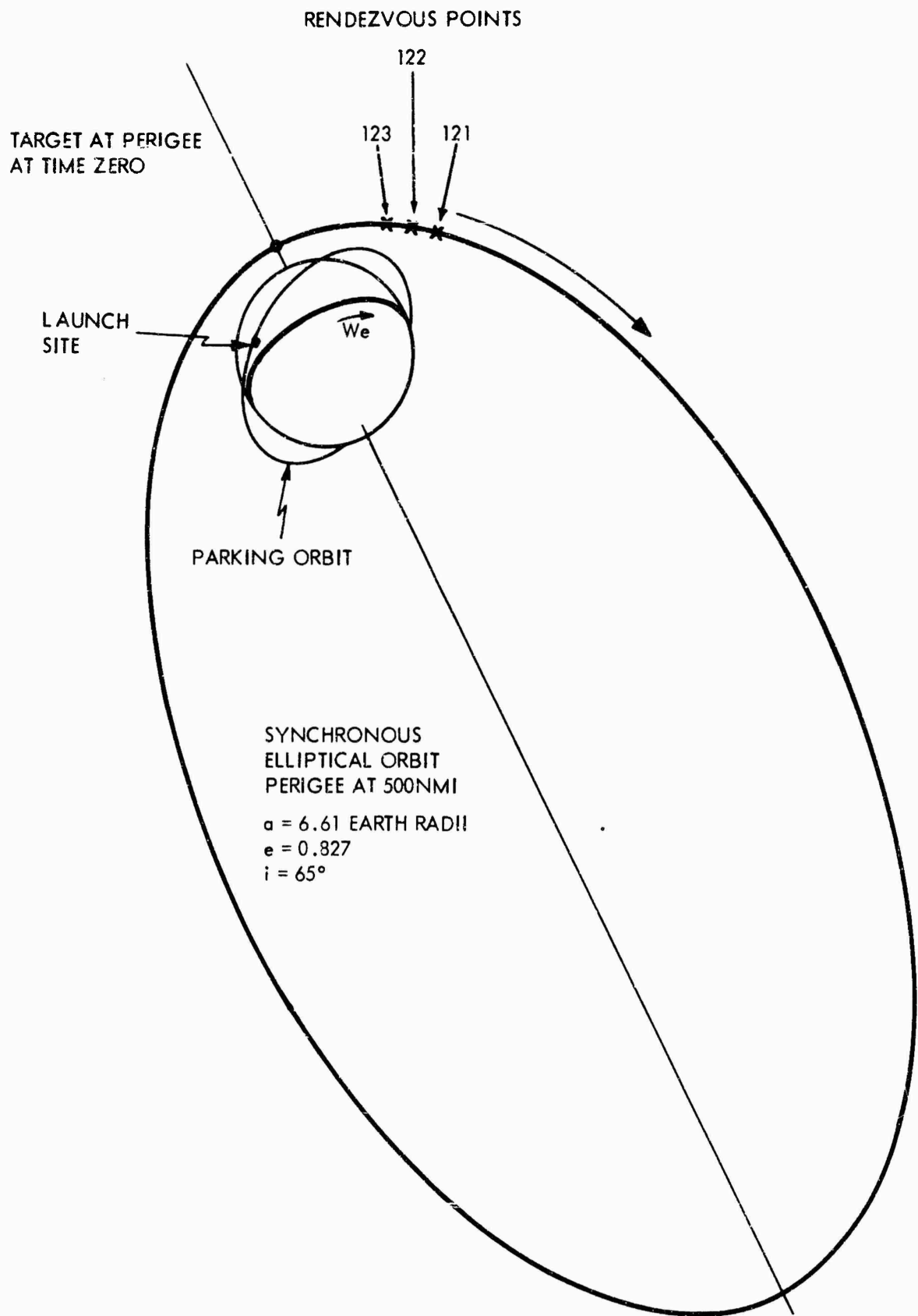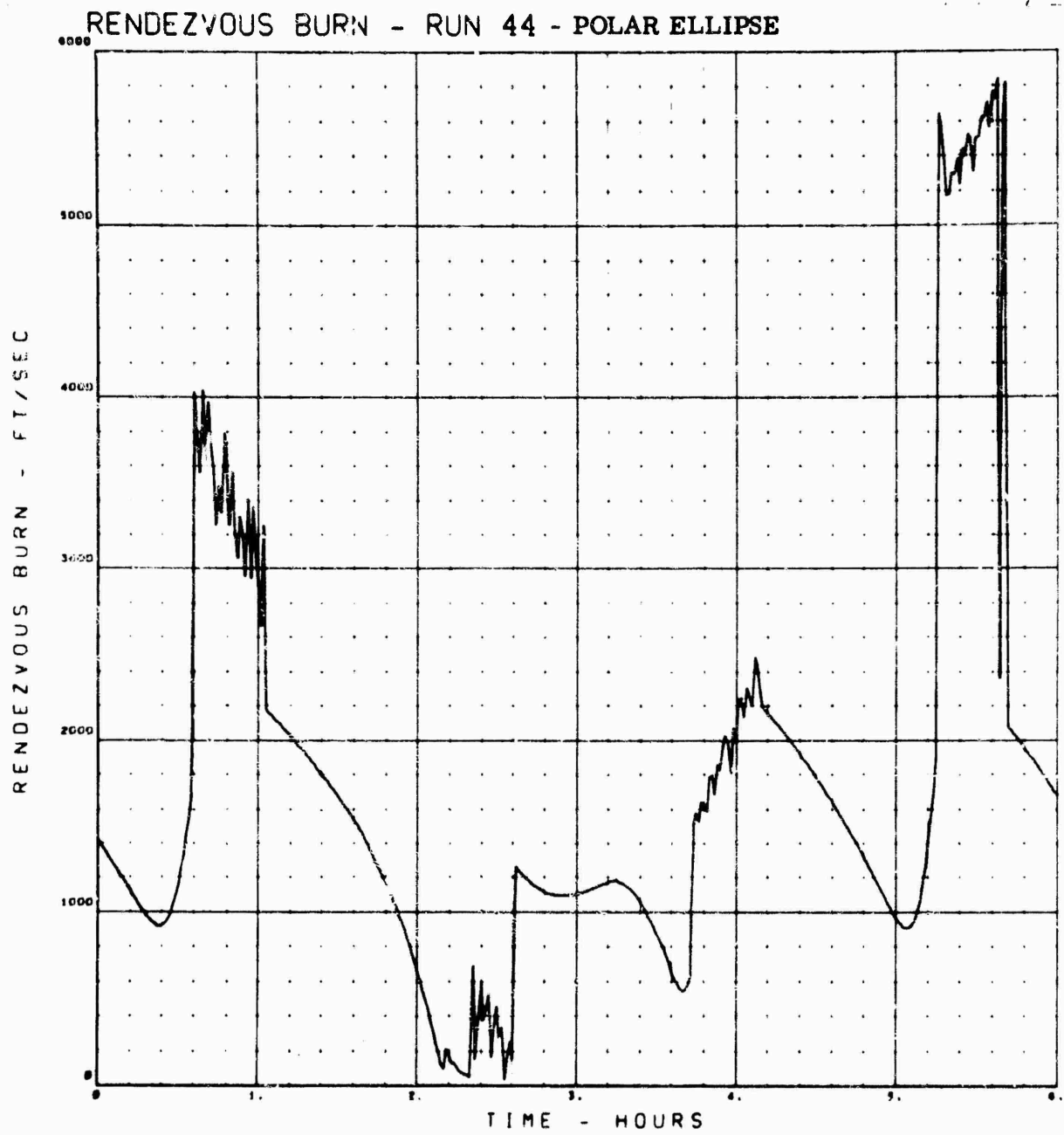Figure 46. Rendezvous Burn as a Function of Lift-Off Time

97
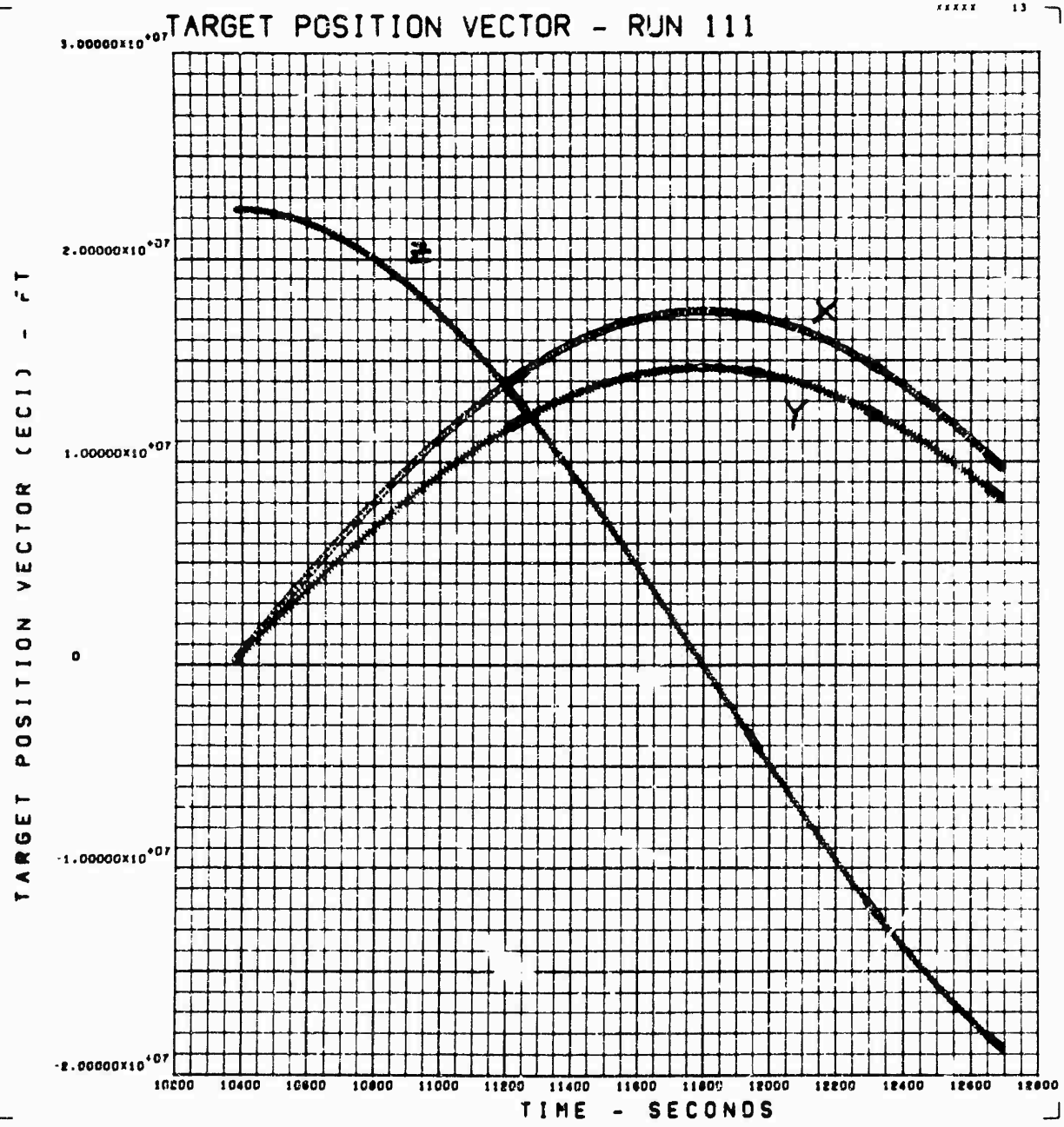
Figure 47. Target Position Vector as a Function of Time

98
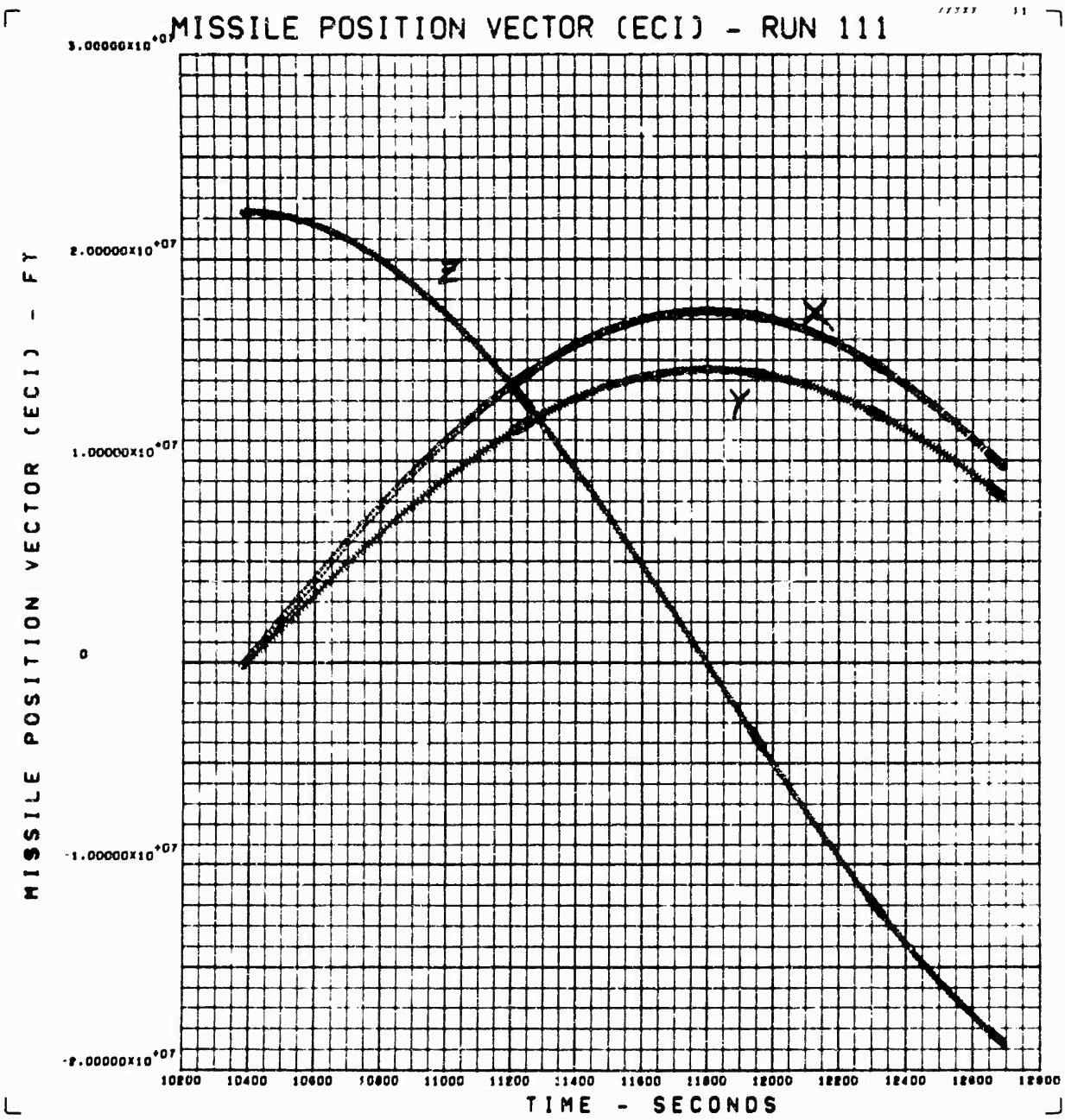
Figure 48. Missile Position Vector as a Function of Time

99
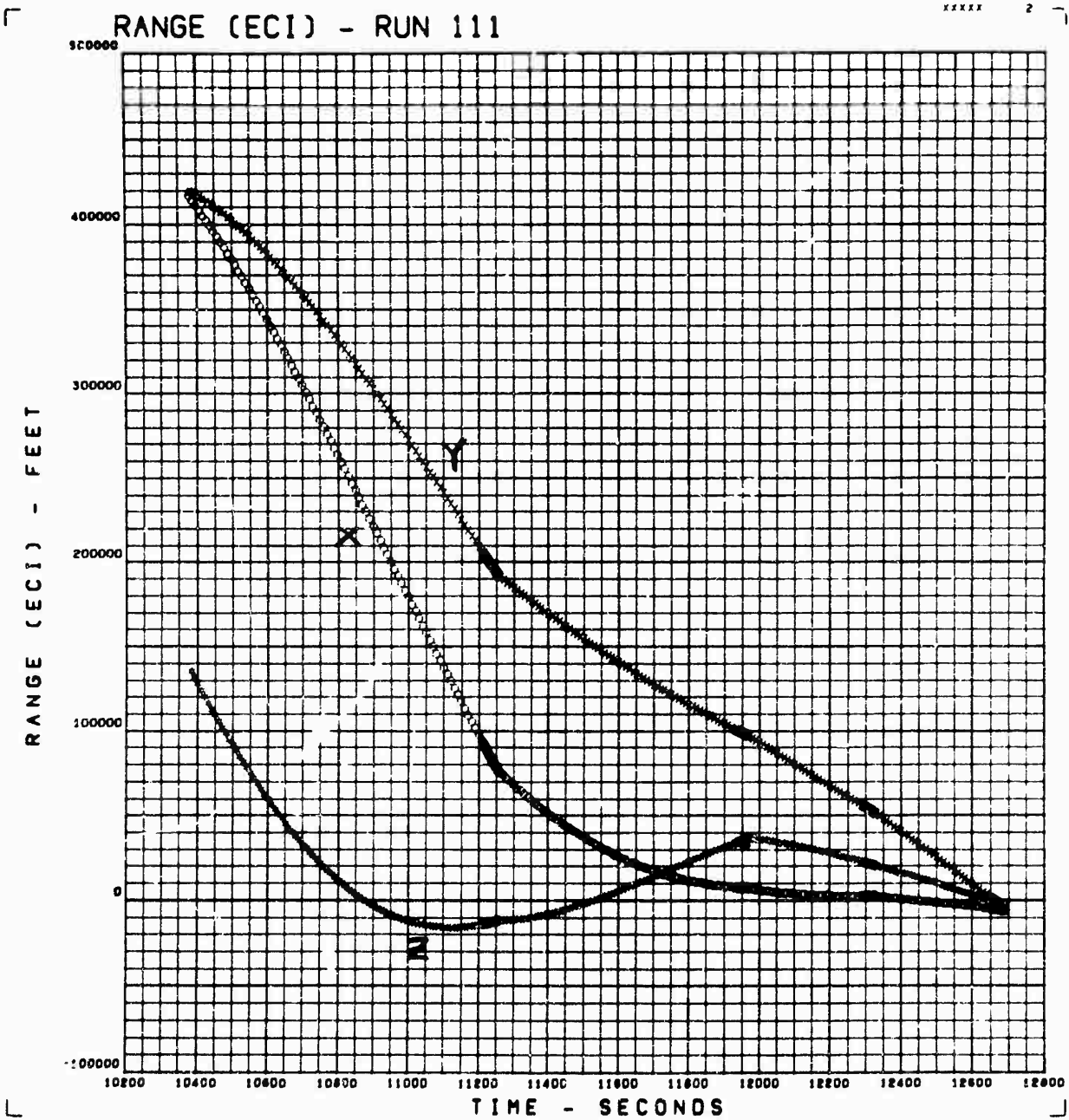
Figure 49. Range (ECI) as a Function of Time

100
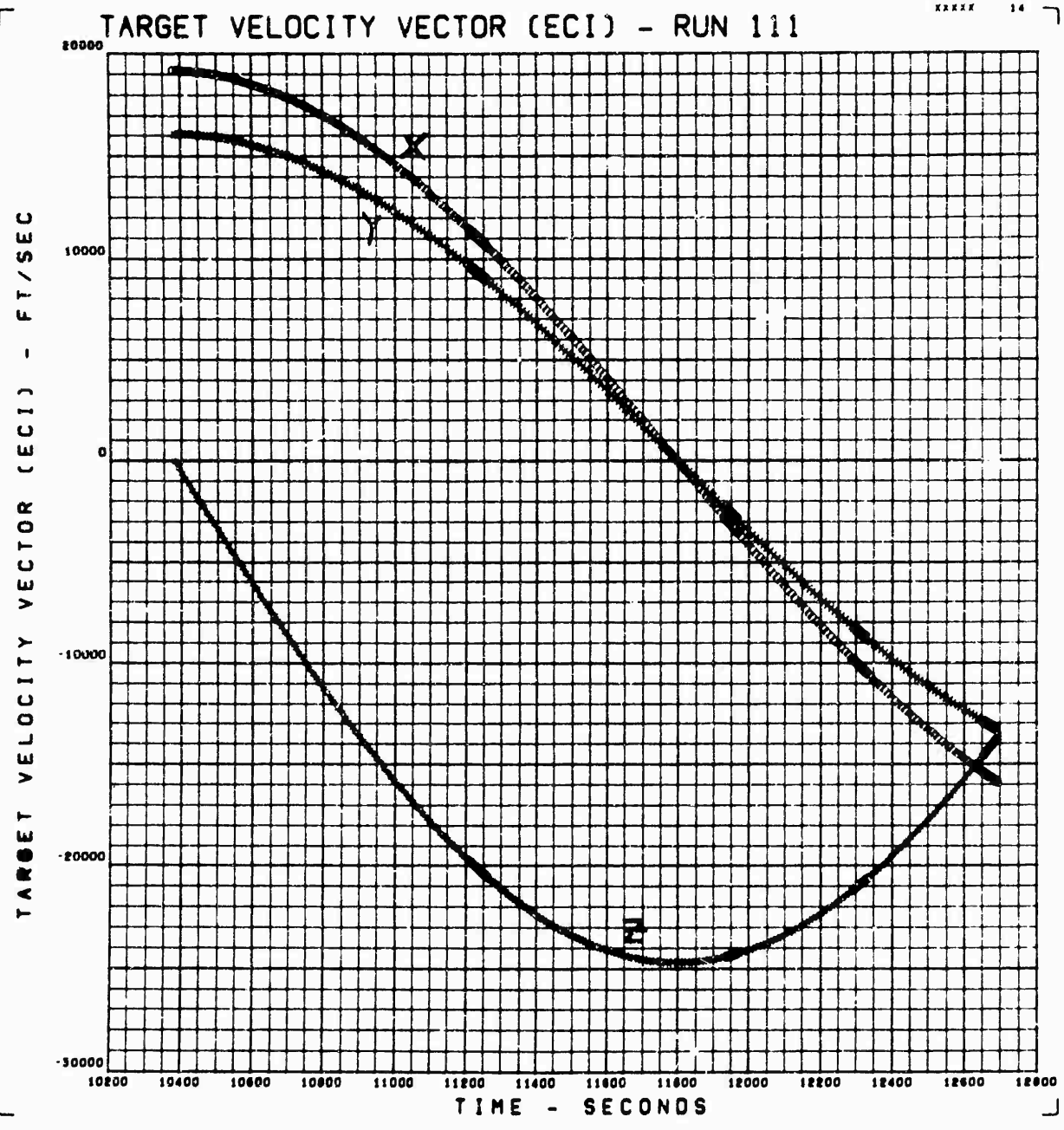
Figure 50. Target Velocity Vector (ECI) as a Function of Time

101
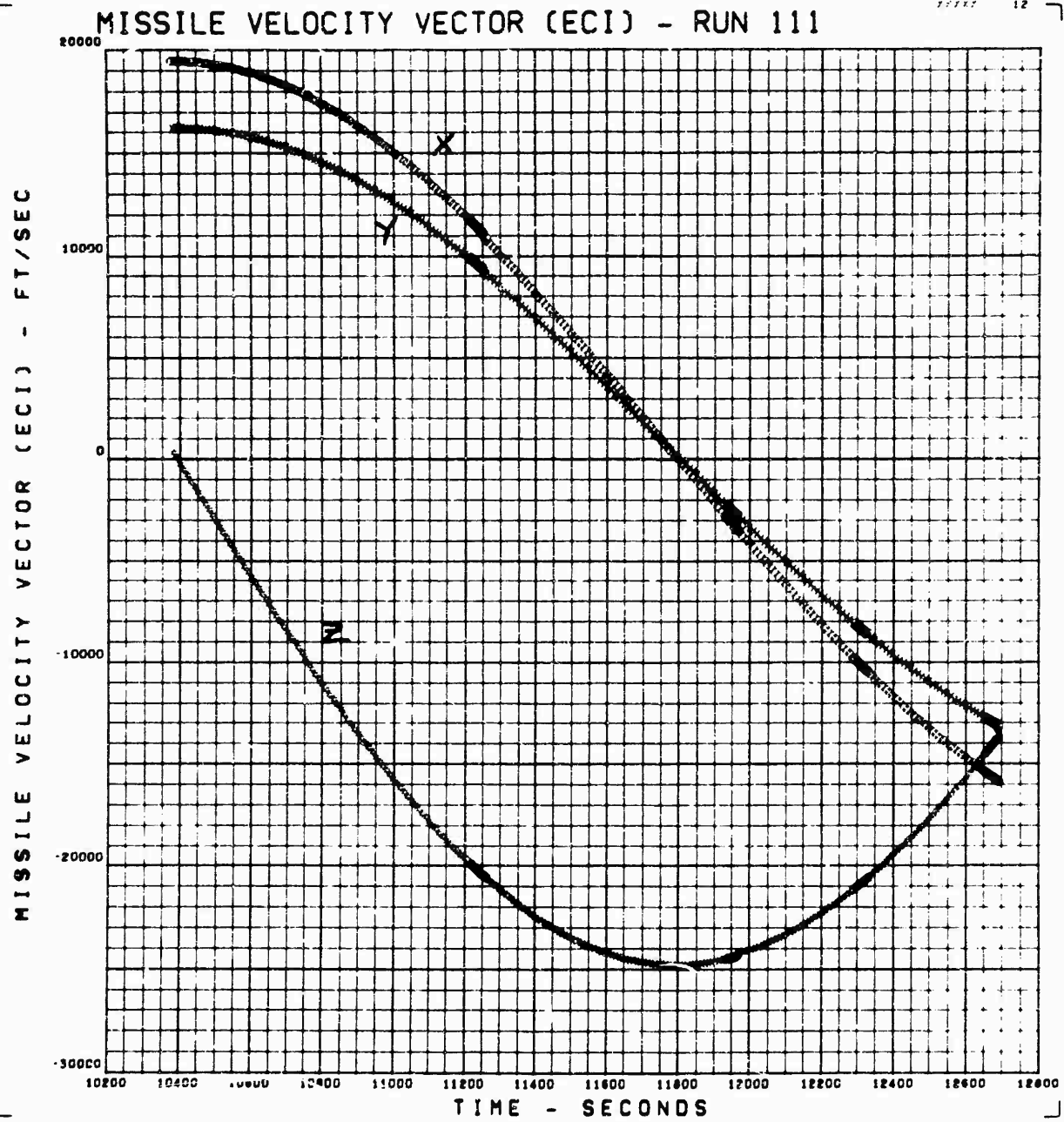
Figure 51. Missile Velocity Vector (ECI) as a Function of Time

102
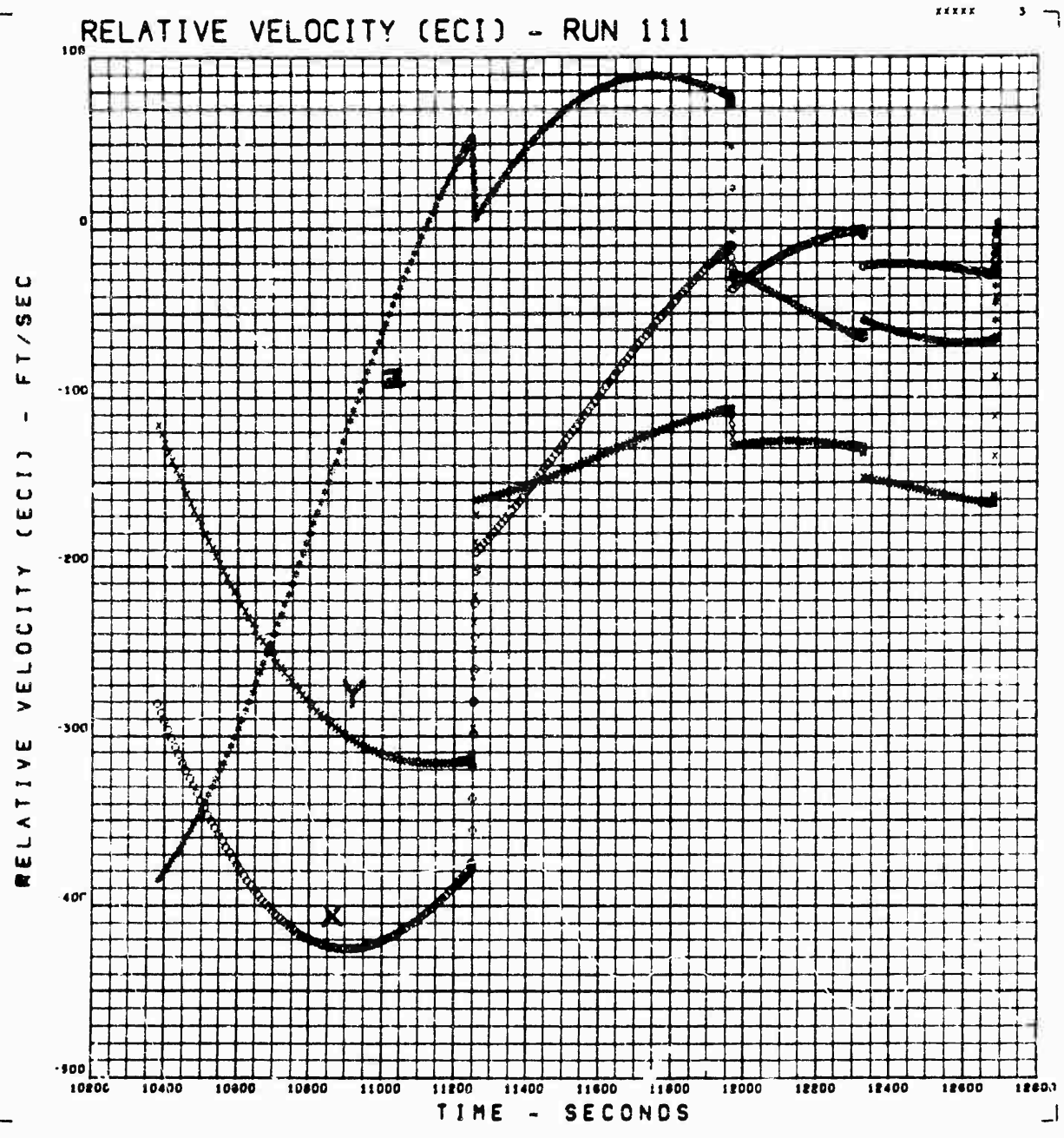
Figure 52. Relative Velocity (ECI) as a Function of Time

103
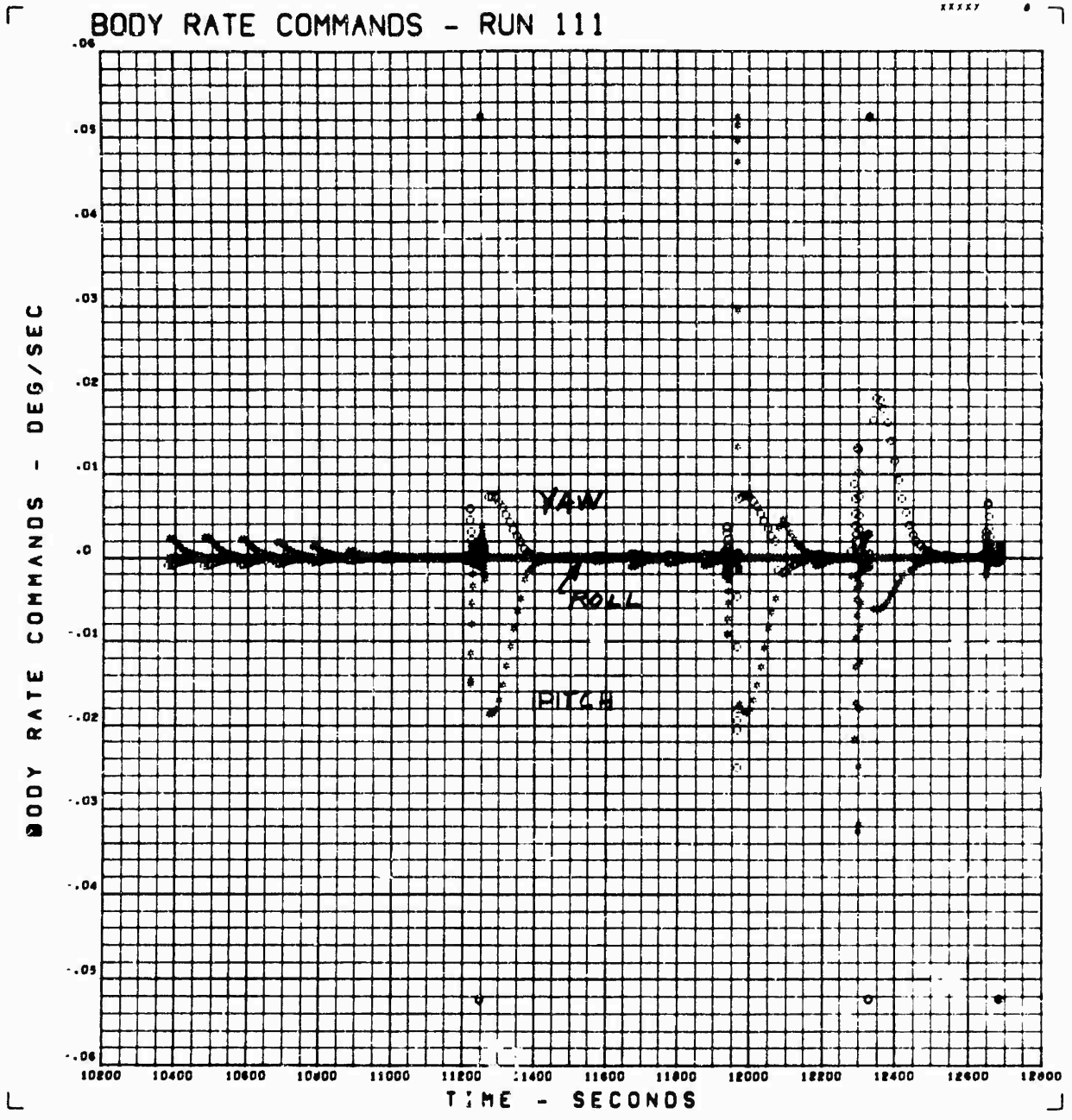
Figure 53. Body Rate Commands as a Function of Time

104
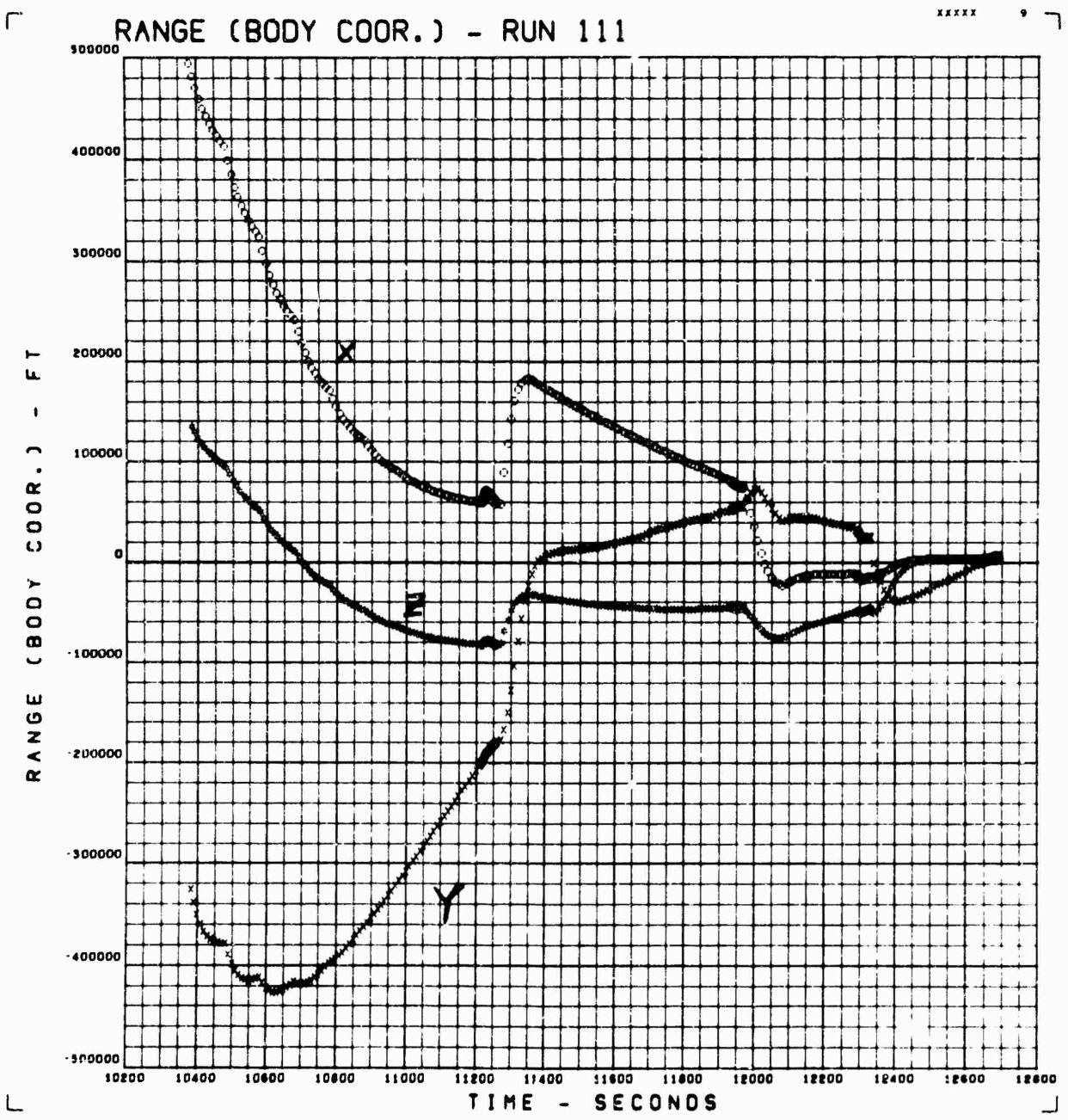
Figure 54. Range as a Function of Time
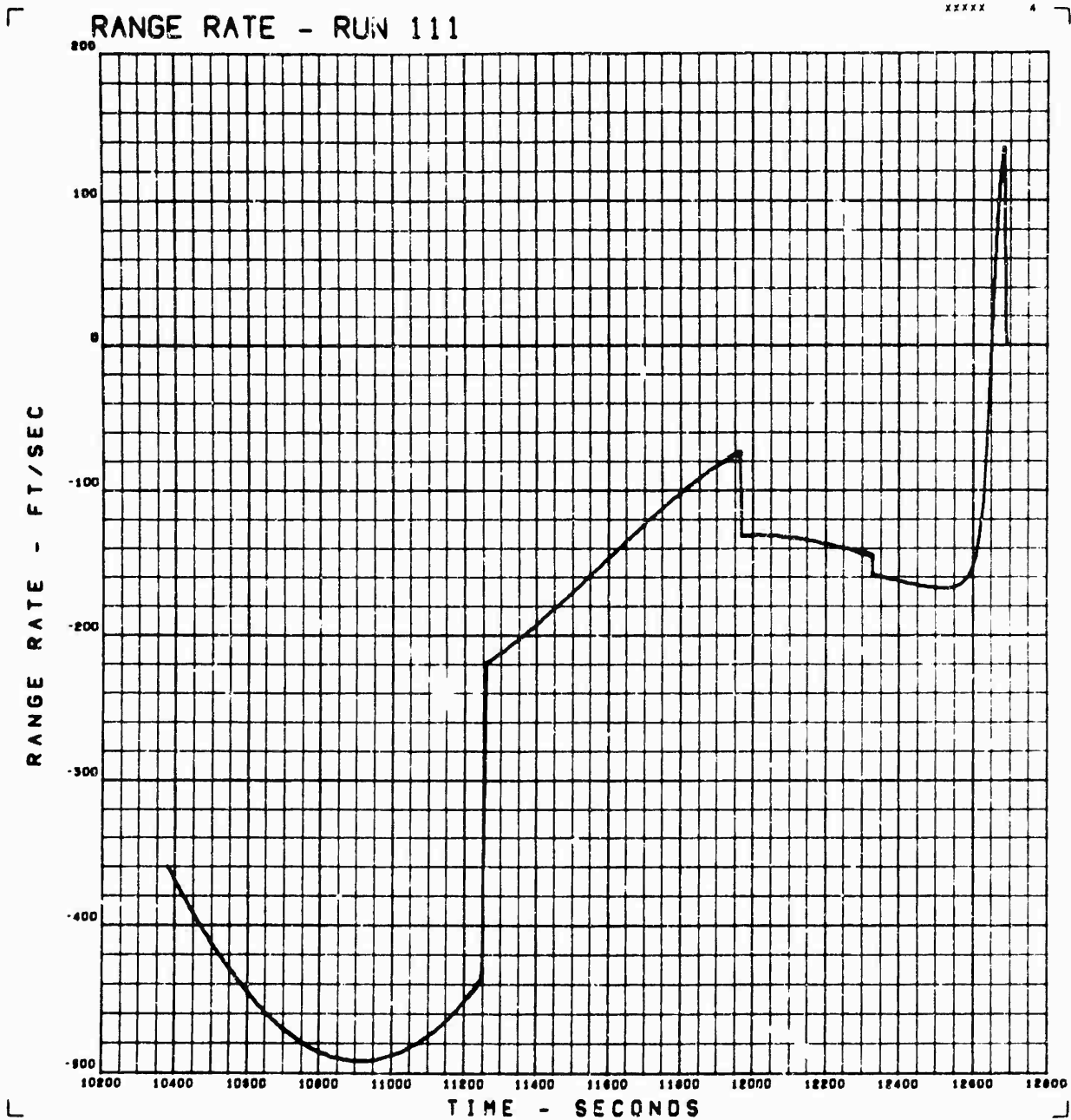
Figure 55. Range Rate as a Function of Time

106
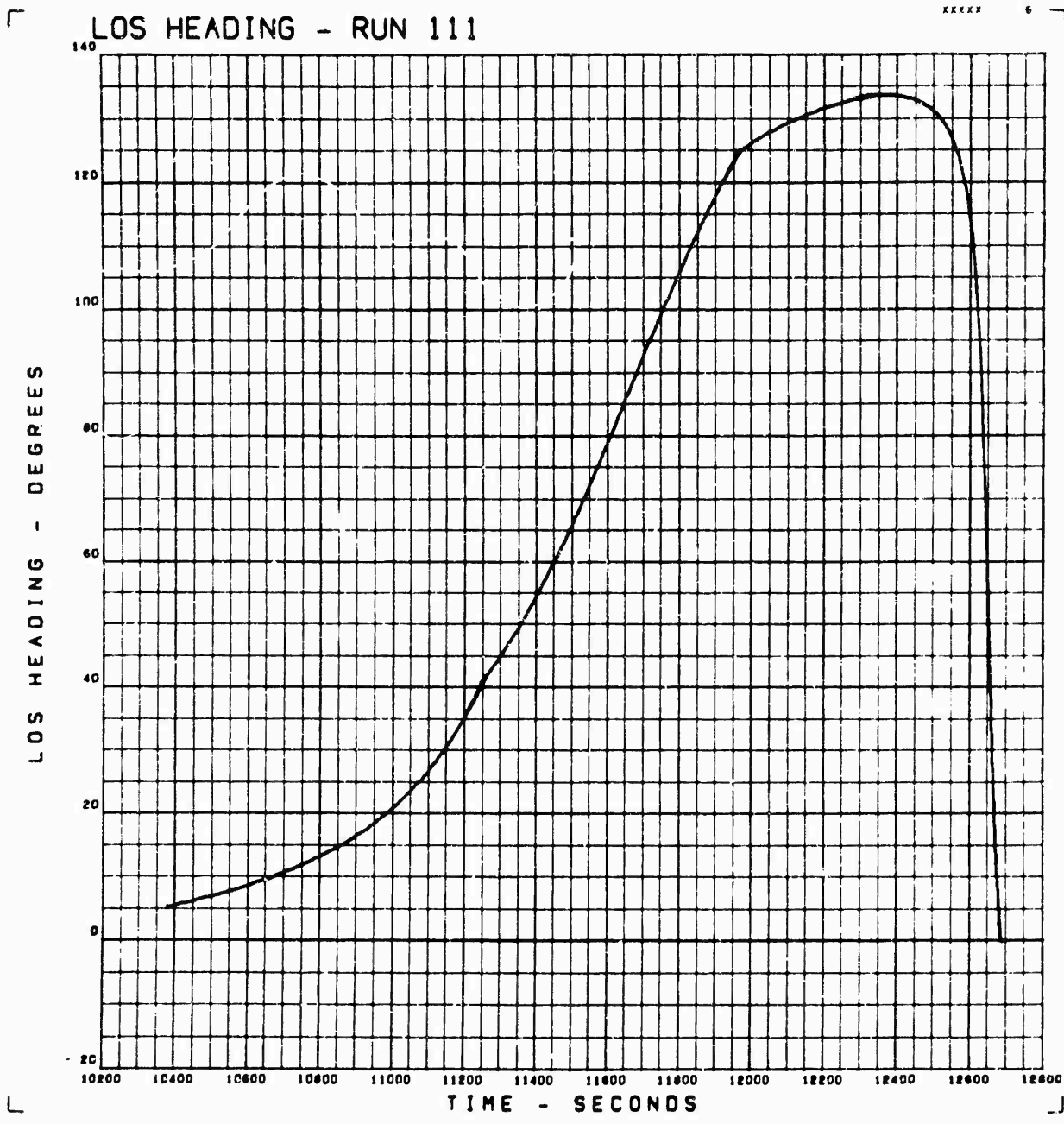
Figure 56. Line of Sight Heading as a Function of Time

107
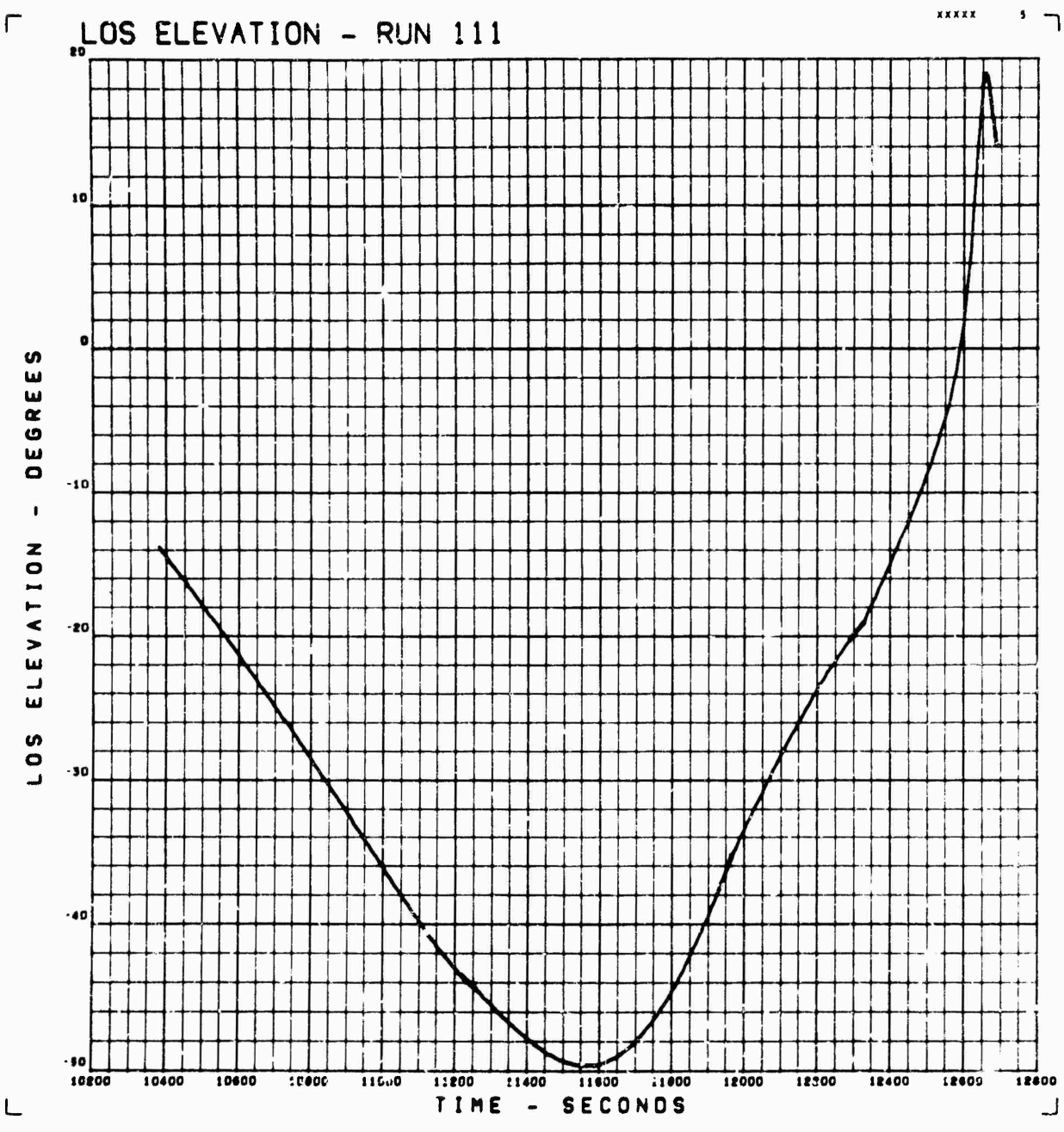
Figure 57. Line of Sight Elevation as a Function of Time

108
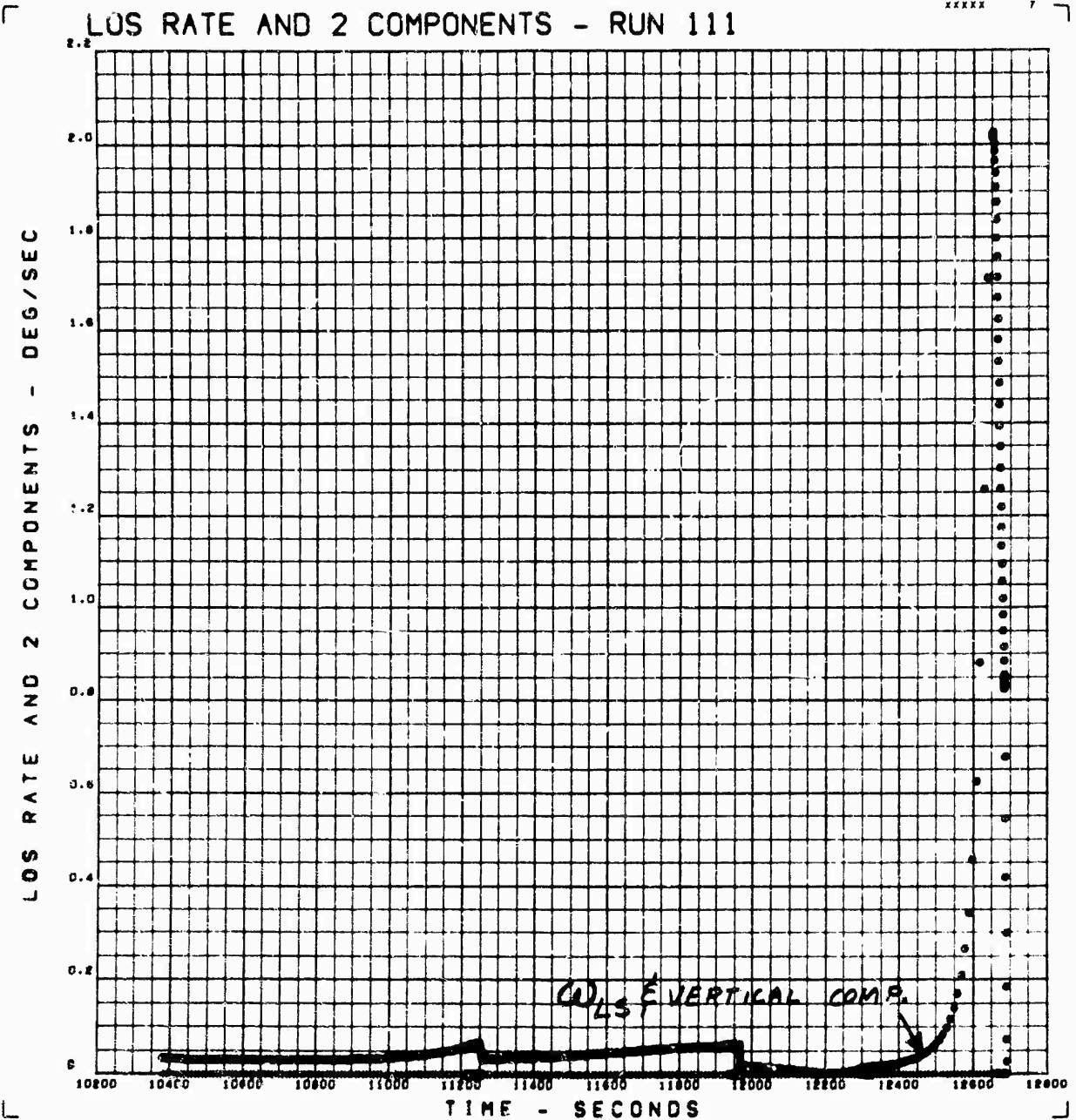
Figure 58. Line of Sight Rate and Two Components as a Function of Time

109
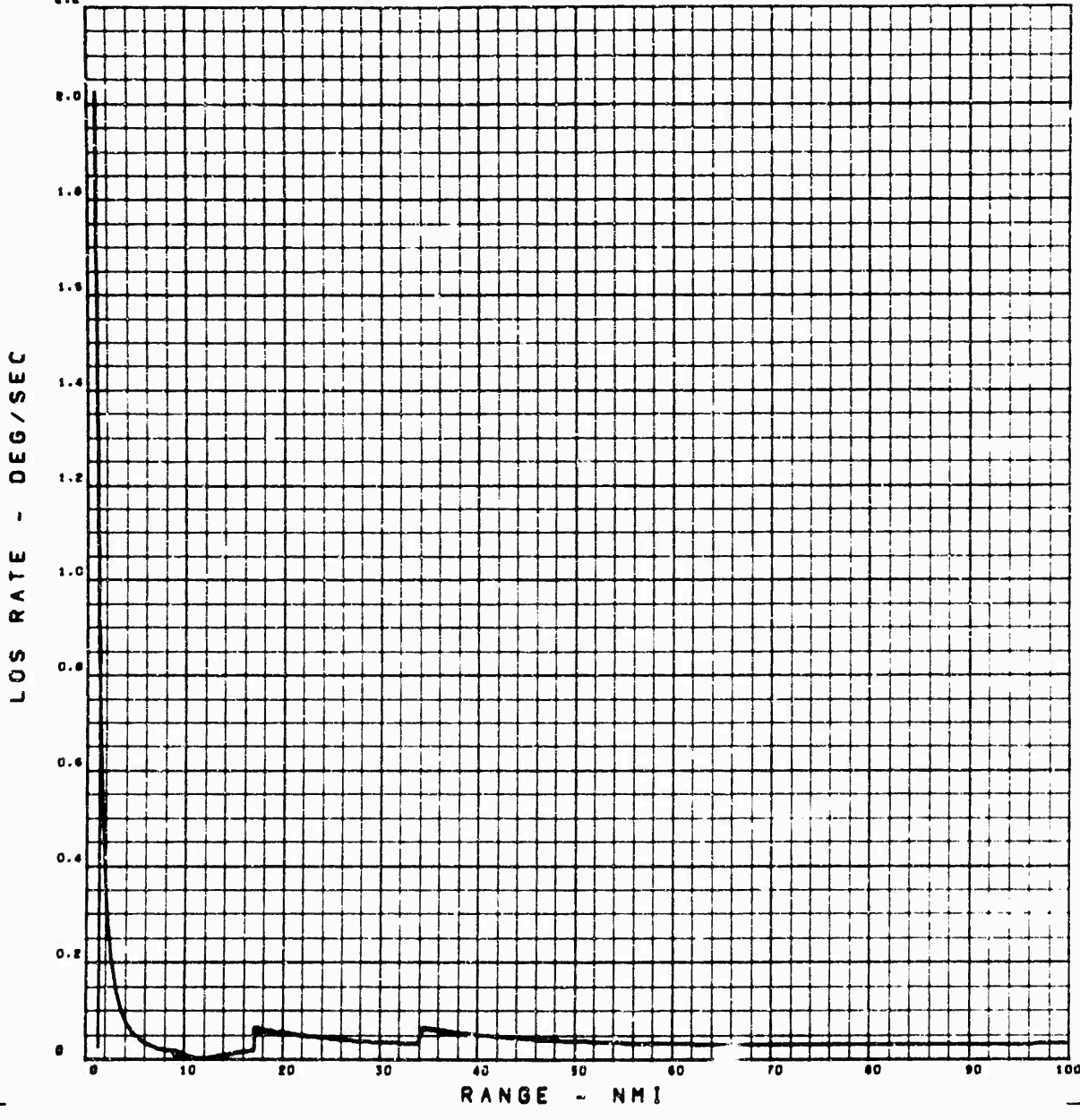
Figure 59.   Line of Sight Rate as a Function of Range

110
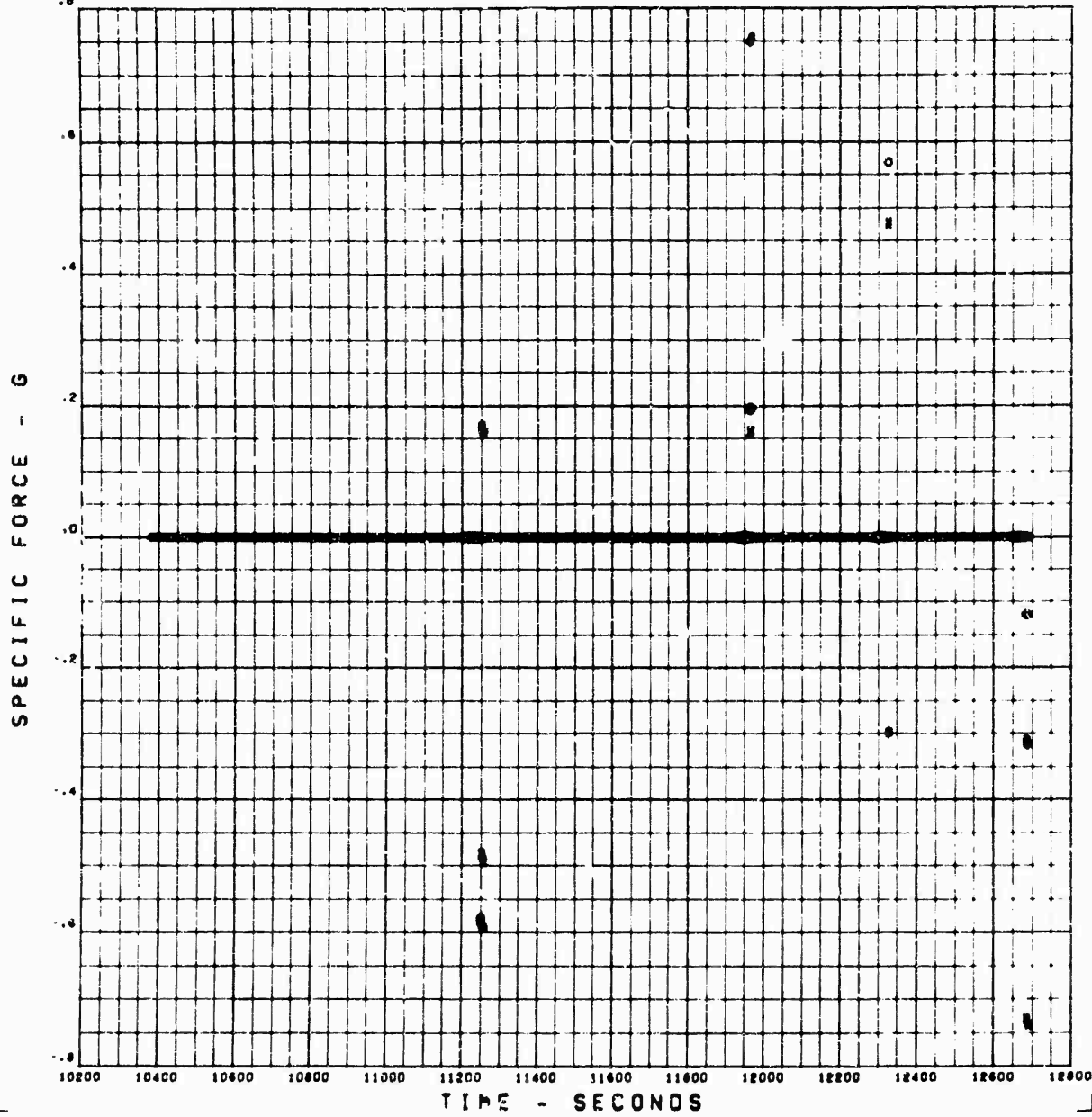
Figure 60. Specific Force as a Function of Range

111

SECTION V

VARIABLE POINT APPLICATIONS

1. **Introduction.** The analysis and simulation results on Variable Point Guidance and Targeting Program have shown that a guidance and targeting method has been developed which covers a wide variety of space missions. The software characteristics in the present state of development can provide both efficient flight plans and guidance commands within one second from insertion of mission objective to potential lift-off time from lift-off through ascent, mid course to terminal phase of the following typical missions:

Satellite Rendezvous (Manned or Unmanned)

    1.) Space station resupply
    2.) Emergency rescue

Single or Multiple Objectives for a Single Launch

    1.) Entry into a circular or an elliptical parking orbit
    2.) Orbit transfer
    3.) Orbit plane change

Placement or Replacement of Payloads into Precise Orbits

    1.) Communications satellites
    2.) Synchronous, equatorial, polar and orbits of any inclination or eccentricity

2. **Satellite Rendezvous (Manned or Unmanned).** The simulation results of Section IV indicated the general capability for the Variable Point Guidance and Targeting to provide the launch operations trade-offs as well as efficient guidance for rendezvous with targets in extremely different orbits.

The targets used for demonstration of the capability of the system were intentionally chosen to be widely different and yet typical of some projected missions. The list of targets is given in Section IV, Table V.

The boost vehicle used in the simulation was representative of boosters currently available using both AMR and PMR as a launch site.

    a. **Space Station Resupply.** The space stations contemplated for the near future are in general of low altitude (i.e., MOL, 150 nautical miles). Future space stations may be higher.

112

Variable Point Guidance and Targeting, in its present form, is ideally suited to the task of space station re-supply since both efficient guidance and control signals and flight plans are continuously available. The computer output can provide rendezvous for any target situation. The same methods are recommended to be used for any vehicle, manned or unmanned. The results have shown that if the station is in circular or elliptical orbits the method is equally applicable. The launch windows available are only dependent upon vehicle capability. Variable Point Guidance and Targeting give maximum launch windows efficient trajectories, early rendezvous, and flexibility for responding quickly to payload changes and to non-standard target orbit characteristics.

The method of solution provides the flexibility to handle alternate missions so that as the number of possible stations in orbit or the number and frequency of missions increases, the need for more flexibility increases. In addition, if rendezvous is required when constraints such as sun line avoidance, launch azimuth restrictions or unavoidable delays are encountered the system flexibility aids in the probability of accomplishing the mission on time since a maximum launch window exists prior to the insertion of other constraints or the delays peculiar to a particular mission actually occurs.

b. Emergency Rescue. A versatile method such as the Variable Point Guidance and Targeting system becomes even more necessary if minimum reaction time is important. The emergency rescue or resupply problem has been considered by many workers as an eventual necessity. Variable Point Guidance and Targeting can handle any target orbit in any orientation. In one computation cycle, it produces a flight plan which can be immediately used for guidance of the rescue vehicle. This method or its equivalent is required for the rapid response to the unplanned situation that the term "rescue" implies. It has been shown that if there is doubt about the ephemeris of the vehicle to be intercepted and rendezvous is to be accomplished, a vehicle with Variable Point Guidance and Targeting can be launched, and an updated ephemeris sent up later when available.

An IR and D study was made by RCA (Reference 13) on the "Cost Effectiveness Study of MCL Resupply and Rescue". An earlier version of the Variable Point Flight Plan Generator portion of the program was used to aid in the generation of tradeoff curves as required for this effort. Three boosters were compared from the points of view of economy, performance, and reaction time. The results indicated that the Titan IIIC was best suited among the three vehicles considered for the rescue mission. The other vehicles considered were Atlas-Agena D and Saturn 1B.

Present operational guidance and targeting methods such as Gemini are not suitable for the unplanned emergency rescue because the planning for rendezvous into new orbits requires several weeks of effort.

The time spent in the planning phase can be costly and for unplanned situations the required reaction time would not generally meet the needs of the resupply or rescue situation involved. The RCA Variable Point Guidance and Targeting system not only can meet fast reaction time requirements, when it is needed, but it accomplishes the cost saving function of planning for any rendezvous mission even if the time to plan were available. As pointed out previously, the targeting, flight plan generator, and guidance are contained in a single flight-borne computer package.

3. Single or Multiple Objectives for a Single Launch. The Variable Point Guidance and Targeting method can be used to place any number of vehicles in any number of desired orbits. This means that one or more payloads may be mounted on a single booster, and

each of these proceeds to its required orbital destination. Alternately, a single vehicle may be placed sequentially into a series of desired orbits. It is necessary that specified end condition and navigation information on the vehicle's own position, velocity and time are known, or can be obtained.

a. Entry Into a Circular or Elliptical Parking Orbit. The entry into a specific orbit is equivalent to rendezvous with a pseudo target in the desired orbit. In the present program the phasing is automatically bypassed if there is not a target in the required orbit.

For synchronous satellite orbits of any eccentricity and various inclinations, nodal crossing, and argument of perigee, the desired target ephemeris is inserted as in any rendezvous problem which depends upon real target and precise knowledge of its time position velocity relationship. The recommended guidance and targeting for these missions is the standard rendezvous method.

4. The Flight Plan Generator as a Launch Operations Aid. As pointed out in Section III, the Variable Point Guidance and Targeting software performs the following functions:

> 1.) Target ephemeris conversion
> 2.) Flight plan generation (targeting)
> 3.) Guidance and control commands.

Functions 1.) and 2.) can be performed by a portion of the total Variable Point Guidance and Targeting system. This portion, called the flight plan generator, can provide launch operations with trade-off data.

There are at present three small programs based on the Variable Point Guidance and Targeting subroutines which were developed to aid in checking out new ideas, and also to define flight plans for various contemplated space missions. These programs can be run on both the RCA 355 and the IBM 7090 and 7094 computers. In addition, the SC4020 plot routine has been tied in so that tradeoff charts are readily produced.

These programs have been proved to be useful in their own right. Specifically, they provide the launch trade-offs data that is so useful to a launch commander. The launch trade-off data is presented as a function of time of lift-off. From the above mentioned programs, from one to four possible choices of rendezvous trajectories can be presented, involving various fuel usages and mission times. This data can be matched to other constraints such as range safety, readout time and location, fuel budget, etc. The data available as outputs of these programs are as follows:

> 1.) Total propellant required
> 2.) Time of flight
> 3.) Time of mission completion
> 4.) Launch azimuth
> 5.) Total plane change angle required
> 6.) Location and time of each burn
> 7.) Number of engine restarts
> 8.) Change in velocity and amount of plane change at each burn
> 9.) Total launch window.

114

The data is useful to answer such questions as the following:

1.) Earliest possible lift-off time
2.) Latest time of lift-off for successful mission completion
3.) The time of lift-off for minimum fuel
4.) Time of lift-off for a particular launch azimuth
5.) Time of lift-off for minimum time to mission completion.

In an operational situation, this data is computed in real time by subroutines of the Variable Point Guidance and Targeting flight plan computations in the vehicle guidance computer. It may be desirable to have a separate special or general purpose ground computer to compute a properly integrated combination of the above subroutines for the purpose of providing the launch commanders with the trade-off data for a 12 or 24 hour look into the future. This will aid him in selecting the best time of launch, scheduling operations, and making rapid changes to plans in case of unexpected delays. At present the above information is printed in tabular form or as SC4020 plots. Automatic display equipment could be used to present the above data as fast as it is computed.

SECTION VI

RECOMMENDATIONS FOR FUTURE WORK

1. Introduction. The development of the Variable Point Guidance and Targeting Program has progressed by a series of evolutionary changes. The program in its present state could be used for guidance and targeting from launch through midcourse to the terminal phase in a typical rendezvous mission. There are, however, several areas where further operational improvements should be made before the program is adapted to a specific rendezvous application. See Table X for recommended follow-on schedule.

There are also many non-rendezvous missions in which rapid flight plans would be useful. The requirement to overfly specific points on the surface of the earth is needed in most missions for the purpose of maintaining communication through telemetry stations.

Range safety must be considered in new missions.

The implementation of the Variable Point Guidance and Targeting technique to specific applications requires consideration of all the detailed hardware and system integration constraints.

General improvements in the equations and logic which would increase the flexibility and efficiency of the system and extend the applicability of the program are discussed in Paragraph 2.

    a. Discussion. An optimized single burn ascent into a low altitude parking orbit should be included in the program. Consideration of yaw turns should be included to increase efficiency in azimuth limited launches. Efficiency can also be increased by comtining yaw turns with optimal placement of the line of nodes.

There are available several simple and close to optimal solutions to the single burn to orbit requirement.

These methods should be examined and compared to the more sophisticated methods. One method should be integrated into the simulation program.

    b. Automatic Range Safety Implementation and Simulation. The purpose of this task is to implement Range and Mission Safety requirements into the Variable Point Targeting System so that it automatically seeks a flight plan which avoids constraints. The items to be included in safety considerations are constraints on launch azimuth and on impact point of various stages of the boost vehicle.

Ea ly integration of range and mission safety into the program will allow continuous study of methods to maximize performance and launch opportunities in the constrained situation. Means will be examined for utilizing off-set points and dog-leg maneuvers as reasonably efficient means of working around the constraints.

117

Table X. Recommended Follow-On Schedule

	1	2	3	4	5	6	7	8	9	10	11	12	13	14	15	16	17	18
SIMULATION COMPATIBILITY																		
REVIEW AND MODULARIZE, PROGRAM, DEBUG AND DEMONSTRATE																		
PROGRAM IMPROVEMENT ASCENT REENTRY ORBIT MANEUVERS																		
COMPLETE CODING 1024																		
CHECKOUT DEBUG																		
FLIGHT TEST																		

118

c.   Flight Plans for Overflight of One or More Specific Sites. All space missions up to the present time have been planned to overfly telemetry stations and for monitoring system performance during periods of thrust, and during other operational sequences.

Flight planning for overflight of points on the surface of the earth should consider range safety limitations.

d.   Terminal Guidance Studies. The present variable point scheme for ascent operates on a target ephemeris input as its basic knowledge of target data. The scheme can be carried into the terminal phase, achieving rendezvous to the accuracy of the target ephemeris itself. In general, this is not sufficiently accurate for typical missions. Rendezvous accuracy can be improved with essentially no change to the variable point formulation if a means existed for obtaining a more accurate ephemeris than that which was used to control ascent. The radar or other sensor measurements on the target in the terminal phase provide the necessary information for improving the ephemeris.

It is proposed to develop equations and incorporate them into the variable point formulation which will convert radar measurements on the target to an improved target ephemeris. An auxiliary problem is that of smoothing, that is, using redundant data acquired over a period of time to reduce the statistical error of the prediction.

e.   Minimum Reaction Time to Mission Completion. The intent of this task is to extend the VPG program to include the minimum reaction time rendezvous trajectory compatible with the full utilization of a prescribed propellant budget, extending the capability still further toward the emergency rescue mission.

There are generally times in a typical launch window when a short range direct ascent (two-burn) rendezvous is possible. The aim point for direct ascent during this period of time can be continuously moved to that location resulting in earliest possible rendezvous.

As the time passes in such a situation the rendezvous point moves down-range and eventually passes a point where accomplishment of earliest rendezvous requires that additional burns must be added.

The approach is to develop the program for minimum time trajectories for direct ascent to rendezvous for a fixed propellant budget. In addition, part of the work of this task will be to develop the policy for transition from the direct ascent to the more general variable point policy.

The program would be exercised by simulation of particular cases and the results would be evaluated.

f.   Reentry Guidance Implementation . A tie in with re-entry guidance should be included to provide maximum flexibility in mission application.

The descent problem may be divided into two distinct steps that should be considered:

1.) Defining the pre-entry trajectory
2.) Guidance through the atmosphere to a landing point.

The primary consideration in planning the pre-entry trajectory is the entry conditions in velocity and flight path angle that will be encountered by the vehicle at entry to the atmosphere.

119

Of special consideration in this work is the requirement for quick return of the vehicle to a specified landing site.

The results of the Variable Point Guidance and Targeting additions necessary for preentry trajectory determination will be to:

1.) Guide the vehicle to a safe entry condition
2.) Position the nominal entry plane so that the vehicle can use its lateral ranging capability to insure landing at the specified site.

g. <u>Displays and Manual Control</u>. Displays for both launch operations and manned vehicles can be developed from the basic Variable Point Guidance and Targeting system. The purpose of this task is to define the information content and gross form of the displays required to allow both the astronaut and/or the launch conductor to monitor, modify or control system operation and performance.

h. <u>Error Analysis</u>. Guidance and Targeting Error Analysis. The purpose of this task is to provide a method for evaluating the accuracy with which the system is able to meet the desired mission objectives. The following subtasks should be performed:

1) Navigation Error Source Model. A mathematical model will be developed to represent the errors originating in the navigation system. This will include inertial instrument errors in the IMU, meaurement errors in the auxiliary sensors used for correcting the IMU, errors in ground-derived data on vehicle and target orbit elements, and errors due to approximations in the navigation equations, and round-off and truncation in the navigation program.

2) Guidance and Targeting Error Source Model. A mathematical model will be developed to represent the errors originating in the guidance and targeting system. This will include approximations in the prediction of the future vehicle and target states, and truncation and roundoff errors in the targeting and guidance programs.

3) Control Error Sources Model. A mathematical model will be developed to represent the errors originating in the control system for each stage. This will include uncertainty of thrust tail-off control errors remaining at engine cutoff, resulting from control system lags, aerodynamic parameter uncertainties and errors in the atmospheric model as they affect aerodynamic control.

4) Error Propagation Model. A mathematical model will be developed to represent the propagation of the errors due to the above sources throughout the mission. This will include both deterministic and stochastic errors and will present the resultant overall error in terms of deviation from the desired state at critical mission times.

APPENDIX I

DERIVATION OF EQUATIONS OF ORBITAL MOTION

1. Introduction. This appendix will derive certain equations pertaining to the motion of a particle in an inverse square centered force field. The form of the equations is chosen to conveniently fit the Variable Point Guidance and Targeting policy. Many of these equations are standard in celestial mechanics; a review for the interested reader. Other equations appearing here are not found in the general literature on orbital mechanics, but have been derived specifically to simplify the programming of real-time space guidance systems.

Consider a central force field in which a particle is at a distance $\overline{r}$. The acceleration of this particle can then be expressed as:

$$\ddot{\overline{R}} = f(R) \, \overline{I}_R \tag{AI-1}$$

where:

$f(R) \, \overline{I}_R$ is any force directed along $\overline{R}$.

Taking cross product of both sides of Equation (AI-1) with $\overline{R}$ gives

$$\overline{R} \times \ddot{\overline{R}} = 0 \tag{AI-2}$$

which is equal to:

$$\frac{d}{dt} (\overline{R} \times \dot{\overline{R}}) = 0 \tag{AI-3}$$

Integrating Equation (AI-3) gives:

$$\overline{R} \times \dot{\overline{R}} = \overline{h} \tag{AI-4}$$

121

where $\bar{h}$ represents a constant vector and is the angular momentum of the orbit of the particle.

Since $\bar{h}$ is a constant vector and is perpendicular to the orbit ($\bar{R}$ and $\dot{\bar{R}}$) the orbit defines a plane in space which passes through the force source.

The definition of the cross product gives:

$$|\bar{R}||\dot{\bar{R}}|\sin\beta = |\bar{h}| = Rv\cos\gamma = R^2\dot{\theta} \tag{AI-5}$$

where β is the angle between the radius and velocity vectors. The angle γ represents $(90 - \beta)$ and is measured from the local horizontal to the velocity vector.

Equation (AI-5) can be solved for time if $\bar{R}$ is known as a function of θ (equation of the path)

$$dt = \frac{R^2}{R_o V_o \cos\gamma_o} \, d\theta \tag{AI-6}$$

The path equation can be defined if the force field characteristics are known. For the inverse square central force field the acceleration is

$$\ddot{\bar{R}} = -\frac{\mu}{R^2} \frac{\bar{R}}{R} \tag{AI-7}$$

where μ is the product GM (product of gravity constant and mass of planet)

From Equation (AI-4) $\bar{R} \times \dot{\bar{R}} = \bar{h}$ which can be crossed with both sides of Equation (AI-7) to give

$$\frac{\ddot{\bar{R}}}{\mu} \times \bar{h} = -\frac{\bar{R}}{R^3} \times (\bar{R} \times \dot{\bar{R}}) = -\frac{1}{R^3}(\bar{R} \cdot \dot{\bar{R}})\bar{R} - (\bar{R} \cdot \bar{R})\dot{\bar{R}} \tag{AI-8}$$

Equation (AI-8) is the simplified giving

$$\frac{\ddot{\bar{R}} \times \bar{h}}{\mu} = \frac{\dot{\bar{R}}}{R} - \frac{\dot{R}}{R} \frac{\bar{R}}{R} \tag{AI-}$$

since Equation (AI-9) is known to be the following derivative

$$\frac{d}{dt}\left(\frac{\dot{\overline{R}} \times \overline{h}}{\mu}\right) = \frac{d}{dt}\left(\frac{\overline{R}}{R}\right) \qquad (AI-10)$$

Equation (AI-9) may be integrated to give

$$\frac{\dot{\overline{R}} \times \overline{h}}{\mu} = \frac{\overline{R}}{R} + e\,\overline{I}_e \qquad (AI-11)$$

where e is a constant and $\overline{I}_c$ is a unit vector along $\overline{e}$. Multiplying Equation (AI-11) by $\overline{R}$.

$$\frac{\overline{R}\cdot\dot{\overline{R}} \times \overline{h}}{\mu} = \frac{\overline{R}\ \ \overline{R}}{R} + e\,\overline{R}\cdot\overline{I}_e \qquad (AI-12)$$

also

$$\frac{\overline{R}\cdot\dot{\overline{R}} \times \overline{h}}{\mu} = \frac{\overline{R} \times \dot{\overline{R}}\cdot\overline{h}}{\mu} = \frac{\overline{h}\cdot\overline{h}}{\mu} = \frac{h^2}{\mu} \qquad (AI-13)$$

h^2/μ is a new constant which may be defined as

$$P = \frac{h^2}{\mu} \qquad (AI-14)$$

Using Equations (AI-13), (AI-14) and simple vector algebra, we can rewrite the vector Equation (AI-12) as the following scalar equation:

$$P = R + e_R \cos \nu \qquad (AI-15)$$

where   is the angle between $\overline{I}_e$ and $\overline{R}$. Solving for R, we obtain

$$R = \frac{P}{1 + e \cos \nu} \qquad (AI-16)$$

2. <u>Orbit Equations.</u> By comparing Equation (AI-16) with the equation of a general conic section in polar coordinates, we identify e as the eccentricity, ν, as the true anomaly,

and P as the semi-latus rectum of the conic section involved. Substituting the expression for "h" from Equation (AI-5) into Equation (AI-14), we obtain another useful form for P as follows:

$$P = \frac{R^2 V^2 \cos^2 \gamma}{\mu} = R \frac{V^2 \cos^2 \gamma}{\frac{\mu}{R}} \tag{AI-17}$$

It will be noted that μ/R is the square of the circular velocity at a radius R. Denote the circular velocity at radius R by V_c. With this definition, division of Equation (AI-17) through by R leads to

$$\frac{P}{R} = \frac{V^2}{V_c} \cos^2 \gamma = u^2 \cos^2 \gamma \tag{AI-18}$$

where $u = V/V_c$. From Equation (AI-18) the horizontal component of velocity is obtained from

$$V_H = \left(\frac{P}{R} \frac{\mu}{R} \right)^{1/2} \tag{AI-19}$$

For any point on the conic, such as an aim point, Equation (AI-16) may be written

$$R_a = \frac{P}{1 + e \cos \nu_a} = \frac{P}{1 + e \cos (\nu + \Omega)} \tag{AI-20}$$

where ν_a is the true anomaly to the aim point and Ω is the downrange angle between the present point (R, ν) and the aim point (R_a, ν_a).

Expanding Equation (AI-19) and converting to non-dimensional form

$$\frac{R_a}{R} = \frac{\frac{P}{R}}{1 + e \cos \nu \cos \Omega - e \sin \nu \sin \Omega} \tag{AI-21}$$

3. Path Equations in Terms of End Conditions. In order to write Equation (AI-21) in terms of initial conditions only, $e \cos \nu$ and $e \sin \nu$ should be written in terms of initial conditions. The downrange angle Ω may be obtained from the dot product to present position and aim point vectors. From Equation (AI-16)

124

$$e \cos \nu = \frac{P}{R} - 1 \tag{AI-22}$$

The function $e \sin \nu$ is obtained from the derivative of Equation (AI-16)

$$\frac{dR}{Rd\nu} = \tan \gamma = \frac{e \sin \nu}{1 + e \cos \nu} \tag{AI-23}$$

and since

$$\frac{P}{R} = 1 + e \cos \nu$$

$$e \sin \nu = \frac{P}{R} \tan \gamma \tag{AI-24}$$

Substituting Equation (AI-22) and (AI-23) into Equation (AI-21) gives

$$\frac{R_a}{R} = \frac{\dfrac{P}{R}}{1 + \left(\dfrac{P}{R} - 1\right) \cos \Omega - \dfrac{P}{R} \tan \gamma \sin \Omega} \tag{AI-25}$$

from Equation (AI-25) the semi-latus section ratio, or the horizontal velocity ratio squared is obtained in terms of initial conditions.

$$\frac{P}{R} = \frac{1 - \cos \Omega}{\dfrac{R}{R_a} - \cos \Omega + \sin \Omega \tan \gamma} \tag{AI-26}$$

and similarly

$$\frac{P}{R_a} = \frac{1 - \cos \Omega}{\dfrac{R_a}{R} - \cos \Omega - \sin \Omega \tan \gamma_a}$$

Equating P in the above two Equations (AI-26) gives the relation between any two flight path angles on a trajectory.

125

$$\tan \gamma = \frac{\sin \Omega}{1 - \cos \Omega} \left(1 - \frac{R}{R_a}\right) - \frac{R}{R_a} \tan \gamma_a \qquad (AI\text{-}27)$$

4. **Required Velocity at the End Points.** The horizontal component of velocity at the point at radius R was given in Equation (AI-19) as

$$V_H = V \cos \gamma = \left(\frac{P}{R} \frac{\mu}{R}\right)^{1/2}$$

The radial component is then obtained by combining Equation (AI-19) and (AI-27) which gives the flight path angle relationship at the end points

$$V_R = V \sin \gamma = V_H \tan \gamma \qquad (AI\text{-}28)$$

The velocity components entering the final point are then:

$$V_{Ha} = V_a \cos \gamma_a = \left(\frac{P}{R_a} \frac{\mu}{R_a}\right)^{1/2} = \frac{R}{R_a} V \cos \gamma$$

and

$$V_{Ra} = V_a \sin \gamma_a = V_{Ha} \tan \gamma_a \qquad (AI\text{-}29)$$

The required reference velocity components which are used to derive $\overline{V}_g$ are

$$V_{req} \cos \gamma_{req} = \left(\frac{P}{R} \frac{\mu}{R}\right)^{1/2} = V_{H\ req}$$

and

$$V_{req} \sin \gamma_{req} = V_{H\ req} \tan \gamma_{req} \qquad (AI\text{-}30)$$

transforming to earth centered coordinates

$$\overline{V}_{req} = \overline{1}_R V_{req} \sin \gamma_{req} + \overline{1}_H V_{req} \cos \gamma_{req} \qquad (AI\text{-}31)$$

126

where $\bar{I}_r$ and $\bar{I}_u$ are unit vectors along the radius vector and perpendicular to the radius vector in the guidance plane or

$$\bar{I}_H = \bar{I}_h \times \bar{I}_R$$

$$\bar{I}_h = \frac{\bar{I}_R \times \bar{I}_{Ra}}{|\bar{I}_R \times \bar{I}_{Ra}|} \qquad \text{(AI-32)}$$

$\bar{V}_g$ is then derived by subtracting the components of present velocity obtained from the navigation computation.

$$\bar{V}_g = \bar{V}_{req} - \bar{V} \qquad \text{(AI-33)}$$

5. Tangent Transfer Trajectories. Equation (AI-27) above can be rearranged to give:

$$\frac{\sin \Omega}{1 - \cos \Omega} = \frac{\tan \gamma - \dfrac{R}{R_a} \tan \gamma_a}{1 - \dfrac{R}{R_a}} \qquad \text{(AI-34)}$$

or

$$\tan \frac{\Omega}{2} = \frac{1 - \dfrac{R}{R_a}}{\tan \gamma - \dfrac{R}{R_a} \tan \gamma_a}$$

Equations (AI-34) are useful for deriving the tangent transfer trajectory equations. The end points and the included angle Ω for the best trajectory need to be found without ambiguity or quadrant problems. Analysis and experiment have shown that the tangent transfer trajectory between two orbits is efficient in propellant usage if the tangency at the higher altitude end is placed at a node. Also the most efficient node is, in general, the higher of the two possible nodal points. Results of detailed studies on the efficiency of the tangent transfer were given in reference 9 .

For circular orbits or for elliptical orbits whose major axes are both aligned with the line of nodes the tangent transfer from node to node with optimal plane change split gives the optimal solution. If the major axes are not aligned or if one ellipse is not aligned with the line of nodes, the tangent transfer at the highest node is close to the optimum transfer

127

and the determination of the end points for the general case is given as follows:

Figure 58 illustrates the general case of the tangent transfer situation when both orbits are elliptical and not aligned.
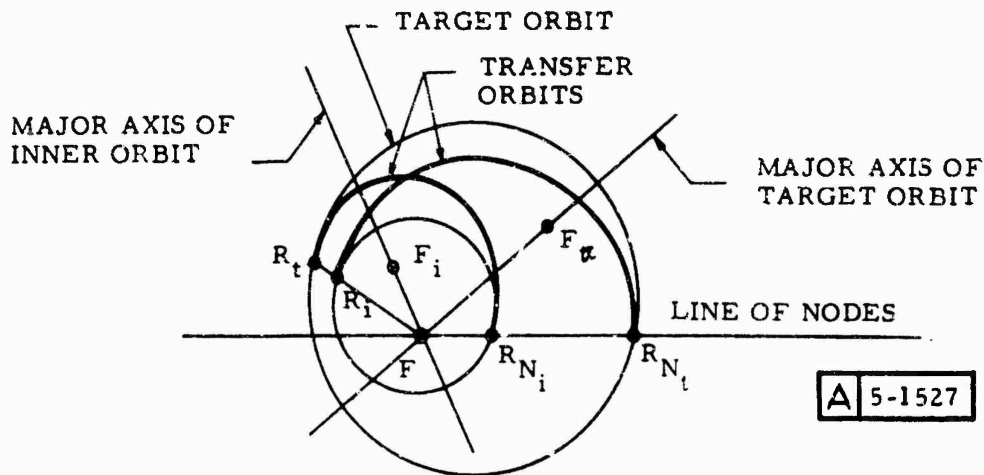
Figure 61. Tangent Transfer Trajectories

Equation (AI-27) which gives the downrange angle function

$$\tan \frac{1}{2} \Omega = \frac{1}{Z}$$

is rewritten in terms of the nomenclature given in Figure 61.

$$\frac{1}{Z} = \frac{\dfrac{R_{Nt}}{R_i} - 1}{\tan \gamma_{Nt} - \dfrac{R_{Nt}}{R_i} \tan \gamma_i}$$

Having defined the tangent transfer, it follows that any tangent trajectory can readily be defined traversing from or to any initial or final point on either trajectory (the transfer always exists for non-intersecting orbits. For intersecting orbits one of the nodes will produce a workable solution). Since the angle from any point on one of the orbits between the lines to the empty foci is equal to twice the flight path angle at the point, the other end point for the tangent trajectory is easily constructed.

The outer orbit in Figure 58 is considered to be the target trajectory with no particular time or position specified. F_t' is the location of its empty focus. F is the center of the

128

force field and is thus one focus for any orbit in this field. The inner orbit is the interceptor trajectory with empty focus at F_i'. R_{Ni} and R_{Nt} are radius vectors along the line of nodes between the two orbits. $\bar{R}_{Ni}$ is the nodal interceptor radius vector and $\bar{R}_{Nt}$ is the nodal target radius vector.

$\bar{R}_T$ and $\bar{R}_i$ are target and interceptor radius vectors at an angle Ω from the line of nodes. $\bar{R}_T$ is in the target orbit plane and $\bar{R}_i$ is in the interceptor orbit plane.

Four trajectories can be passed between the four points shown above. The object of the proof here is to show that all four of these trajectories contain the same angle Ω and are all tangent to each other at the indicated end points. We have already defined one of these trajectories.

Two other tangent trajectories are tangent by definition. They both lie on the two original orbits and in their own respective planes. The same angle is traversed, from a crossing vector (the line of nodes) to another point along their original orbits. The above three trajectories contain the same central angle and have end points of radii as stated.

As previously stated the fourth trajectory is considered as one starting in the target plane at point $\bar{R}_t$ and arriving at $\bar{R}_{Ni}$ in the target orbit plane. To prove that these four trajectories have the same flight path angles at their respective end points which contain the same included angle requires that the tangency conditions exist for the fourth specific trajectory just defined.

Let $X = \tan \gamma$ and write Equation (AI-28) for each trajectory

$$X_i = \frac{1 - \dfrac{R_i}{R_{Ni}}}{(\tan \frac{\Omega}{2})} - \frac{R_i}{R_{Ni}} X_{Ni}$$

also

$$X_i = \frac{1 - \dfrac{R_i}{R_{Nt}}}{(\tan \frac{\Omega}{2})} - \frac{R_i}{R_{Nt}} X_{Nt} \qquad \text{(AI-35)}$$

and

$$X_t = \frac{1 - \dfrac{R_t}{R_{Nt}}}{(\tan \frac{\Omega}{2})} - \frac{R_t}{R_{Nt}} X_{Nt}$$

129

For the fourth trajectory

$$X'_t = \frac{1 - \dfrac{R_t}{R_{Ni}}}{(\tan \dfrac{\Omega}{2})} - \frac{R_t}{R_{Ni}} X_{Ni} \qquad \text{(AI-36)}$$

To prove the conjecture equate the first of the above two equations and solve for X_{Ni}, then substitute the solution for X_{Nt} from the third into the last equation. This gives the desired result

$$X_t = X'_t$$

Further algebraic manipulation of these equations then gives the range angle Ω as a function of the radii and flight path angles of each orbit along a node as follows:

$$\text{Tan } \frac{\Omega}{2} = \frac{\dfrac{R_{Nt}}{R_{Ni}} - 1}{\tan \gamma_{Nt} - \dfrac{R_{Nt}}{R_{Ni}} \tan \gamma_{Ni}} \qquad \text{(AI-37)}$$

since:

$$\tan \frac{\Omega}{2} = \frac{1}{Z}$$

$$\sin \Omega_{12} = \frac{2Z}{Z^2 + 1} \qquad \text{(AI-38)}$$

$$\cos \Omega_{12} = 1 - \frac{2}{Z^2 + 1}$$

These are convenient forms for use in the program. The details of application are given in Volume I part 2.

6. <u>Time of Flight.</u> Up to this point the equation of a path has been specified with associated initial conditions which pass through a specific point in space, also the tangent

130

transfer trajectory parameters have been derived but one or more paths may be required which fits an overall time constraint.

In solving Equation (AI-6) for time, using the path equation, it is useful to first derive some of the orbit elements in terms of end conditions.

From Equation (AI-22) and (AI-24)

$$e^2 = (e \sin \nu)^2 + (e \cos \nu)^2$$

or

$$e^2 = \frac{P}{R} \left[\frac{P}{R} (1 + \tan^2 \gamma) - 2 \right] + 1 \qquad \text{(AI-38)}$$

also from Equation (AI-18) and (AI-28)

$$e^2 = 1 - u^2 \cos^2 \gamma (2 - u^2) \qquad \text{(AI-39)}$$

The major axis ratio is then found from Equation (AI-16) as the mean of perigee and apogee distance

$$\frac{a}{R} = \frac{\frac{P}{R}}{1 - e^2} \qquad \text{(AI-40)}$$

in terms of initial velocity

$$\frac{a}{R} = \frac{1}{2 - u^2} = \frac{1}{2 - \frac{P}{R} (1 + \tan^2 \gamma)} \qquad \text{(AI-41)}$$

from Equation (AI-39)

$$e^2 = 1 - \frac{P}{a} \qquad \text{(AI-42)}$$

and

$$b^2 = a^2 (1 - e^2) \tag{AI-43}$$

then

$$\left(\frac{b}{a}\right)^2 = \left(\frac{P}{a}\right) \tag{AI-44}$$

also

$$\left(\frac{b}{R}\right)^2 = \left(\frac{a}{R}\right)\left(\frac{P}{R}\right) \tag{AI-45}$$

The time of flight from start point to aim point can now be found by integration of Equation (AI-6).

First let

$$\tau = \frac{R}{V_c} \tag{AI-46}$$

for non-dimensional time. Then equation (AI-6) in non-dimensional form is:

$$\frac{dt}{\tau} = \left(\frac{P}{R}\right)^{-1/2} \left(\frac{R_a}{R}\right)^2 d\Theta \tag{AI-47}$$

Then from Equation (AI-20) and (AI-25)

$$\frac{t}{\tau} = \left(\frac{P}{R}\right)^{3/2} \int_0^\Omega \frac{d\Theta}{\left| 1 + \left(\frac{P}{R} - 1\right) \cos\Theta - \frac{P}{R} \tan\gamma \, \sin\Theta \right|^2} \tag{AI-48}$$

$$= \left(\frac{P}{R}\right)^{3/2} \int_{\Theta_0}^{\Theta_0 + \Omega} \frac{d(\Theta + \Theta_0)}{\overline{1 + e \cos(\Theta + \Theta_0)}^2} \tag{AI-49}$$

132

from Pierce's tables with

$$e < 1 \tag{AI-50}$$

The time equation then may be written for any start point to any angle to 2π as

$$\frac{t}{\tau} = \left(\frac{a}{R}\right)^{3/2} \left[2 \text{ arc cot } \frac{b}{R} \left(\frac{\sin \Omega}{1 - \cos \Omega} - \tan \gamma \right) \right.$$

$$\left. - \frac{b}{a} (\tan \gamma_a - \tan \gamma) \right] \tag{AI-51}$$

Similar solutions of the time equation are readily obtained for the cases where $e = 1$ and $e > 1$. For the case where $e > 1$

$$\frac{t}{\tau}\bigg|_{e > 1} = \left(\frac{a}{R}\right)^{3/2} \left[- 2 \text{ arc coth } \frac{b}{R} \left(\frac{\sin \Omega}{1 - \cos \Omega} - \tan \gamma \right) \right.$$

$$\left. + \frac{b}{a} (\tan \gamma_a - \tan \gamma) \right] \tag{AI-52}$$

which gives the time of flight on an hyperbolic trajectory and for $e = 1$

$$\frac{t}{\tau}\bigg|_{e = 1} = \frac{1}{3} \left(\frac{P}{R}\right)^{1/2} \left[\frac{P_a}{R} (\tan \gamma_a) \left(1 + \frac{P}{R_a} \right) - (\tan \gamma) \left(1 + \frac{P}{R} \right) \right] \tag{AI-53}$$

which gives the time of flight on a parabolic trajectory. This equation is useful when the ratio R/a approaches zero.

Since for the parabolic trajectory the velocity anywhere along its path is equal to the escape velocity, the semi-latus rectum ratio is a function of the radius vector to the point and the flight path angle at the point or

$$\frac{P}{R}\bigg|_{e = 1} = 2 \cos^2 \gamma = \frac{2}{1 + \tan^2 \gamma}$$

and

$$\left.\frac{P}{R_a}\right|_{e=1} = 2 \cos^2 \gamma_a = \frac{2}{1 + \tan^2 \gamma_a}$$

In terms of flight path angles, range angle and radius ratio

$$\left.\frac{t}{\tau}\right|_{e=1} = \frac{1}{3} \left(\frac{2}{1 + \tan^2 \gamma}\right)^{1/2} \left[\frac{R_a}{R} \left(\frac{3 + \tan^2 \gamma_a}{1 + \tan^2 \gamma_a}\right) \tan \gamma_a \right.$$

$$\left. - \left(\frac{3 + \tan^2 \gamma}{1 + \tan^2 \gamma}\right) \tan \gamma\right] \qquad \text{(AI-54)}$$

where

$$\tan \gamma_a = \frac{\sin \Omega}{1 - \cos \Omega} \left(\frac{R_a}{R} - 1\right) - \frac{R_a}{R} \tan \gamma$$

and

$$\tau = \left(\frac{R_o^3}{GM}\right)^{1/2}$$

7. **Time-To-Start-Burn for a Two-Stage Vehicle.** One of the basic functions of Variable Point Guidance is to determine the remainder of an ascent trajectory based on present situation parameters. This trajectory, if successfully executed by the vehicle in response to the commands of the guidance computer, will lead to rendezvous with the intended orbital target. Determination of an ascent trajectory and issuance of suitable commands to achieve this trajectory are continually performed by the Variable Point Guidance Computer while the vehicle is both on the pad and in its ascent flight. The ascent trajectory decided upon is computed based on impulsive burns located at aim points in space which are varied in position to satisfy the time constraint for rendezvous (within certain vehicle safety constraints). The number of aim points required is determined by the guidance computer.

As the intercepting vehicle approaches an aim point, the guidance computer must decide when to start the (finite) vehicle thrust to match the effect of the impulsive maneuver planned to take place at that aim point. It can be shown that under generally applicable

134

conditions, a finite burn can be made equivalent to an impulsive maneuver (requiring zero time) if the finite burn is begun at the proper time and is properly oriented through its duration.

In this section the correct time to start such a burn is derived for the case in which the maneuver is to be executed by a two-stage rocket vehicle, each stage of which has a predictable initial thrust, a thrust time-history predictable by the rocket equation, and known cutoff conditions.

Consider the vehicle as initially on a path which if continued unaltered would pass through the computed aim point at the correct time associated with that aim point. The trajectory leaving this point must then be changed to one that will arrive at the next selected aim point at its assigned time. Figure 59 illustrates the situation at this time. All vectors shown represent 3 x 1 column matrices in an earth-centered inertial coordinate system. As the vehicle approaches aim point "a" the guidance computer attacks the problem of reaching aim point "a + 1" on time. The known conditions are:

1.) $\overline{R}_o$ = present vehicle position

2.) $\overline{V}_o$ = present vehicle velocity

3.) T_o = present time

4.) $\overline{R}_{a+1}$ = aim point location

5.) T_{a+1} = time at aim point "a + 1"

6.) γ_{a+1} = flight path angle at arrival at "a + 1".

From the above, the guidance computer determines $\overline{V}_{REQ}$, the velocity necessary at the present time to arrive at "a + 1" with a flight path angle of γ_{a+1}. The velocity vector that must be added, $\overline{V}_g$, is therefore computed by:

$$\overline{V}_g = \overline{V}_{REQ} - \overline{V}_o \tag{AI-55}$$

If the vehicle thrust acceleration amplitude profile is a known function of time, a(t), and the thrust acceleration vector is kept parallel to $\overline{V}_g$, the predicted time required for thrusting, T, is defined by the scalar equation:

$$V_g = \int_0^T a(t) \, dt \tag{AI-56}$$

The position of the vehicle, $\overline{R}_{co}$, at the predicted end of the thrust period is given by:
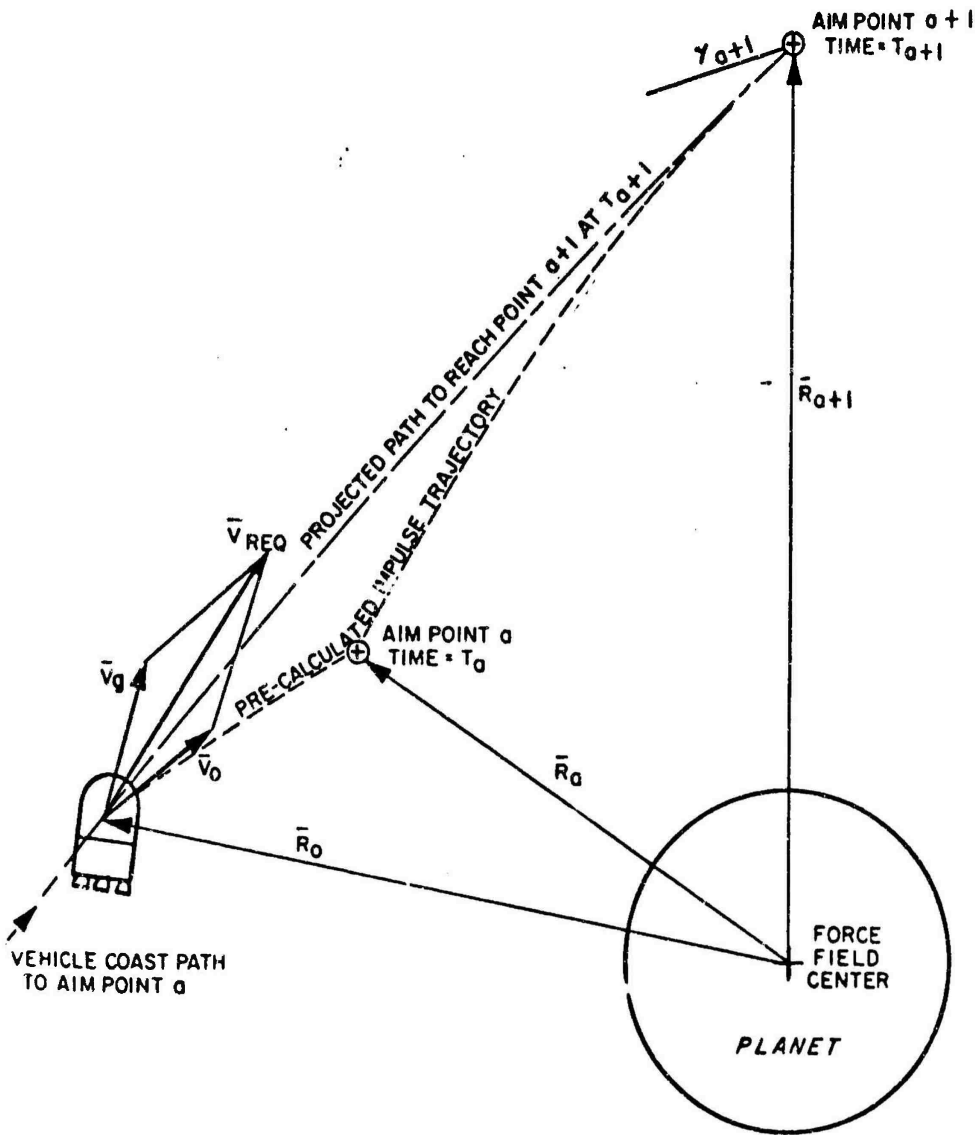
135

Figure 62. Time to Start Burn Situation Parameters

$$\overline{R}_{co} = \overline{R}_o + \overline{V}_o T + \int_0^T \int_0^t \overline{a}(t) \, dt \, dt + \overline{E}_{\overline{R}(t)} + \overline{E}_{\overline{V}(t)} \qquad (AI-57)$$

where:

$$\overline{E}_{\overline{R}(t)} = \int_0^T \int_0^t \left[- \frac{GM}{R(t)^2} + \left(\frac{\overline{V}(t) \cdot \overline{R}(t)}{R(t)} \right)^2 \frac{1}{R(t)} \right] dt \, dt$$

and

$$\overline{E}_{\overline{V}(t)} = \int_0^T \int_0^t \left(\overline{V}_o - \frac{\overline{V}(t) \cdot \overline{R}(t)}{R(t)} \right) dt \, dt$$

The effects introduced in the cutoff position ($\overline{R}_{co}$) by errors $\overline{E}_{\overline{R}(t)}$ along $\overline{R}(t)$ and $E_{\overline{V}(t)}$ along $\overline{V}(t)$, which are due to gravity during the burn, are not considered. This approximation is justified to the extent that the burn duration is short and the gravity gradient associated with the difference in positions at initiation and cutoff is small.

Equation (AI-57) may then be rewritten as:

$$\overline{R}_{co} = \overline{R}_o + \overline{V}_o T + \int_0^T \int_0^t \overline{a}(t) \, dt \, dt \qquad (AI-58)$$

If the time interval from start of thrust to the time the impulse was to occur is called T_s, the desired position, R_d, at the end of time interval T (i.e., that where an impulsive vehicle would be) is:

$$R_d(T) = \overline{R}_o + \overline{V}_o T_s + \overline{V}_T (T - T_s) \qquad (AI-59)$$

The time to start the burn is then found by equating Equation (AI-58) and (AI-59), setting $\overline{R}_{co}$ equal to $\overline{R}_d(T)$.

$$\overline{R}_d(T) = \overline{R}_{co}$$

$$\overline{R}_o + \overline{V}_o T_s + V_T (T - T_s) = \overline{R}_o + \overline{V}_o T + \int_0^T \int_0^t \overline{a}(t) \, dt \, dt \qquad (AI-60)$$

137

Equation (AI-60) is illustrated in Figure 60 in which both the impulsive vehicle and the real vehicle are shown in the same positions with the same velocity at the times of initiation and cutoff of the burn. The components of distance which comprise the total position change are also shown. Equation (AI-60) reduces to:

$$T_s = T - \frac{1}{V_g} \int_0^T \int_0^t a(t) \, dt \, dt \tag{AI-61}$$

Interval T_s is the "lead time" required in the start of the burn, T being computed from Equation (AI-56).

A two-stage vehicle with constant thrust and mass flow rate for each stage is assumed. The thrust parameters for each stage are represented as follows:

	Stage 1	Stage 2
Initial Thrust Acceleration	a_{o1}	a_{o2}
Exhaust Velocity	C_1	C_2
Burn Time Remaining	T_1	T_2

If the second stage is started at some time ΔT after the remaining burn time, T_1, of the first stage the vehicle acceleration profile at a time t (measured from initiation) will be:

$$a = \frac{a_{o1}}{1 - \frac{a_{o1}}{C_1} t}, \quad t < T_1 \tag{AI-62}$$

$$a = 0, \quad\quad T_1 < t < T_1 + \Delta T \tag{AI-63}$$

$$a = \frac{a_{o2}}{1 - \frac{a_{o2}}{C_1} (t - T_1 - \Delta T)}, \quad T_1 + \Delta T < t < T \tag{AI-64}$$

By integrating the acceleration profile, the velocity gained during use of the first stage becomes:

$$V_1 = - C_1 \ln \left[1 - \frac{a_{o1} t}{C_1} \right], \quad t < T_1 \tag{AI-65}$$
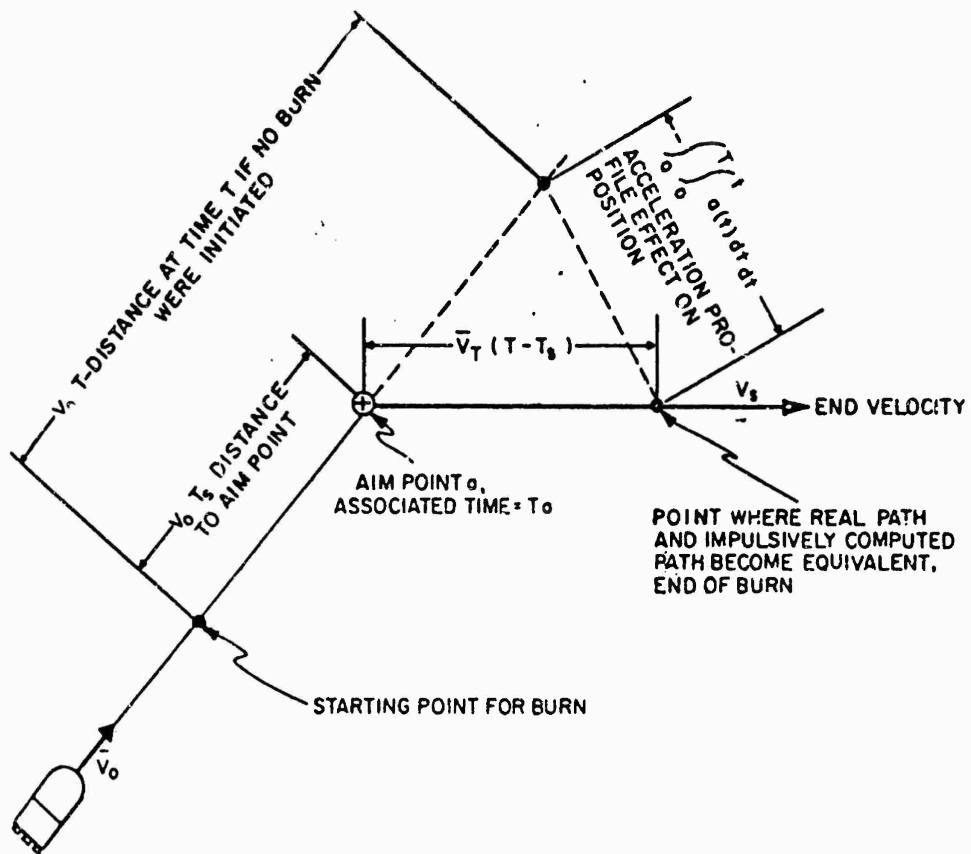
138

Figure 63. Equivalent Position Burn Computation

139

No velocity is gained through the "dead time", ΔT (referencing the development of Equation (Al-58). The velocity gained through use of both the first and second stages is:

$$V_T = V_1 + V_2$$

$$V_T = V_1 + C_2 \ln \left[1 - \frac{a_{o2}}{C_2} (t - T_1 - \Delta T) \right], \quad T_1 + \Delta T < t < T \qquad (AI-66)$$

Equation (AI-62) may be used to find thrust time T in terms of V_g as:

$$T = \frac{C_1}{a_{o1}} \left[1 - \exp \left(\frac{-V_g}{C_1} \right) \right], \quad V_g < V_1 \qquad (AI-67)$$

$$T = T_1 + \Delta T + \frac{C_2}{a_{o2}} \left[1 - \exp \left(\frac{V_g - V_1}{C_2} \right) \right], \quad V_g > V_1 \qquad (AI-68)$$

Integrating Equation (AI-65) to determine the distance S covered during the burns as a result of burn acceleration only gives:

$$S = \int_0^t \int_0^t a(t) \, dt \, dt = \int_0^t V(t) \, dt \qquad (AI-69)$$

$$S = \frac{C_1^2}{a_{o1}} \left[\left(1 - \frac{a_{o1} t}{C_1} \right) \ln \left(1 - \frac{a_{o1} t}{C_1} \right) - 1 \right], \quad t < T_1 \qquad (AI-70)$$

$$S = S_1 \qquad\qquad\qquad t = T_1 \qquad (AI-71)$$

$$S = S_1 + V_1 (t - T_1) \qquad\qquad T_1 < t < T_1 + \Delta T \qquad (AI-72)$$

$$S = S_1 + V_1 (t - T_1) + \frac{C_2^2}{a_{o2}} \left\{ \left[1 - \frac{a_{o2}}{V_{e2}} (t - T_1 - \Delta T \right] \right.$$

$$\left. \left[\ln \left(1 - \frac{a_{o2}}{C_2} \left\{ t - T_1 - \Delta T \right\} \right) - 1 \right] + 1 \right\} \qquad \text{(AI-73)}$$

where:

$$t_1 = \Delta t < t < T$$

Expressing S in terms of T and substituting into Equation (AI-61) yields:

$$T_s = \frac{C_1}{a_{o1}} \left\{ 1 - \frac{C_1}{a_{o1}} \left[1 - \exp \left(\frac{V_g}{C_1} \right) \right] \right\} , \quad V_1 > V_g \qquad \text{(AI-74)}$$

$$T_s = T_1 - \frac{(S_1 + V_1 \Delta T)}{V_g} + \frac{V_g - V_1}{V_g} \frac{C_2}{a_{o2}} \left\{ 1 - \frac{C_2}{a_{o2}} \right\}$$

$$\qquad \text{(AI-75)}$$

$$\left\{ 1 - \exp \left(- \frac{V_g - V_1}{C_2} \right) \right\} , \quad V_1 < V_g$$

It can be seen that the above equations are readily adaptable to computer solution. A possible computation sequence for the situation shown in Figure 1 is as follows:

(a) From $\bar{R}_o$, $\bar{V}_o$, T_o, T_{a+1}, $\bar{R}_{a+1}$, and γ_{a+1}, compute $\bar{V}_{REQ}$ and $\bar{V}_g$

(b) Compute present stage velocity capability remaining, V_1, using Equation (AI-65)

(c) Compare V_1 to V_g

    1.) If $V_1 \geq V_g$, compute time to start burn (T_s) using Equation (AI-74).

    2.) If $V_1 < V_g$, compute T_s using Equations (AI-70) and (AI-75).

(d) Compare T_o to $(T_a - T_s)$

1.) If $T_o < (T_a - T_s)$, do not thrust until next computation cycle

2.) If $T_o \geq (T_a - T_s)$, start engine; cutoff when forward component of V_g passes through zero.

After the engine is started, the variable point $\overline{V}_g$ steering control will command a precision cutoff consistent with successful arrival at aim point "a + 1".

APPENDIX

LIST OF ABBREVIATIONS AND SYMBOLS

<u>Symbol</u>		<u>Definition</u>
A, B	=	Coefficients depending on subscripts
a	=	Semi major axis of an orbit
a(t)	=	Acceleration as a function of time
b	=	Semi minor axis of an orbit
c	=	Exhaust velocity
E	=	Eccentric anomaly of an orbit
e	=	Eccentricity of an orbit
F	=	Force vector
f	=	Specific force (thrust to mass ratio)
g	=	Gravity vector
G	=	Gravitational constant
H, h	=	Angular momentum of an orbit
i	=	inclination of an orbit
I_{sp}	=	Specific impulse
J	=	Oblateness coefficient
K	=	Coefficient or constant depending upon subscript
L	=	Lattitude of planet surface location
M	=	Mean anomaly, mass of planet
m	=	Mass of vehicle
n	=	Number of orbits (parking or phasing)

143

Symbol		Definition
p	=	Semi latus rectum of an orbit
R	=	Radius vector from center of force field
T	=	Time or time interval denoted by subscript
u	=	Velocity ratio
v	=	Velocity vector
V_{req}	=	Velocity required
V_g	=	Velocity to be gained
α	=	Plane change angle
β	=	Coefficient
γ	=	Flight path angle
δ, Δ	=	Finite difference
λ	=	Lagrange multiplier
μ	=	GM = gravitational constant for specific planet
ν	=	True anomaly of point on an orbit
ρ	=	Relative range
τ	=	Period of an orbit
ω	=	Argument of perigee of an orbit
Ω	=	Angle between two points on an orbit, also the right ascention of the ascending mode

Subscripts

α	=	Refers to apogee
a	=	Refers to aim point
B	=	Body axes
H	=	Horizontal
i,j	=	Points at beginning and end of arc

Symbol		Definition
p	=	Refers to platform axes
M	=	Refers to intercepting vehicle
π	=	Refers to perigee
r	=	Point R
t	=	Refers to target vehicle
ϕ	=	Refers to phasing unit
x, y, z	=	Earth centered inertial (ECI) axes
ξ, η, ζ	=	Steering axes

COORDINATE SYSTEMS
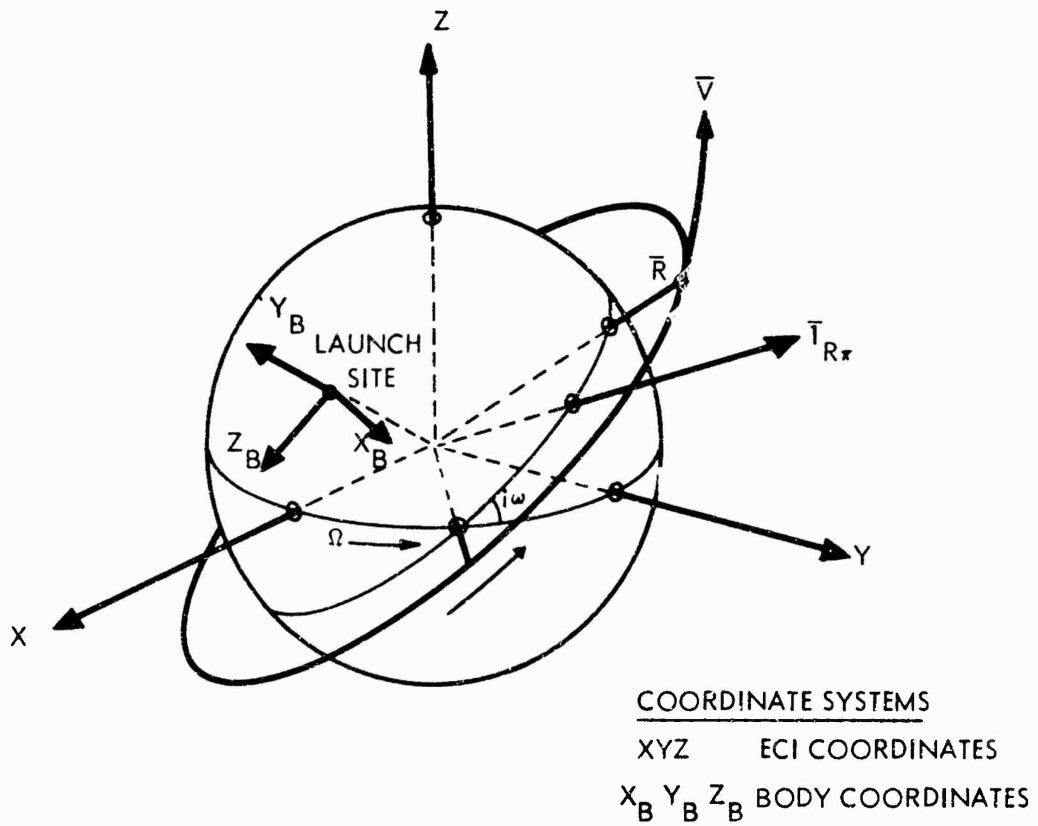XYZ   ECI COORDINATES
$X_B Y_B Z_B$ BODY COORDINATES

Figure 64. Coordinates
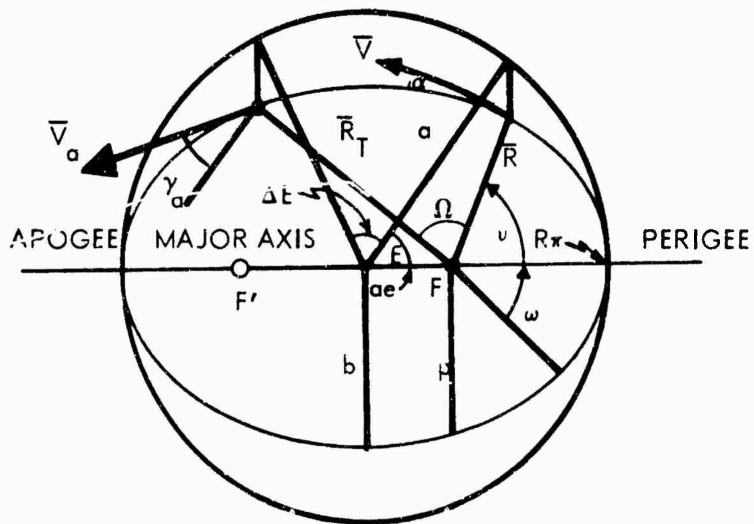

Figure 65. Orbit Parameters
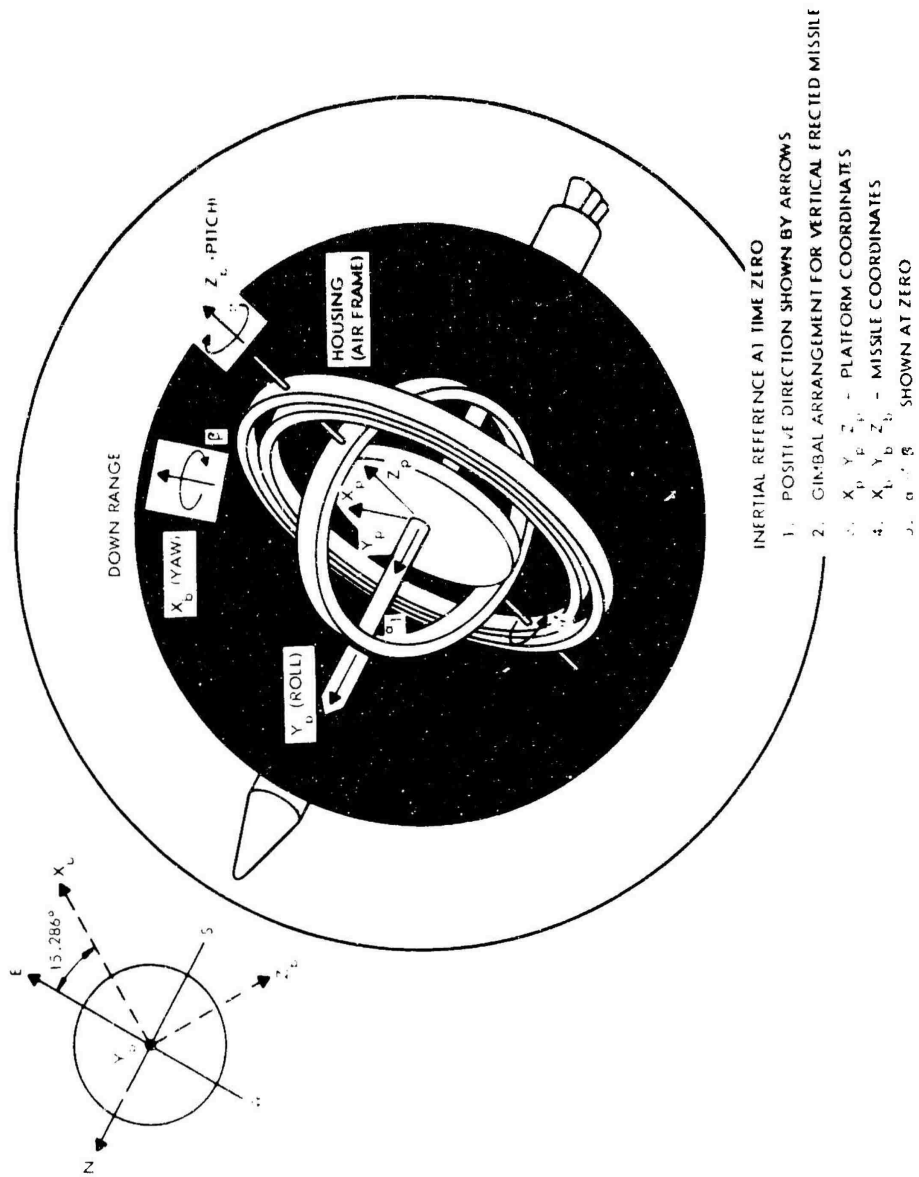
Figure 66. Inertial Reference at Time Zero

$$[d_{ij}] = \begin{bmatrix} \begin{Bmatrix} \cos\theta'\cos\alpha\cos 0 \\ -\sin 0\sin 0'\cos\alpha\cos\beta \\ +\sin 0\sin\alpha\sin\beta \end{Bmatrix} & \begin{Bmatrix} -\cos 0'\cos\alpha\sin\theta \\ -\cos 0\sin\theta'\cos\alpha\cos\beta \\ +\cos\theta\sin\alpha\sin\beta \end{Bmatrix} & \begin{Bmatrix} \sin\theta'\cos\alpha\sin\beta \\ +\sin\alpha\cos\beta \end{Bmatrix} \\ \begin{Bmatrix} \sin 0'\cos 0 \\ +\cos 0'\cos\beta\sin\theta \end{Bmatrix} & \begin{Bmatrix} -\sin 0'\sin\theta \\ +\cos 9'\cos\beta\cos\theta \end{Bmatrix} & \begin{Bmatrix} -\cos\theta'\sin\beta \end{Bmatrix} \\ \begin{Bmatrix} -\cos 0'\sin\alpha\cos\theta \\ +\sin 0\sin 0'\sin\alpha\cos\beta \\ +\sin 0\cos\alpha\sin\beta \end{Bmatrix} & \begin{Bmatrix} \cos\theta'\sin\alpha\sin\theta \\ +\cos\theta\sin 0'\sin\alpha\cos\beta \\ +\cos\theta\cos\alpha\sin\beta \end{Bmatrix} & \begin{Bmatrix} -\sin\theta'\sin\alpha\sin\beta \\ +\cos\alpha\cos\beta \end{Bmatrix} \end{bmatrix}$$
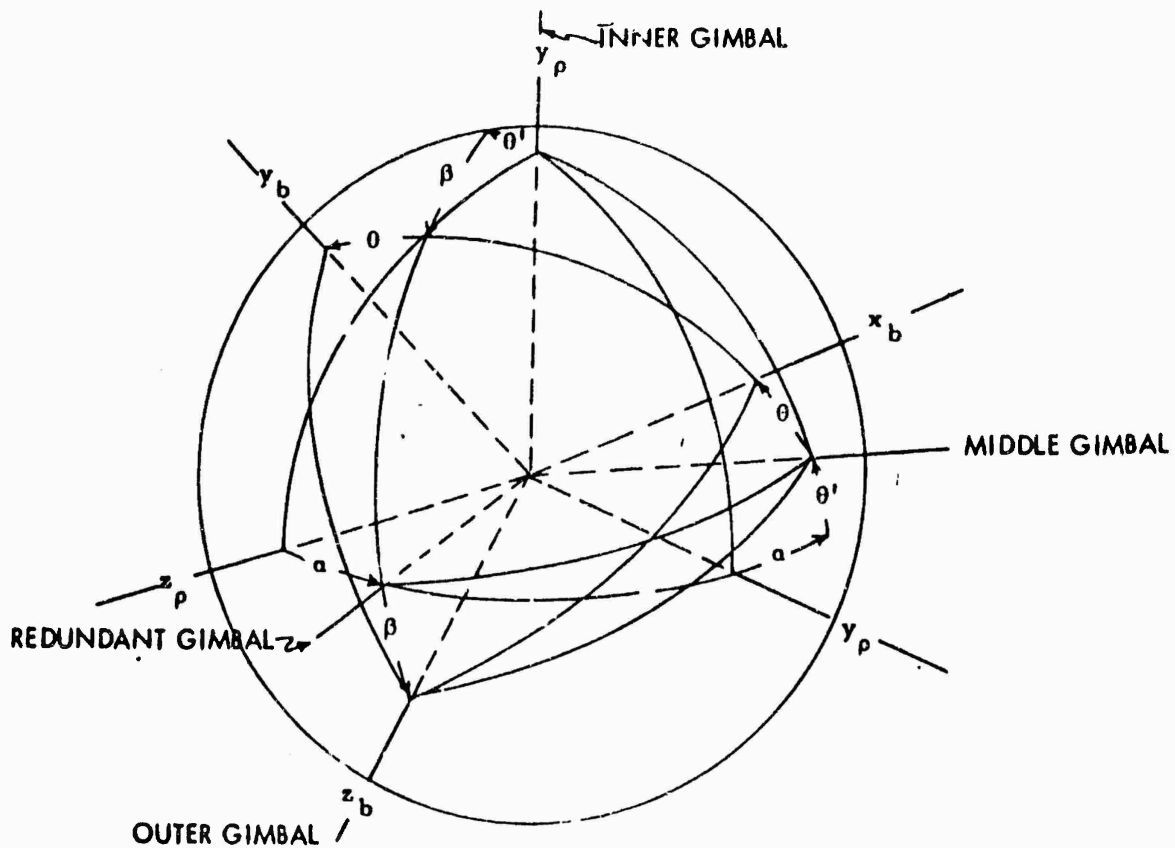

Figure 67.   Platform to Body Coordinate Relation

148

REFERENCES

1) Schneider, A. M. and Capen, E. B. , "Variable Point Guidance for Space Missions", AIAA Paper Number 64-640. Presented at AIAA-ION Astrodynamics Guidance and Control Conference, Los Angles, California, August 24-26, 1964.

2) Wallner, E. P. and Camiel, J. J. , "Plane Change in Circular Orbits", AIAA Journal of Spacecraft and Rockets. April, 1966.

3) Robbins, H. M. , "An Analytical Study of the Impulsive Approximation", AIAA Paper Number 66-12. Presented at AIAA Third Aerospace Sciences Meeting, New York, New York, January 24-26, 1966.

4) McCue, G. A. and Bender, D. F. , "Numerical Investigation of Minimum Impulse Orbital Transfer", AIAA Journal 3 (12), pages 2328-2334, December 1965.

5) Kupfrian, E. E. , "Optimum Two Impulse Orbit Transfer", MS Thesis, M. I. T. Department of Electrical Engineering, 1965.

6) MacPherson, D. , "An Explicit Solution to the Powered Flight Dynamics of a Rocket Vehicle", ASTIA Document AD2930-2, October 31, 1962.

7) Cherry, G. W. , "A General, Explicit, Optimizing Guidance Law for Rocket-Propelled Spacecraft", AIAA Paper Number 64-638. Presented at AIAA-ION Astrodynamics Guidance and Control Conference, Los Angeles, California, August 24-26, 1964.

8) Schneider, A. M. , Capen E. B. , Camiel J. J. , "Recent Development in Variable Point Guidance for Space Rendezvous and Rescue". Presented at the AIAA/5ASS Guidance and Control Conference, University of Washington, Seattle, Washington, August 1966.

9) Capen, E. et al. , "Variable Point Guidance Study,"Radio Corporation of America - Aerospace Systems Division, Document Number SSD-TDR-65-100 (Final Report for Contract AF04-(695)-633), July 15, 1965.

10) "Program 624A Mission Specification for Flight Plan VII", Aerospace Corporation. El Segundo, California. Report Number TOR-469(5116-54)-6 Reissue A, July 1965.

11) Capen, E. et al. , "Guidance Analysis", Radio Corporation of America, Aerospace Systems Division, Document Number SSD-TDR-63-399 (Final Report for Contract AF04-(695)-273). December 31, 1963 (Secret).

12) "Space Data", TRW/STL, Redondo Beach California, 1965.

REFERENCES (Continued)

13) Camiel, J. J. and Capen E. B., "Cost Effectiveness Study of MOL Resupply and Rescue", November 16, 1964 (EM 64-588-27).

14) "Programming for the S-C 4020, Section 74 of Engineers Computing Manual", North American Aviation Inc., October 15, 1963. (Available from VAIDE Library reference number 006.)

15) Kalik and Martikan, "Derivation of Nodal Period", AIAA Journal, Volume I, No. 9, p. 2041, September 1963.

16) Capen, et al., "Variable Point Guidance Study", RCA Aerospace Systems Division Burlington, Massachusetts, number CR-588-15 (SSD-TDR-65-100), 15 July 1965.

DOCUMENT CONTROL DATA - R&D

(Security classification of title, body of abstract and indexing annotation must be entered when the overall report is classified)

1 ORIGINATING ACTIVITY (Corporate author)	2a. REPORT SECURITY CLASSIFICATION
Radio Corporation of America	UNCLASSIFIED
Aerospace Systems Division Burlington, Massachusetts	2b GROUP

3 REPORT TITLE

VARIABLE POINT GUIDANCE AND TARGETING FINAL REPORT
(Volume I Part 1 Basic Principals and Results, Volume I Part 2 Programmers Manual and Volume II, Program Specification and Coding Report)

4 DESCRIPTIVE NOTES *(Type of report and inclusive dates)*

Final Report 1 May 1966 to 28 March 1967

5 AUTHOR(S) *(Last name, first name, initial)*

Capen, Edward B., Camiel, Joseph J., McNaughton Ruth V.,

6 REPORT DATE	7a. TOTAL NO. OF PAGES	7b. NO. OF REFS
28 March 1967	784	

8a. CONTRACT OR GRANT NO.	9a. ORIGINATOR'S REPORT NUMBER(S)
AF 04(695)-946	
b PROJECT NO	SSD TR-67-102
681D	
c	9b. OTHER REPORT NO(S) (Any other numbers that may be assigned this report)
d	CR-67-588-2

10 AVAILABILITY/LIMITATION NOTICES

Each transmittal of this document outside the Department of Defense must have prior approval of Headquarters, Space Systems Division (AFSC), AF Unit Post Office, Los Angeles, California 90045.

11 SUPPLEMENTARY NOTES	12 SPONSORING MILITARY ACTIVITY
	U.S. Air Force Space Systems Division
	Los Angeles Air Force Station L.A. Calif.

13 ABSTRACT The primary objective of the development of the Variable Point Guidance and Targeting Technique is to devise a quick reaction guidance and targeting system for space vehicles which does not limit the intrinsic propulsion capability of the booster and upper stages in applications involving arbitrary rendezvous missions. Logic and equations for such a system which operate in real time and which fit a modern aerospace computer have been developed and simulated. The system is provided with the ability of accepting a revised target ephemeris or the ephemeris of a completely new target after lift-off, giving the operational flexibility which permits in-flight changing of mission objectives at any time. The purpose of the present work has been (1) to improve the efficiency and effectiveness of the techniques, (2) to verify the modifications by a detailed simulation containing a representation of a typical booster and upper-stage configuration, (3) document the complete program and (4) to code an aerospace computer to the extent that an accurate sizing and timing estimate can be made. The program was exercised by complete simulation of twelve rendezvous missions against four widely different target situations. An evaluation of the results of the rendezvous simulation studies indicates that the efficiency, effectiveness and general applicability of the computer program was improved and extended so that any satellite rendezvous mission that is within the potential capability of the booster and its associated hardware can successfully be initiated and completed by the insertion of the target ephemeris.

KEY WORDS	LINK A		LINK B		LINK C	
	ROLE	WT	ROLE	WT	ROLE	WT
Space Vehicle Guidance						
Rendezvous Guidance						
Rescue Guidance for Space Missions						
Guidance and Control for Orbital Missions						
Satellite Vehicle Guidance						
Targeting, Guidance and Navigation						

INSTRUCTIONS

1. ORIGINATING ACTIVITY: Enter the name and address of the contractor, subcontractor, grantee, Department of Defense activity or other organization (corporate author) issuing the report.

2a. REPORT SECURITY CLASSIFICATION: Enter the overall security classification of the report. Indicate whether "Restricted Data" is included. Marking is to be in accordance with appropriate security regulations.

2b. GROUP: Automatic downgrading is specified in DoD Directive 5200.10 and Armed Forces Industrial Manual. Enter the group number. Also, when applicable, show that optional markings have been used for Group 3 and Group 4 as authorized.

3. REPORT TITLE: Enter the complete report title in all capital letters. Titles in all cases should be unclassified. If a meaningful title cannot be selected without classification, show title classification in all capitals in parenthesis immediately following the title.

4. DESCRIPTIVE NOTES: If appropriate, enter the type of report, e.g., interim, progress, summary, annual, or final. Give the inclusive dates when a specific reporting period is covered.

5. AUTHOR(S): Enter the name(s) of author(s) as shown on or in the report. Enter last name, first name, middle initial. If military, show rank and branch of service. The name of the principal author is an absolute minimum requirement.

6. REPORT DATE: Enter the date of the report as day, month, year; or month, year. If more than one date appears on the report, use date of publication.

7a. TOTAL NUMBER OF PAGES: The total page count should follow normal pagination procedures, i.e., enter the number of pages containing information.

7b. NUMBER OF REFERENCES: Enter the total number of references cited in the report.

8a. CONTRACT OR GRANT NUMBER: If appropriate, enter the applicable number of the contract or grant under which the report was written.

8b, 8c, & 8d. PROJECT NUMBER: Enter the appropriate military department identification, such as project number, subproject number, system numbers, task number, etc.

9a. ORIGINATOR'S REPORT NUMBER(S): Enter the official report number by which the document will be identified and controlled by the originating activity. This number must be unique to this report.

9b. OTHER REPORT NUMBER(S): If the report has been assigned any other report numbers (either by the originator or by the sponsor), also enter this number(s).

10. AVAILABILITY/LIMITATION NOTICES: Enter any limitations on further dissemination of the report, other than those imposed by security classification, using standard statements such as:

(1) "Qualified requesters may obtain copies of this report from DDC."

(2) "Foreign announcement and dissemination of this report by DDC is not authorized."

(3) "U. S. Government agencies may obtain copies of this report directly from DDC. Other qualified DDC users shall request through

_____."

(4) "U. S. military agencies may obtain copies of this report directly from DDC. Other qualified users shall request through

_____."

(5) "All distribution of this report is controlled. Qualified DDC users shall request through

_____."

If the report has been furnished to the Office of Technical Services, Department of Commerce, for sale to the public, indicate this fact and enter the price, if known.

11. SUPPLEMENTARY NOTES: Use for additional explanatory notes.

12. SPONSORING MILITARY ACTIVITY: Enter the name of the departmental project office or laboratory sponsoring (paying for) the research and development. Include address.

13. ABSTRACT: Enter an abstract giving a brief and factual summary of the document indicative of the report, even though it may also appear elsewhere in the body of the technical report. If additional space is required, a continuation sheet shall be attached.

It is highly desirable that the abstract of classified reports be unclassified. Each paragraph of the abstract shall end with an indication of the military security classification of the information in the paragraph, represented as (TS), (S), (C), or (U).

There is no limitation on the length of the abstract. However, the suggested length is from 150 to 225 words.

14. KEY WORDS: Key words are technically meaningful terms or short phrases that characterize a report and may be used as index entries for cataloging the report. Key words must be selected so that no security classification is required. Identifiers, such as equipment model designation, trade name, military project code name, geographic location, may be used as key words but will be followed by an indication of technical context. The assignment of links, rules, and weights is optional.